

Distributed Control of Large-Scale Systems

A Takagi-Sugeno Fuzzy Model-based Approach

by **Rodrigo Farias Araújo**

supervised by

Prof. Dr. Reinaldo Martinez Palhares

Prof. Dr. Leonardo Antônio Borges Tôres

Graduate Program in Electrical Engineering

Universidade Federal de Minas Gerais

Belo Horizonte, MG - Brasil

November 28th, 2019

UNIVERSIDADE FEDERAL DE MINAS GERAIS
ESCOLA DE ENGENHARIA
PROGRAMA DE PÓS-GRADUAÇÃO EM ENGENHARIA ELÉTRICA

Distributed Control of Large-Scale Systems

A Takagi-Sugeno Fuzzy Model-based Approach

Rodrigo Farias Araújo

Tese de doutorado submetida à Banca Examinadora designada pelo Colegiado do Programa de Pós-Graduação em Engenharia Elétrica da Escola de Engenharia da Universidade Federal de Minas Gerais, como requisito para obtenção do Título de Doutor em Engenharia Elétrica.

Orientador: Prof. Reinaldo Martinez Palhares
Coorientador: Prof. Leonardo Antônio Borges Tôrres

Belo Horizonte - MG, 28 de Novembro de 2019.

| | |
|-------|--|
| A663d | <p>Araújo, Rodrigo Farias. Distributed control of large-scale systems [recurso eletrônico] : a Takagi-Sugeno fuzzy model-based approach / Rodrigo Farias Araújo. - 2019. 1 recurso online (xiii, 73 f. : il., color.) : pdf. Orientador: Reinaldo Martinez Palhares. Coorientador: Leonardo Antônio Borges Tôres.</p> <p>Tese (doutorado) - Universidade Federal de Minas Gerais, Escola de Engenharia.</p> <p>Bibliografia: f. 68-73. Exigências do sistema: Adobe Acrobat Reader.</p> <p>1. Engenharia elétrica - Teses. 2. Sistemas não- lineares - Teses. I. Palhares, Reinaldo Martinez. II. Tôres, Leonardo Antônio Borges. III. Universidade Federal de Minas Gerais. Escola de Engenharia. IV. Título.</p> <p style="text-align: right;">CDU: 621.3(043)</p> |
|-------|--|

TESE DE DOUTORADO Nº 316

**DISTRIBUTED CONTROL OF LARGE-SCALE SYSTEMS: A
TAKAGI-SUGENO FUZZY MODEL-BASED APPROACH**

Rodrigo Farias Araújo

DATA DA DEFESA: 28/11/2019

**"Distributed Control of Large-scale Systems: a Takagi-Sugeno
Fuzzy Model-based Approach"**

Rodrigo Farias Araújo

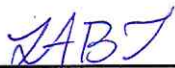
Tese de Doutorado submetida à Banca Examinadora designada pelo Colegiado do Programa de Pós-Graduação em Engenharia Elétrica da Escola de Engenharia da Universidade Federal de Minas Gerais, como requisito para obtenção do grau de Doutor em Engenharia Elétrica.

Aprovada em 28 de novembro de 2019.

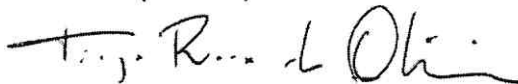
Por:



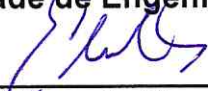
Prof. Dr. Reinaldo Martinez Palhares
DELT (UFMG) - Orientador



Prof. Dr. Leonardo Antônio Borges Tôres
DELT (UFMG) - Coorientador



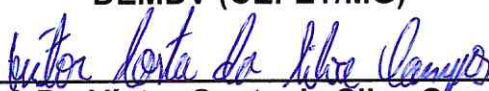
Prof. Dr. Tiago Roux de Oliveira
Faculdade de Engenharia (UERJ)



Prof. Dr. Eduardo Nunes Gonçalves
DEE (CEFET/MG)



Prof. Dr. Václav J. de Souza Leite
DEMDV (CEFET/MG)



Prof. Dr. Víctor Costa da Silva Campos
DELT (UFMG)

To my parents

Acknowledgements

Life consists of creating relationships wherever we go. We are just one in a “large-scale distributed network”, where we interact and learn continuously from others. This example illustrates the study of this thesis, which would not be possible without the contribution of several people. I’m grateful to god for this wonderful opportunity.

I thank my dear parents, Raimunda and Reginaldo, for all the love, support, and encouragement, mainly durant these years I was away. To my girlfriend, Adria, for always encouraging me and support during the doctorate.

I want to thank my advisors, Reinaldo and Léo, for all the teachings, advice, guidance and support throughout the doctorate, and to the numerous conversations on the various themes, which undoubtedly made me evolve as a student and person.

To my dear friends from D!FCOM Lab: Luiz Jr., Matheus, Iury, Pedro, Murilo, Fúlvia, Rosileide, Márcia, Gabriela, Klenilmar and Tiago, who made these years lighter even in the most challenging times. Thank you all for the productive conversations and mainly the unproductive ones. Especially, to Amazonenses, Luiz Jr. and Matheus, for putting up with me and sharing the apartment with me.

To PPGEE/UFGM team of professors who helped to sediment this formation.

Finally, I would like to thank the Brazilian agency CNPq by funding provided during my years at UFGM.

“Always pass on what you have
learned.”

“Much to learn you still have...
my old padawan. ... This is
just the beginning!”

Jedi Master Yoda, *Star Wars*

Abstract

Large-scale systems have become increasingly common in modern society where many real systems are widely distributed in space and consist of a large number of interconnected subsystems with strong coupling among them. In this context, this thesis addresses the problem of distributed control of large-scale nonlinear systems which are described by Takagi-Sugeno (TS) fuzzy models interconnected by sector nonlinearities.

An approach based on Lyapunov theory is used as a starting point for the distributed controller synthesis. A quadratic block-diagonal Lyapunov function is used to check the asymptotic stability of large-scale systems via sufficient conditions described in terms of Linear Matrix Inequalities (LMIs).

In the first moment, this thesis deals with networked systems such no decomposition technique is applied to large-scale systems. Creating a large number of LMIs usually generated when dealing with large-scale systems is prevented by defining an augmented vector created with state vectors and association functions of subsystems. In this case, state constraints and saturation in the control input are also considered, which are often found in practice and are generated by limitations in the physical system or in the description of models that represent them. Besides that, the proposed approach also allows to maximize the estimate of the domain of attraction where initial conditions belonging to the region converge asymptotically to the equilibrium point.

In the sequel, the synthesis problem of distributed controllers for large-scale nonlinear systems is solved utilizing the so-called chordal decomposition. This decomposition takes advantage of the sparsity pattern of the graph associated with the large-scale system to decrease the computational complexity of the problem. Thus, the analysis of the computational complexity and the running time of the method show that solutions can be provided with reasonable computational efforts, even though the number of subsystems is very large.

Finally, aiming to illustrate the effectiveness of the proposed methods for distributed control design, the stabilization of multiple inverted pendulums connected by nonlinear springs and the control of electrical power systems are considered.

Resumo

O contexto de sistemas de grande escala tornou-se razoavelmente comum na sociedade moderna já que muitos sistemas reais são de fato distribuídos no espaço e consistem em um grande número de subsistemas interconectados e, em muitos casos, com forte acoplamento entre os mesmos. Nesse contexto, esta tese considera o problema de controle distribuído de sistemas de grande escala não-lineares, os quais são descritos por modelos fuzzy Takagi-Sugeno interconectados por não-linearidades setoriais.

Uma abordagem baseada na teoria de Lyapunov é usada como ponto de partida para obter a síntese de controladores distribuídos. Uma função de Lyapunov bloco-diagonal quadrática é utilizada para se obter condições suficientes para a checagem da estabilidade assintótica do sistema de grande escala.

Em um primeiro momento, a tese lida com sistemas em rede, uma vez que nenhuma técnica de decomposição é aplicada aos sistemas de grande escala. A criação de um grande número de desigualdades matriciais lineares geradas quando lidamos com sistemas de grande escala é evitada a partir do uso de um vetor aumentado formado com os vetores de estado e funções de pertinência dos subsistemas. Neste caso, também considera-se restrições nos estados e saturação na entrada de controle, restrições estas que podem estar frequentemente presentes em sistemas reais pois podem ser geradas por limitações no sistema físico ou na descrição dos modelos que o representam. Além disso, a abordagem também nos permite maximizar a estimativa do domínio de atração para o qual condições iniciais que pertencem à região convergem assintoticamente para o ponto de equilíbrio.

Posteriormente, o problema de síntese de controladores distribuídos para sistemas de grande escala não-lineares é resolvido utilizando a decomposição *chordal*, que aproveita o padrão de esparsidade do grafo associado ao sistema de grande escala para diminuir a complexidade computacional do problema. A análise da complexidade computacional e tempos de execução do método mostra que soluções podem ser fornecidas com esforços computacionais razoáveis, mesmo que o número de subsistemas seja grande.

Por último, visando verificar a efetividade da abordagem proposta, o projeto de controle distribuído é aplicado a problemas reais como, por exemplo, estabilização de múltiplos

pêndulos invertidos conectados por molas não-lineares e controle de sistemas elétricos de potência.

Contents

| | |
|---|-------------|
| List of Figures | ix |
| List of Tables | xi |
| Notation | xii |
| List of Acronyms | xiii |
| 1 Introduction | 1 |
| 1.1 Motivation | 1 |
| 1.1.1 Control of Large-Scale Systems | 3 |
| 1.2 Objectives | 6 |
| 1.3 Outline and Contributions | 7 |
| 2 Background | 9 |
| 2.1 Chordal Graph | 9 |
| 2.1.1 Maximal Cliques and Clique Trees | 11 |
| 2.1.2 Sparse Symmetric Matrices and Chordal Decomposition | 13 |
| 2.2 Takagi-Sugeno Fuzzy Models | 15 |
| 2.2.1 Takagi-Sugeno Fuzzy Models with Nonlinear Consequents | 19 |
| 2.3 Interconnected N-TS Fuzzy Systems | 23 |
| 2.3.1 Fuzzy Summations and Interconnected Systems | 27 |
| 3 Networked Systems | 30 |
| 3.1 Introduction | 30 |
| 3.1.1 Regional Stability | 31 |
| 3.2 Problem Statement | 35 |
| 3.3 Stabilization of Interconnected N-TS Fuzzy Systems | 37 |
| 3.4 Illustrative Examples | 44 |

| | | |
|----------|---|-----------|
| 3.4.1 | Two-machine Subsystems | 45 |
| 3.4.2 | Multiple Inverted Pendulums | 48 |
| 3.5 | Conclusions | 49 |
| 4 | Large-Scale Systems | 52 |
| 4.1 | Introduction | 52 |
| 4.1.1 | Sparse Block Matrices and Chordal Decomposition | 53 |
| 4.2 | Problem Statement | 55 |
| 4.3 | Stabilization of Large-Scale Systems | 57 |
| 4.4 | Analysis of the Computational Complexity | 58 |
| 4.4.1 | Multiple Inverted Pendulums | 59 |
| 4.5 | Conclusions | 64 |
| 5 | Conclusions and Future Directions | 65 |
| 5.1 | An Overview of the Research | 65 |
| 5.2 | Main Conclusions | 65 |
| 5.3 | Possible Future Directions | 66 |
| | Bibliography | 68 |

List of Figures

| | | |
|-----|---|----|
| 1.1 | A large-scale system represented by its subsystems S_i , $i \in \mathcal{I}_5$. Continuous arrows represent the physical couplings between subsystems. | 2 |
| 1.2 | Centralized control structure. The states and control inputs of each subsystem S_i are denoted by x_i and u_i , respectively. Dashed arrows indicate that the states (blue) of each subsystem are sent to a centralized controller that computes and transmits control inputs (red) back to each subsystem. | 4 |
| 1.3 | Decentralized control structure. Dashed arrows indicate that the states (blue) of each subsystem are sent to a local controller that computes and transmits control inputs (red) back each corresponding subsystem. | 5 |
| 1.4 | Distributed control structure. Dashed arrows (gray) between local controllers indicate that the states or control inputs of subsystems in the neighborhood are sent to a local controller to compute the control signal for its corresponding subsystem. | 5 |
| 2.1 | Examples of undirected graphs. | 11 |
| 2.2 | Clique tree associated to chordal extension of undirected graph shown in Figure 2.1(b). | 12 |
| 2.3 | Two-inverted pendulums connected via linear springs. | 21 |
| 2.4 | Graph of interconnected system. | 25 |
| 3.1 | Validity region $\mathcal{D}_{\mathbf{x}}$ and Domain of Attraction (DoA). | 33 |
| 3.2 | DoA and sets $\mathcal{D}_{\mathbf{x}}$ and $\mathcal{D}_{\mathbf{u}}$ | 35 |
| 3.3 | Trajectories of angular positions of two-machines in Section 3.4.1 – Extension of (Lin, Wang, and Yang 2007). | 46 |
| 3.4 | Control signals of two-machines in Section 3.4.1 – Extension of (Lin, Wang, and Yang 2007). | 47 |
| 3.5 | Trajectories of angular positions of two-machines in Section 3.4.1 – Corollary 3.1. | 47 |
| 3.6 | Control signals of two-machines in Section 3.4.1 – Corollary 3.1. | 48 |

| | | |
|-----|--|----|
| 3.7 | Networked system graph of the interconnected inverted pendulums. | 49 |
| 3.8 | Time evolution of the angular positions for the nine interconnected inverted pendulums in Section 3.4.2. | 50 |
| 3.9 | Control signals of the nine interconnected inverted pendulums in Section 3.4.2. | 50 |
| 4.1 | Graph of large-scale system. | 54 |
| 4.2 | Clique tree of the chordal graph in Figure 4.1. | 55 |
| 4.3 | Comparison of the computational complexity associated with Theorems 3.2 and 4.2, considering the largest maximal clique size $\tau = 2$ | 60 |
| 4.4 | Comparison of the computational complexity of Theorems 3.2 and 4.2, considering the largest maximal clique size $\tau = 6$ | 61 |
| 4.5 | Comparison of the computational complexity of Theorems 3.2 and 4.2, considering the largest maximal clique size $\tau = 10$ | 61 |
| 4.6 | Comparison of the total running time associated with Theorems 3.2 and 4.2, considering the largest maximal clique size $\tau = 2$ | 62 |
| 4.7 | Comparison of the Yalmip parser plus solver running time and only solver running time associated with Theorems 3.2 and 4.2, considering the largest maximal clique size $\tau = 2$ | 63 |
| 4.8 | Comparison of the total running time associated with Theorems 3.2 and 4.2, considering the largest maximal clique size $\tau = 6$ | 63 |
| 4.9 | Comparison of the Yalmip parser plus solver running time and only solver running time associated with Theorems 3.2 and 4.2, considering the largest maximal clique size $\tau = 6$ | 64 |

List of Tables

| | | |
|-----|--|----|
| 3.1 | Values of $\det(\mathbf{Q}_N)^{1/n_x}$ obtained with extension of (Lin, Wang, and Yang 2007) and Corollary 3.1. | 46 |
| 3.2 | Parameters of the multiple inverted pendulums. | 48 |
| 3.3 | Values of $\det(\mathbf{Q}_N)^{1/n_x}$ obtained with Corollary 3.1, and alternatives of control in the Remark 3.1. | 49 |
| 4.1 | Comparison of the number of LMI rows in Theorems 3.1, 3.2 and 4.2. | 59 |

Notation

| | |
|---------------------------|---|
| \mathbb{R}^n | The set of n -dimensional real vector |
| $\mathbb{R}^{n \times m}$ | The set of $n \times m$ real matrix |
| \mathbf{S}^n | The set of $n \times n$ symmetric matrices |
| \mathbf{S}_+^n | The set of $n \times n$ symmetric positive semidefinite matrices |
| \mathcal{I}_n | The set of natural numbers from 1 to n |
| a | Scalar |
| \mathbf{a} | Vector |
| a_i | i -th component of vector \mathbf{a} |
| \mathbf{a}_i | i -th vector |
| A | Matrix $A = [a_{ij}]$ |
| A^\top | Transpose of matrix A |
| $A_{(i)}$ | i -th row vector of matrix A |
| $A \otimes B$ | Kronecker product between matrices A and B |
| $A \circ B$ | Hadamard product between matrices A and B |
| A_i | i -th matrix |
| \mathbf{A} | Block matrix, i.e., $\mathbf{A} = [A_{ij}]$ |
| $\bigoplus_{i=1}^n X_i$ | Direct sum of matrices, i.e., $\bigoplus_{i=1}^n X_i = \text{diag}(X_1, X_2, \dots, X_n)$ |
| I_n | Identity matrix of n -th order |
| \star | Transpose elements inside of a symmetric matrix |
| $P \succ (\prec) 0$ | The matrix P is positive (negative) definite |
| $P \succeq (\preceq) 0$ | The matrix P is positive (negative) semidefinite |
| $\text{co}\{x, y\}$ | Convex hull of two points x and y |
| $\mathbf{0}_n$ | Vector, with n elements, whose components are all equal to zero |
| $\mathbf{1}_n$ | Vector, with n elements, whose components are all equal to one |
| $\mathbf{0}_{n \times m}$ | Matrix in $\mathbb{R}^{n \times m}$ whose elements are all equal to zero |
| $\mathbf{1}_{n \times m}$ | Matrix in $\mathbb{R}^{n \times m}$ whose elements are all equal to one |

List of Acronyms

| | |
|-------------|--------------------------|
| DoA | Domain of Attraction |
| LMI | Linear Matrix Inequality |
| N-TS | Nonlinear Takagi-Sugeno |
| TS | Takagi-Sugeno |

1 Introduction

1.1 Motivation

Large-scale systems have become increasingly common in modern society where many practical systems are widely distributed in space and consist of a large number of interconnected heterogeneous subsystems with strong physical coupling among them, such as transportation systems, water and energy distribution, mobile robots, industrial processes and communication networks (Antoulas 2005; Mahmoud 2011; Meyn 2007; Šiljak 2007).

However, the notion of *large-scale* is very subjective and several definitions have been presented in the literature. The definition adopted in this thesis is: a system is large-scale when its dimensions are so large that conventional techniques of modeling, analysis, control, and computation fail to provide solutions with reasonable computational efforts and, further, it is necessary to use some decomposition techniques to solve the problem (Jamshidi 1997).

Due to structural characteristics such as high dimensionality, information structure constraints, uncertainty and induced delays (Bakule 2008; Lunze 1992), the analysis of large-scale systems stability can be very challenging. The large-scale systems addressed in this thesis consist of several nonlinear interconnected heterogeneous subsystems by linear or nonlinear physical couplings, where the subsystems are represented by TS fuzzy models, which is a powerful way to represent nonlinearities, since one can, in principle, smoothly approximate nonlinear systems with an arbitrary precision by relying on this mathematical description (Nguyen et al. 2019; Takagi and Sugeno 1985).

In such cases, it is usual to represent a large-scale system by means of a *graph* and if interactions between subsystems are mutual, an *undirected* graph can be used (Godsil and Royle 2001). Figure 1.1 depicts an example of a large-scale system composed by five subsystems; a continuous arrow indicates that the dynamics of subsystem i depends on the states of the subsystem j interconnected to it and vice versa. In this case, we say that subsystem j belongs to the neighborhood \mathcal{N}_i of the i -th subsystem. For example, in Figure 1.1, $\mathcal{N}_4 = \{1, 3, 5\}$. In general, the graph that represents a large-scale system is

sparse, thus this thesis exploits this feature to develop an approach to the synthesis of controllers for large-scale systems.

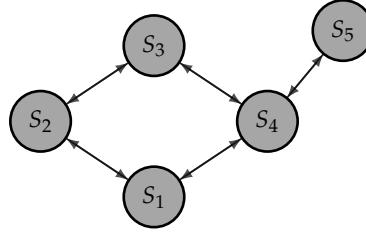


Figure 1.1: A large-scale system represented by its subsystems S_i , $i \in \mathcal{I}_5$. Continuous arrows represent the physical couplings between subsystems.

In this context, the problem of handling nonlinear interconnections between subsystems can be considered as one of the great challenges in the design of controllers for large-scale systems, since usually only linear interconnections are considered in many works in the current literature on the subject.

Different alternatives to deal with this problem have been employed. In general, it may be assumed that the nonlinear interconnections satisfy a few particular conditions. For instance, a Lipschitz condition is considered in (Li, Wu, and He 2018; Zhang and Lin 2014), and the same assumption together with equal interconnected systems was considered in (Li, Wu, and He 2018). In (Ye 2011), unknown nonlinear interconnections satisfying a polynomial bounding condition were assumed. In (Dhbaibi et al. 2009; Liu and Li 2002) uncertain norm-bounded interconnections were considered, while a quadratic bounding was used in (Stanković, Stipanović, and Šiljak 2007; Zečević and Šiljak 2004), in the context of dynamic and static output feedback, respectively. Interconnected Lur'e systems are discussed in (Zečević, Cheng, and Šiljak 2010) in which the nonlinear interconnections satisfy a sector-bounded condition. Chang et al. 2014 proposed a decomposition of nonlinear interconnections into a combination of a linear term and an uncertain linear one.

Except for the reference (Chang et al. 2014), all the previous papers mentioned in the last paragraph do not consider a fuzzy TS framework, which is a powerful way to represent nonlinearities since one can, in principle, smoothly approximate nonlinear systems with arbitrary precision by relying on this mathematical description (Nguyen et al. 2019; Takagi and Sugeno 1985). Besides that, TS fuzzy model representations have successfully been combined with Lyapunov theory to derive powerful stability and stabilization conditions (Nguyen et al. 2019). However, if each nonlinear interconnection is transformed into a set of fuzzy rules, this can lead to the so-called *rule-explosion* problem (Tanaka and Wang 2001). This happens in (Zhang, Zhong, and Dang 2012), where the authors transform all nonlinearities into a set of fuzzy rules and focus on considering the time-varying delay in the subsystems, and also in (Zhong, Zhu, and Lam 2018), where the problem of distributed

event-triggering control is examined. To avoid incorporating an excessive number of rules in the TS models, Kim, Park, and Joo [2017](#) employ TS fuzzy modeling to represent local nonlinearities of the subsystems, and nonlinear interconnections are considered to be norm-bounded ones, while in (Koo, Park, and Joo [2014](#)) nonlinear interconnections satisfy a quadratic bounding.

Note that, when TS fuzzy models with linear consequent are used, only the local nonlinearity of subsystems are represented by fuzzy rules, while it is assumed that the interconnections satisfy some particular condition. In this context, when TS fuzzy models are used in a way that they incorporate in the model sector-bounded functions, it is generated the so-called Nonlinear Takagi-Sugeno (N-TS) fuzzy models (Dong, Wang, and Yang [2009](#); Dong, Wang, and Yang [2011](#)), i.e. TS fuzzy models with nonlinear consequent. It is noteworthy that the sector-bounded function is similar to the one in the Lur'e problem, however, it is a function of system's states rather than a function of system's output.

1.1.1 Control of Large-Scale Systems

One of the main issues in large-scale systems is related to the control design under information structure constraints (Lunze [1992](#); Mahmoud [2011](#); Šiljak and Zečević [2005](#)). In other words, the problem is how to define a control strategy from the information flow in the large-scale system since its complexity can increase rapidly according to the number of subsystems. In this case, standard control structures may not be applicable. In the following, we highlight the main drawbacks of centralized control and we discuss alternatives for the control structures of large-scale systems such as decentralized and distributed control.

Centralized versus Decentralized Control

Centralized control structures have been popular choices in most of the approaches in the past, and several methods for stability analysis and control design of linear and nonlinear systems are available in the literature (Khalil [2002](#); Skogestad and Postlethwaite [2005](#)). Its structure is characterized by computing the control inputs from all the systems' states. Figure 1.2 depicts the centralized control scheme applied to control the large-scale system in Figure 1.1.

As a matter of fact, centralized techniques depend on a central entity that receives from subsystems all data available and determines all control input signals. In other words, all information is assumed to be available for a single unit capable of influencing all subsystems by means of control actions that depend on globally available information.

However, when this kind of approach is used in large-scale systems it leads to some problems such as *high computational complexity*, which increases with the number of subsystems; and also *low reliability*, since a data transmission failure from a single subsystem

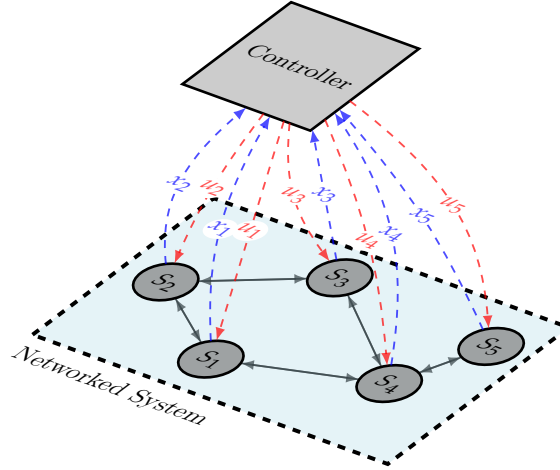


Figure 1.2: Centralized control structure. The states and control inputs of each subsystem S_i are denoted by x_i and u_i , respectively. Dashed arrows indicate that the states (blue) of each subsystem are sent to a centralized controller that computes and transmits control inputs (red) back to each subsystem.

can compromise the operation of the overall networked system. Furthermore, large-scale systems often have sensors and actuators geographically separated and, owing to economic reasons or to delays in data transmission, centralized control can become an impracticable solution, such that decentralized control structures can be considered more attractive (Lunze 1992).

The main idea of decentralized control is dividing the large-scale system into independent or quasi-independent subsystems to design local controllers. In a decentralized control architecture, each subsystem in the network has a local controller whose action is computed based only on local information on the subsystem's internal variables, as depicted in Figure 1.3 (see surveys (Bakule 2008, 2014; Šiljak and Zečević 2005) and references therein).

As a result, a decentralized control structure can achieve higher reliability than a centralized one, since unlike in the centralized approach, if one decentralized controller fails, only one part rather than the whole control system fails. However, local controllers may not be effective to ensure a suitable level of performance of large-scale systems, or a proper set of local controllers that can stabilize the overall network might not even exist (Lunze 1992), mainly when the interconnections among subsystems are very strong and the local controllers are designed not taking this into consideration.

Distributed Control

In distributed control, the local controllers can make use of information on internal variables along with those of the subsystems in the neighborhood of the controlled subsystem to compute its control input, see Figure 1.4. In contrast to centralized and decentralized

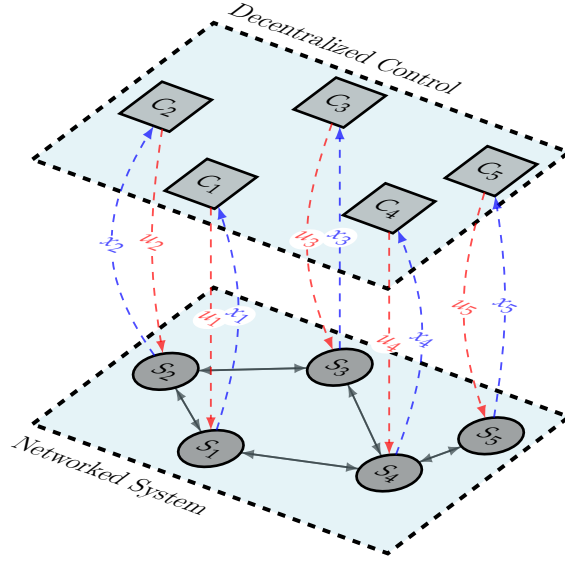


Figure 1.3: Decentralized control structure. Dashed arrows indicate that the states (blue) of each subsystem are sent to a local controller that computes and transmits control inputs (red) back each corresponding subsystem.

control architectures, the distributed control structure appears as an alternative aiming to provide greater reliability with respect to communication failures in the network in comparison to centralized controllers, while still being able to improve performance and stabilization capability (Lunze 1992; Zečević and Šiljak 2010). In addition, distributed control approaches have the potential to overcome some computational issues associated with the design of centralized strategies for high dimensional systems.

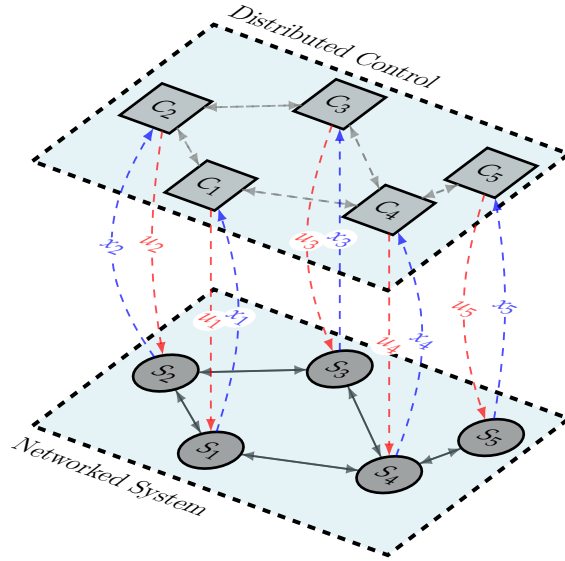


Figure 1.4: Distributed control structure. Dashed arrows (gray) between local controllers indicate that the states or control inputs of subsystems in the neighborhood are sent to a local controller to compute the control signal for its corresponding subsystem.

Distributed control has been applied mainly in cooperative and coordinated control of multi-agent systems (Bullo, Cortés, and Martínez 2009; Yu et al. 2016), and in this context, the subsystems are often considered equal. Furthermore, many papers have considered networked distributed control structures where subsystems are connected over an underlying communication network, and the analysis is focused on network induced problems. For instance, a distributed model predictive control strategy for nonlinear networked control systems with asynchronous communication is proposed in (Zhou et al. 2018). For linear subsystems and linear interconnections, Kazempour and Ghaisari 2013 developed networked distributed control systems subject to both random delay and packet loss induced by non-ideal communication links. Peng et al. 2015 presented a data-based framework for distributed actuator fault identification and accommodation in networked process control systems, and again each subsystem was modeled as a linear system.

1.2 Objectives

The main objective of this thesis is to design distributed control laws for a class of continuous-time large-scale nonlinear heterogeneous systems. This objective will be pursued by exploiting features of interconnection graphs and of distributed control architectures to improve flexibility and efficiency in the design of controllers for large-scale systems described by interconnected N-TS fuzzy models, i.e. TS fuzzy models with nonlinear consequents. Therefore, based on what was previously discussed, the following specific objectives are pursued:

1. To propose a new representation of large-scale system through interconnected N-TS fuzzy models (namely, TS fuzzy models with nonlinear consequents), aiming to avoid the *rule-explosion* problem that occurs in traditional TS fuzzy models;
2. To obtain sufficient conditions for distributed control design of networked systems based on quadratic block-diagonal Lyapunov functions and derived and expressed in terms of LMIs (Boyd et al. 1994), while both state and control input constraints are taken into account in the synthesis of controllers, and the maximizing the volume of the estimated DoA for the closed-loop system;
3. To obtain sufficient conditions for distributed control design of large-scale systems based on chordal decomposition and quadratic block-diagonal Lyapunov functions in order to get solutions to the case where the number of subsystems is large;
4. To propose a methodology able to be used in the synthesis for both distributed and decentralized controllers.

1.3 Outline and Contributions

The outline and main contributions of the thesis are:

- Chapter 2 provides an overview of the concepts, definitions, and results utilized throughout this thesis with regard to chordal graphs and TS and N-TS fuzzy models. This chapter also introduces how large-scale systems can be represented by interconnected N-TS fuzzy systems which is the first contribution of this thesis.
- Chapter 3 presents the main results obtained for the distributed stabilization of *networked nonlinear systems*¹, where quadratic stabilization conditions are obtained through distributed control structures. Besides, it presents and discusses the results of applying the developed approach in two types of systems. The results in this chapter have been published in (Araújo, Torres, and Palhares 2020).
- Chapter 4 demonstrates how the chordal decomposition can be used to exploit the sparsity properties of the graph associated with the large-scale system and, thus, it proposed an alternative to the results presented in Chapter 3 to the case when the number of subsystems is large. In addition, the analysis of computational complexity and running time of the proposed methods are provided.
- Chapter 5 points out conclusions and directions for the continuity of the research.

Publications

The results of this thesis have led to the following publications.

- Araújo, R. F., L. A. B. Torres, and R. M. Palhares (2020). “Distributed Control of Networked Nonlinear Systems via Interconnected Takagi-Sugeno Fuzzy Systems with Nonlinear consequent”. In: *IEEE Transactions on Systems, Man, and Cybernetics: Systems*, pp. 1-10. To appear.
- Araújo, R. F., L. A. B. Torres, and R. M. Palhares (2019). “Controle Descentralizado de Sistemas Interconectados por Não-Linearidades Setoriais Sujeitos a Saturação nos Atuadores”. In: *14º Simpósio Brasileiro de Automação Inteligente (SBAI)*, Ouro Preto, MG, Brasil.

In addition, other results for N-TS models have been obtained although they are not covered in this thesis.

¹In Chapter 3, we refer to large-scale system as a networked system because no decomposition technique is applied to large-scale systems.

- Coutinho, P. H. S., R. F. Araújo, A.-T. Nguyen, and R. M. Palhares (2020). “A Multiple-Parameterization Approach for Local Stabilization of Constrained Takagi-Sugeno Fuzzy Systems with Nonlinear Consequents”. In: *Information Sciences* 506, pp. 295-307.
- Araújo, R. F., Coutinho, P. H. S., A.-T. Nguyen, and R. M. Palhares (2019). ”Delayed Nonquadratic \mathcal{L}_2 -Stabilization of Continuous-Time Takagi-Sugeno Fuzzy Models with Nonlinear Consequents”. In: *Submitted to IEEE Transactions on Fuzzy Systems*.

2 Background

In this chapter, we present the fundamental concepts on graph theory and TS fuzzy models used in this thesis. Firstly we introduce the notion of chordal graphs, its main features, and roles in decomposition of sparse symmetric matrices. Next, we show how TS and N-TS fuzzy models can be used to describe nonlinear systems using different sets of fuzzy rules. Finally, as an initial contribution of this thesis, we introduce how large-scale systems can be represented by interconnected N-TS fuzzy systems.

2.1 Chordal Graph

Graph Theory provides a natural and powerful framework for studying relationships among interconnected systems in a network. A graph $\mathcal{G}(\mathcal{V}, \mathcal{E})$ is composed by a set of vertices $\mathcal{V} = \{1, 2, \dots, n\}$ and a set of edges $\mathcal{E} = \{(i, j) \mid i, j \in \mathcal{V}\}$. A graph is called *complete* if any two vertices are connected by an edge.

A path in \mathcal{G} is a sequence of edges that connect a sequence of distinct vertices. A graph is called *connected* if there is a path between every pair of vertices. A *clique* is a subset of vertices $\mathcal{C} \subseteq \mathcal{V}$ that induces a complete subgraph $\mathcal{G}_{\mathcal{C}}(\mathcal{C}, \mathcal{E}_{\mathcal{C}})$, i.e., $(i, j) \in \mathcal{E}$ for any distinct vertices $i, j \in \mathcal{C}$. If \mathcal{C} is not a subset of any other clique, then it is called a *maximal clique*. The number of vertices in \mathcal{C} is denoted by $|\mathcal{C}|$. A *cycle* of length k in a graph \mathcal{G} is a set of pairwise distinct vertices $\{1, 2, \dots, k\} \subseteq \mathcal{V}$ such that $(k, 1) \in \mathcal{E}$ and $(i, i+1) \in \mathcal{E}$ for $i = \{1, 2, \dots, k-1\}$.

A *chord* is an edge between nonconsecutive vertices on the path. In a cycle, a chord is an edge connecting two non-adjacent vertices. Throughout this thesis, we are interested in a particular class of chordal graphs, called *undirected* graphs, in which two connected vertices interact mutually, i.e. $(i, j) \in \mathcal{E} \Leftrightarrow (j, i) \in \mathcal{E}$. Next, the definition of chordal graph is given.

Definition 2.1: Chordal graph

An undirected graph \mathcal{G} is called *chordal* if every cycle of length greater than three has at least one chord.

Nonchordal graphs can always be extended to a chordal graph by adding additional edges to the original one. A chordal extension can be efficiently generated from heuristics, such as the minimum degree ordering followed by a symbolic Cholesky factorization (Vandenberghe and Andersen 2015).

Definition 2.2: Chordal extension

A *chordal extension* of a graph $\mathcal{G}(\mathcal{V}, \mathcal{E})$ is a chordal graph $\hat{\mathcal{G}}(\mathcal{V}, \hat{\mathcal{E}})$, where $\mathcal{E} \subseteq \hat{\mathcal{E}}$.

Given an undirected graph \mathcal{G} , its corresponding Adjacency matrix $A_{\mathcal{G}} = [\alpha_{ij}] \in \mathbb{R}^{n \times n}$ is such that $\alpha_{ij} = 1$, if $(i, j) \in \mathcal{E}$, indicating a connection/edge between vertices i and j , and $\alpha_{ij} = 0$, otherwise. Since the graph is undirected, the Adjacency matrix is symmetric, i.e. $A_{\mathcal{G}} \in \mathbb{S}^n$. In addition, the neighborhood of the i -th vertex is defined by the set of vertices $\mathcal{N}_i = \{j \in \mathcal{V} \mid \alpha_{ij} \neq 0\}$. The Degree matrix of a graph, $D_{\mathcal{G}} = [d_{ij}] \in \mathbb{R}^{n \times n}$, is a diagonal matrix that contains information on the number of edges attached to each vertex, such that $d_{ii} = \sum_{j=1}^n \alpha_{ij}$, $\forall i \in \mathcal{V}$; and $d_{ij} = 0$, if $i \neq j$. From the Adjacency and Degree matrices one can compute the Laplacian matrix $L_{\mathcal{G}} = [\ell_{ij}] \in \mathbb{R}^{n \times n}$ of a graph: $L_{\mathcal{G}} \triangleq D_{\mathcal{G}} - A_{\mathcal{G}}$. Since both the degree and the Adjacency matrices are symmetric, the Laplacian is also a symmetric matrix and it satisfies the following properties (Godsil and Royle 2001):

Property 2.1: Laplacian matrix of an undirected graph

$$L_{\mathcal{G}} \mathbf{1}_N = \mathbf{0}_N, \quad \sum_{j=1}^N \ell_{ij} = 0, \forall i \in \mathcal{V}.$$

Example 2.1. Consider the two undirected graphs illustrated in Figure 2.1. The graph in Fig. 2.1(a) is chordal, because has a cycle of length 4 with one chord, i.e. edge $(1, 3)$. The following vertices sets define its cliques: $\{1, 2\}$, $\{1, 3\}$, $\{1, 4\}$, $\{2, 3\}$, $\{3, 4\}$, $\{1, 2, 3\}$ and $\{1, 3, 4\}$. Further, its maximal cliques are only $\mathcal{C}_1 = \{1, 2, 3\}$ and $\mathcal{C}_2 = \{1, 3, 4\}$, which are not subsets of any other clique.

On the other hand, the graph in Fig. 2.1(b) is nonchordal. However, a chordal extension can be obtained through the addition of a chord, e.g. adding the edge $(1, 3)$ or the edge $(2, 4)$. Note that, the chordal extension is not unique and can be performed in different ways.

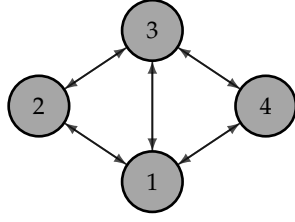
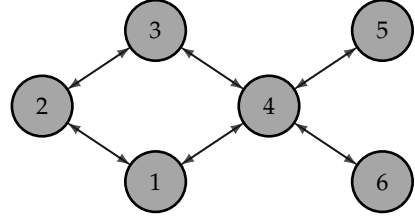
(a) Graph \mathcal{G}_a - chordal graph.(b) Graph \mathcal{G}_b - nonchordal graph.

Figure 2.1: Examples of undirected graphs.

The Laplacian matrices of the above graphs satisfy Property 2.1 and are defined as follows:

$$L_{\mathcal{G}_a} = \begin{bmatrix} 3 & -1 & -1 & -1 \\ -1 & 2 & -1 & 0 \\ -1 & -1 & 3 & -1 \\ -1 & 0 & -1 & 2 \end{bmatrix}, \quad L_{\mathcal{G}_b} = \begin{bmatrix} 2 & -1 & 0 & -1 & 0 & 0 \\ -1 & 2 & -1 & 0 & 0 & 0 \\ 0 & -1 & 2 & -1 & 0 & 0 \\ -1 & 0 & -1 & 4 & -1 & -1 \\ 0 & 0 & 0 & -1 & 1 & 0 \\ 0 & 0 & 0 & -1 & 0 & 1 \end{bmatrix}.$$

Perfect Elimination Ordering

A vertex of an undirected graph is called *simplicial* if the subgraph induced by its neighborhood \mathcal{N}_i is complete, i.e. all its neighbors are connected to each other. An ordering (or equivalently a numbering of the vertices) $\sigma = \langle 1, \dots, n \rangle$ of an undirected graph \mathcal{G} is a *perfect elimination ordering* if each i th vertex, for $i = \{1, 2, \dots, n\}$, is a simplicial vertex in the subgraph induced by the vertices $\{i, i+1, \dots, n\}$. Theorem 2.1 is used to check the chordality of a graph and is equivalent to Definition 2.1.

Theorem 2.1: Theorem 4.1 in (Vandenberghe and Andersen 2015)

A graph $\mathcal{G}(\mathcal{V}, \mathcal{E})$ is chordal if and only if \mathcal{G} has a perfect elimination ordering.

2.1.1 Maximal Cliques and Clique Trees

Given a perfect elimination ordering, the maximal cliques of a chordal graph can be identified in linear time (Blair and Peyton 1993). Let \mathcal{G} be a connected chordal graph with a set of maximal cliques $\mathcal{V}_{\mathcal{T}} = \{\mathcal{C}_1, \mathcal{C}_2, \dots, \mathcal{C}_t\}$. These maximal cliques can be arranged in a clique tree $\mathcal{T} = (\mathcal{V}_{\mathcal{T}}, \mathcal{E}_{\mathcal{T}})$ with $\mathcal{E}_{\mathcal{T}} \subseteq \mathcal{V}_{\mathcal{T}} \times \mathcal{V}_{\mathcal{T}}$, which satisfies the *clique-intersection property*, i.e. $\mathcal{C}_i \cap \mathcal{C}_j \subseteq \mathcal{C}_k$ if clique \mathcal{C}_k lies on the path between cliques \mathcal{C}_i and \mathcal{C}_j in the tree (Blair and Peyton 1993).

A related notion is the so-called *running intersection property*, an ordering of the maximal cliques $\mathcal{C}_1, \dots, \mathcal{C}_t$ satisfies the running intersection property if for every $k \in \mathcal{I}_{t-1}$,

one has that

$$\left(\mathcal{C}_{k+1} \cap \bigcup_{j=1}^k \mathcal{C}_j \right) \subseteq \mathcal{C}_s, \text{ for some } s \leq k. \quad (2.1)$$

The Theorems 2.2 and 2.3 are obtained from the discussed properties above and, similar to Theorem 2.1, they are also equivalent to Definition 2.1.

Theorem 2.2: Theorem 3.2 in (Blair and Peyton 1993)

A connected graph $\mathcal{G}(\mathcal{V}, \mathcal{E})$ is chordal if and only if there exists a clique tree that satisfies the clique-intersection property.

Theorem 2.3: Theorem 3.4 in (Blair and Peyton 1993)

A connected graph $\mathcal{G}(\mathcal{V}, \mathcal{E})$ is chordal if and only if there exists an ordering of its maximal cliques that satisfies the running-intersection property.

Example 2.2. To illustrate these concepts, consider a chordal extension of undirected graph shown in Figure 2.1(b). The chordal extension can be obtained by adding one edge to cycle $\{1, 2, 3, 4\}$, e.g. the undirected edge $(1, 3)$.

Therefore, the maximal cliques of the graph are $\mathcal{C}_1 = \{1, 2, 3\}$, $\mathcal{C}_2 = \{1, 3, 4\}$, $\mathcal{C}_3 = \{4, 5\}$ and $\mathcal{C}_4 = \{4, 6\}$. Notice that, the clique tree shown in Figure 2.2 satisfies the clique-intersection property. Consider maximal cliques \mathcal{C}_1 and \mathcal{C}_4 , one has $\mathcal{C}_1 \cap \mathcal{C}_4 = \emptyset \subseteq \mathcal{C}_2$. Further, one can verify that the ordering $\mathcal{C}_1, \mathcal{C}_2, \mathcal{C}_3, \mathcal{C}_4$ satisfies also the running-intersection property (2.1).

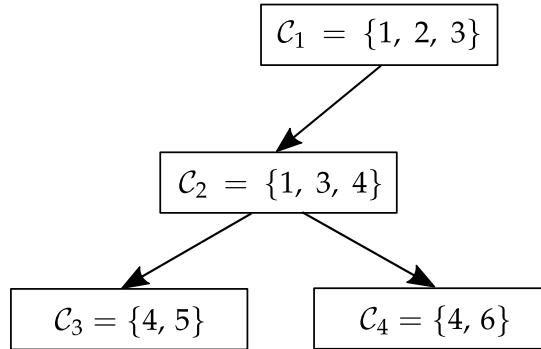


Figure 2.2: Clique tree associated to chordal extension of undirected graph shown in Figure 2.1(b).

2.1.2 Sparse Symmetric Matrices and Chordal Decomposition

In this subsection, we present the applications of chordal graphs to sparse positive semidefinite matrices. The notation used in the following text is the same one proposed in (Zheng, Mason, and Papachristodoulou 2018).

Given an undirected graph $\mathcal{G}(\mathcal{V}, \mathcal{E})$, a matrix $X = [x_{ij}] \in \mathbb{S}^n$ has a sparsity pattern \mathcal{E} if $x_{ij} = x_{ji} = 0$, whenever $i \neq j$ and $(i, j) \notin \mathcal{E}$. Basically, the sparsity pattern of a graph is incorporated into its Adjacency and Laplacian matrices, as we can see in Example 2.1. Thus, the space of symmetric matrices with sparsity pattern \mathcal{E} is defined as

$$\mathbb{S}^n(\mathcal{E}, 0) = \{X \in \mathbb{S}^n \mid x_{ij} = x_{ji} = 0, \text{ if } i \neq j \text{ and } (i, j) \notin \mathcal{E}\}.$$

In addition, if $X \in \mathbb{S}^n(\mathcal{E}, 0)$ and $\mathcal{E} \subset \hat{\mathcal{E}}$, then X also has sparsity pattern $\hat{\mathcal{E}}$, i.e. $X \in \mathbb{S}^n(\hat{\mathcal{E}}, 0)$. Notice that, if $\hat{\mathcal{G}}(\mathcal{V}, \hat{\mathcal{E}})$ is chordal, this denotes the chordal extension given in Definition 2.2. Further, we define the set of positive semidefinite matrices with sparsity pattern \mathcal{E} as

$$\mathbb{S}_+^n(\mathcal{E}, 0) = \{X \in \mathbb{S}^n(\mathcal{E}, 0) \mid X \succeq 0\}.$$

For instance, given a graph $\mathcal{G}(\mathcal{V}, \mathcal{E})$, its Laplacian matrix is $L_{\mathcal{G}} \in \mathbb{S}_+^n(\mathcal{E}, 0)$. Given a clique \mathcal{C}_k of a graph $\mathcal{G}(\mathcal{V}, \mathcal{E})$ with maximal cliques $\{\mathcal{C}_1, \dots, \mathcal{C}_t\}$, the principle submatrices of a sparsity pattern \mathcal{E} are defined matrices $E_{\mathcal{C}_k} \in \mathbb{R}^{|\mathcal{C}_k| \times n}$, $\forall k \in \mathcal{I}_t$ with entries

$$(E_{\mathcal{C}_k})_{ij} = \begin{cases} 1, & \text{if } \mathcal{C}_k(i) = j, \\ 0, & \text{otherwise,} \end{cases}$$

where $\mathcal{C}_k(i)$ is the i -th vertex in \mathcal{C}_k , whose vertices are sorted in the natural ordering. These submatrices will then be used in the chordal decomposition theorem.

Theorem 2.4: Chordal decomposition theorem (Agler et al. 1988; Kakimura 2010)

Let $\mathcal{G}(\mathcal{V}, \mathcal{E})$ be a chordal graph with maximal cliques $\{\mathcal{C}_1, \mathcal{C}_2, \dots, \mathcal{C}_t\}$. Then, $X \in \mathbb{S}_+^n(\mathcal{E}, 0)$ if and only if there exist matrices $X_k \in \mathbb{S}_+^{|\mathcal{C}_k|}$ for $k \in \mathcal{I}_t$ such that

$$X = \sum_{k=1}^t E_{\mathcal{C}_k}^\top X_k E_{\mathcal{C}_k}.$$

Example 2.3. As an illustration of the decomposition discussed above, consider the graph in Figure 1.1. Although the graph is nonchordal, a chordal extension $\hat{\mathcal{G}}$ can be performed by adding the undirected edge $(1, 3)$. Consider the Laplacian matrix of the nonchordal

graph shown in Figure 1.1:

$$L_{\mathcal{G}} = \begin{bmatrix} 2 & -1 & 0 & -1 & 0 \\ -1 & 2 & -1 & 0 & 0 \\ 0 & -1 & 2 & -1 & 0 \\ -1 & 0 & -1 & 3 & -1 \\ 0 & 0 & 0 & -1 & 1 \end{bmatrix} \succeq 0. \quad (2.2)$$

The corresponding maximal cliques of the extended graph $\hat{\mathcal{G}}(\mathcal{V}, \hat{\mathcal{E}})$ are $\mathcal{C}_1 = \{1, 2, 3\}$, $\mathcal{C}_2 = \{1, 3, 4\}$, $\mathcal{C}_3 = \{4, 5\}$. In this case, since the Laplacian matrix of $\hat{\mathcal{G}}(\mathcal{V}, \hat{\mathcal{E}})$ has the same sparsity pattern of the Laplacian matrix associated with $\mathcal{G}(\mathcal{V}, \mathcal{E})$, from Theorem 2.4, matrix (2.2) can also be decomposed in the same way as follows:

$$L_{\mathcal{G}} = E_{\mathcal{C}_1}^\top \underbrace{\begin{bmatrix} a_1 & -1 & 0 \\ -1 & 2 & -1 \\ 0 & -1 & a_3 \end{bmatrix}}_{\succeq 0} E_{\mathcal{C}_1} + E_{\mathcal{C}_2}^\top \underbrace{\begin{bmatrix} a_2 & 0 & -1 \\ 0 & a_4 & -1 \\ -1 & -1 & a_5 \end{bmatrix}}_{\succeq 0} E_{\mathcal{C}_2} + E_{\mathcal{C}_3}^\top \underbrace{\begin{bmatrix} a_6 & -1 \\ -1 & 1 \end{bmatrix}}_{\succeq 0} E_{\mathcal{C}_3},$$

with $a_1 + a_2 = 2$, $a_3 + a_4 = 2$ and $a_5 + a_6 = 3$. The principle submatrices related to the maximal cliques of the extended graph are:

$$\begin{aligned} \mathcal{C}_1 = \{1, 2, 3\} &\Rightarrow E_{\mathcal{C}_1} = \begin{bmatrix} 1 & 0 & 0 & 0 & 0 \\ 0 & 1 & 0 & 0 & 0 \\ 0 & 0 & 1 & 0 & 0 \end{bmatrix}, \\ \mathcal{C}_2 = \{1, 3, 4\} &\Rightarrow E_{\mathcal{C}_2} = \begin{bmatrix} 1 & 0 & 0 & 0 & 0 \\ 0 & 0 & 1 & 0 & 0 \\ 0 & 0 & 0 & 1 & 0 \end{bmatrix}, \\ \mathcal{C}_3 = \{4, 5\} &\Rightarrow E_{\mathcal{C}_3} = \begin{bmatrix} 0 & 0 & 0 & 1 & 0 \\ 0 & 0 & 0 & 0 & 1 \end{bmatrix}. \end{aligned}$$

Remark 2.1

Theorem 2.4 plays an important role in the context of sparse semidefinite problems since that if a LMI constraint has a chordal sparsity pattern, then it can be equivalently replaced by a set of smaller LMIs and a set of equality constraints, the Example 2.3 illustrates the chordal decomposition. Therefore, according to (Fukuda et al. 2001; Nakata et al. 2003), using this theorem brings substantial computational enhancement to solving large sparse semidefinite problems, mainly if the number of vertices in maximal cliques is small.

2.2 Takagi-Sugeno Fuzzy Models

TS fuzzy models (Takagi and Sugeno 1985) have become one of the most popular modelling frameworks used to represent nonlinear systems, since they can approximate any smooth nonlinear function with an arbitrary precision from fuzzy rules with linear consequents. The main feature of this modelling approach is its capability to represent nonlinear systems by a convex combination of local linear dynamics and, as a consequence, it facilitates the employment of Lyapunov stability theory based analysis and design techniques (Nguyen et al. 2019; Tanaka and Wang 2001).

Consider a continuous-time and input affine nonlinear system given by:

$$\dot{\mathbf{x}}(t) = f(\mathbf{x}(t)) + g(\mathbf{x}(t))\mathbf{u}(t), \quad (2.3)$$

where $\mathbf{x}(t) \in \mathbb{R}^{n_x}$ is the state vector; $\mathbf{u}(t) \in \mathbb{R}^{n_u}$ is the control input vector; and $f(\cdot) \in \mathbb{R}^{n_x}$ and $g(\cdot) \in \mathbb{R}^{n_x \times n_u}$ are smooth nonlinear function matrices.

A continuous-time TS fuzzy model which represents the nonlinear system (2.3) can be expressed by the following fuzzy rules (Nguyen et al. 2019; Rhee and Won 2006):

$$\begin{aligned} \text{Rule } i : \text{ IF } z_1(t) \in \mathcal{M}_1^{\alpha_{i1}} \text{ and } \cdots \text{ and } z_p(t) \in \mathcal{M}_p^{\alpha_{ip}}, \\ \text{ THEN } \dot{\mathbf{x}}(t) = A_i \mathbf{x}(t) + B_i \mathbf{u}(t), \end{aligned} \quad (2.4)$$

where $i \in \mathcal{I}_r$, with r the number of fuzzy rules; $\mathbf{z}(t) \in \mathbb{R}^p$ is the premise variables vector ($z_j(t)$ is the j -th element of vector $\mathbf{z}(t)$); $A_i \in \mathbb{R}^{n_x \times n_x}$ and $B_i \in \mathbb{R}^{n_x \times n_u}$ are matrices describing the local linear dynamics of the system; $\mathcal{M}_j^{\alpha_{ij}}$ is the fuzzy set related to the premise variable $z_j(t)$; α_{ij} is an index that relates each fuzzy set of the premise variable $z_j(t)$ with rule i , e.g. an index $\alpha_{32} = 1$ indicates that the first fuzzy set of the premise variable $z_2(t)$ is used on the third rule; and $1 \leq \alpha_{ij} \leq r_j$ with r_j the number of fuzzy sets related to the premise variable $z_j(t)$.

The grade of membership $0 \leq \omega_j^{\alpha_{ij}}(z_j(t)) \leq 1$ associated with premise variable $z_j(t)$ and fuzzy set $\mathcal{M}_j^{\alpha_{ij}}$ such that a corresponding normalized grade of membership can be obtained as

$$\mu_j^{\alpha_{ij}}(z_j(t)) = \frac{\omega_j^{\alpha_{ij}}(z_j(t))}{\sum_{\alpha_{ij}=1}^{r_j} \omega_j^{\alpha_{ij}}(z_j(t))}.$$

These normalized grade of membership satisfy the convex sum properties:

$$\mu_j^{\alpha_{ij}}(z_j(t)) \geq 0, \quad \sum_{\alpha_{ij}=1}^{r_j} \mu_j^{\alpha_{ij}}(z_j(t)) = 1.$$

In addition, these properties are inherited by the inferred TS membership functions $\varsigma(\mathbf{z}(t))$ given by Definition 2.3. Thus, $\varsigma_i(\mathbf{z}(t))$ satisfies Property 2.2.

Definition 2.3: Inferred TS membership functions

$$\varsigma_i(\mathbf{z}(t)) = \prod_{j=1}^p \mu_j^{\alpha_{ij}}(z_j(t)), \quad (2.5)$$

Property 2.2: Convex sum property

$$\varsigma_i(\mathbf{z}(t)) \geq 0, \quad \sum_{i=1}^r \varsigma_i(\mathbf{z}(t)) = 1.$$

where $r = \prod_{j=1}^p r_j$ is the TS model's total rule number.

The set of rules (2.4) and membership functions (2.5) yield the following inferred TS fuzzy model:

$$\dot{\mathbf{x}}(t) = \sum_{i=1}^r \varsigma_i(\mathbf{z}(t)) (A_i \mathbf{x}(t) + B_i \mathbf{u}(t)). \quad (2.6)$$

Different methods can be used to obtain a TS fuzzy model from nonlinear system equations. The most common approaches in the literature are the fuzzy local approximation and sector nonlinearity approach (Tanaka and Wang 2001). Example 2.4 illustrates how to build a TS fuzzy model using the sector nonlinearity approach, which is the technique used throughout this thesis.

Example 2.4. Consider the following nonlinear system (Tanaka and Wang 2001, Chapter 2):

$$\begin{aligned} \dot{x}_1 &= -x_1 + x_1 x_2^3 \\ \dot{x}_2 &= -x_2 + (3 + x_2) x_1^3. \end{aligned} \quad (2.7)$$

We need to find a representation such that $\dot{\mathbf{x}} = \mathbf{g}(\mathbf{x})\mathbf{x}$, however, notice that this choice is not unique. Defining as premise variables, $z_1 = x_1 x_2^2$ and $z_2 = (3 + x_2) x_1^2$, one has that

$$\dot{\mathbf{x}} = \begin{bmatrix} -1 & z_1 \\ z_2 & -1 \end{bmatrix} \mathbf{x}.$$

Assuming that $x_1 \in [-1, 1]$ and $x_2 \in [-1, 1]$, the premise variables' bounds are given by

$$\begin{aligned} \max z_1 &= 1, & \max z_2 &= 4, \\ \min z_1 &= -1, & \min z_2 &= 0. \end{aligned}$$

From the maximum and minimum values, z_1 and z_2 can be represented by

$$\begin{aligned} z_1 &= \mu_1^1(z_1) \cdot 1 + \mu_1^2(z_1) \cdot (-1), \\ z_2 &= \mu_2^1(z_2) \cdot 4 + \mu_2^2(z_2) \cdot 0, \end{aligned}$$

with

$$\begin{aligned} \mu_1^1(z_1) + \mu_1^2(z_1) &= 1, \\ \mu_2^1(z_2) + \mu_2^2(z_2) &= 1. \end{aligned}$$

Therefore the membership functions can be calculated as

$$\begin{aligned} \mu_1^1(z_1) &= \frac{z_1 + 1}{2}, & \mu_1^2(z_1) &= \frac{1 - z_1}{2}, \\ \mu_2^1(z_2) &= \frac{z_2}{4}, & \mu_2^2(z_2) &= \frac{4 - z_2}{4}. \end{aligned}$$

In this case the nonlinear system (2.7) is represented by the following TS fuzzy model:

$$\begin{aligned} \textbf{Rule } i : \textbf{ IF } z_1(t) \in \mathcal{M}_1^{\alpha_{i1}} \textbf{ and } z_2(t) \in \mathcal{M}_2^{\alpha_{i2}}, \\ \textbf{ THEN } \dot{\mathbf{x}} = A_i \mathbf{x}, \end{aligned}$$

and the inferred TS membership functions $h_i(\mathbf{z})$ are constructed as follows

$$\begin{aligned} \alpha_{11} = 1, \alpha_{12} = 1, & \quad \varsigma_1(\mathbf{z}) = \mu_1^1(z_1)\mu_2^1(z_2), \\ \alpha_{21} = 1, \alpha_{22} = 2, & \quad \varsigma_2(\mathbf{z}) = \mu_1^1(z_1)\mu_2^2(z_2), \\ \alpha_{31} = 2, \alpha_{32} = 1, & \quad \varsigma_3(\mathbf{z}) = \mu_1^2(z_1)\mu_2^1(z_2), \\ \alpha_{41} = 2, \alpha_{42} = 2, & \quad \varsigma_4(\mathbf{z}) = \mu_1^2(z_1)\mu_2^2(z_2). \end{aligned}$$

Finally, the inferred fuzzy model is described by

$$\dot{\mathbf{x}} = \sum_{i=1}^4 \varsigma_i(\mathbf{z}) A_i \mathbf{x},$$

with

$$A_1 = \begin{bmatrix} -1 & 1 \\ 4 & -1 \end{bmatrix}, \quad A_2 = \begin{bmatrix} -1 & 1 \\ 0 & -1 \end{bmatrix}, \quad A_3 = \begin{bmatrix} -1 & -1 \\ 4 & -1 \end{bmatrix}, \quad A_4 = \begin{bmatrix} -1 & -1 \\ 0 & -1 \end{bmatrix}.$$

Remark 2.2

As mentioned before, different choices of premise variables can be made in order to represent $g(\mathbf{x})$. In Example 2.4, considering the defined premise variables, z_1 and z_2 , the required number of fuzzy rules (r) to described the TS fuzzy model is $r = 2^2$. However, if one decides to define three premise variables, e.g., $z_1 = -1 + x_2^3$, $z_2 = 3x_1^2$ and $z_3 = -1 + x_1^3$, then $r = 2^3$ fuzzy rules are necessary to describe the same nonlinear system. Notice that the number of rules grows exponentially with the number of sector nonlinearities used to construct the fuzzy model.

In addition, the TS fuzzy model obtained via sector nonlinearity approach can exactly represent the nonlinear system in a *local region* of the state space, i.e. within the compact set defined by the limits considered for the state variables such that the convex sum property holds.

Fuzzy Summations

In general, the analysis and synthesis conditions for TS systems are expressed as matrix inequalities and in terms of membership functions. In particular, the synthesis conditions are commonly written as the following double fuzzy summation:

$$\sum_{i=1}^r \sum_{j=1}^r \varsigma_i \varsigma_j Y_{ij} \succ 0. \quad (2.8)$$

The inequality (2.8) is nonlinear and has infinite dimension. Thus, several sufficient conditions based on a finite set of LMIs have been proposed in the literature to guarantee that (2.8) is valid. Next, two of these conditions used throughout this thesis will be presented.

Lemma 2.1: Double fuzzy summation (Tanaka and Wang 2001)

A sufficient condition for expression (2.8) to be valid, with $i, j \in \mathcal{I}_r$, is

$$\begin{aligned} Y_{ii} &\succ 0, \\ Y_{ij} + Y_{ji} &\succ 0, \quad j \succ i. \end{aligned}$$

Proof. Note that

$$\sum_{i=1}^r \sum_{j=1}^r \varsigma_i \varsigma_j Y_{ij} = \sum_{i=1}^r \varsigma_i^2 Y_{ii} + \sum_{i=1}^{r-1} \sum_{j=i+1}^r \varsigma_i \varsigma_j (Y_{ij} + Y_{ji})$$

Therefore the conditions on the lemma are sufficient for expression (2.8). \square

When multiple fuzzy summations are obtained instead of a double summation (2.8), the following Lemma ensures its positiveness.

Lemma 2.2: Multiple fuzzy summation (Sala and Ariño 2007)

A sufficient condition for

$$\sum_{i_1=1}^r \cdots \sum_{i_p=1}^r \left(\prod_{\ell=1}^p \zeta_{i_\ell} \right) Y_{(i_1, \dots, i_p)} \succ 0,$$

is that, for every combination of (i_1, i_2, \dots, i_p) with $i_\ell \in \mathcal{I}_r$, the sum of its permutations is positive definite.

2.2.1 Takagi-Sugeno Fuzzy Models with Nonlinear Consequents

When the TS fuzzy model previously described is used to represent a complex dynamical system, the so-called problem of rules explosion occurs due to a large number of nonlinearities. Stability analysis and control synthesis for such T-S fuzzy models often are very challenging, since the large number of fuzzy rules leads to high computational complexity as well. The fuzzy local approximation method is employed to obtain a TS fuzzy model with fewer fuzzy rules to overcome this drawback. However, the designed control laws based on the fuzzy model may not guarantee the stability of the original nonlinear system (Tanaka and Wang 2001).

In this context, N-TS models, i.e. TS fuzzy models with nonlinear consequent, have been employed to avoid using an excessive number of fuzzy rules while increasing the model accuracy. Two approaches have emerged: the first one consists of using TS fuzzy models with polynomial consequent (Sala 2009; Sala and Ariño 2009; Tanaka et al. 2009), and the other one is the method introduced in (Dong, Wang, and Yang 2009; Dong, Wang, and Yang 2011) in which sector-bounded functions are added to the traditional TS fuzzy models, with linear local models, resulting in nonlinear consequent. More discussion on the latter approach is given in the sequel since this is the method used throughout this work.

Assuming that the nonlinear function $f(\mathbf{x}(t))$ in (2.3) can be rewritten as follows:

$$f(\mathbf{x}(t)) = f_a(\mathbf{x}(t)) + f_b(\mathbf{x}(t))\bar{\boldsymbol{\phi}}(\mathbf{x}(t)), \quad (2.9)$$

in which $\bar{\boldsymbol{\phi}}(\mathbf{x}(t)) = [\bar{\phi}_1(\mathbf{x}(t)) \ \bar{\phi}_2(\mathbf{x}(t)) \ \cdots \ \bar{\phi}_{n_\phi}(\mathbf{x}(t))]^\top$, $\bar{\phi}_i(\mathbf{x}(t)) \in \mathbb{R}$, $\forall i \in \mathcal{I}_{n_\phi}$, are sector-bounded nonlinear functions, i.e. each one satisfies Property 2.3.

Property 2.3: Sector-bounded nonlinearity

A sector-bounded nonlinearity $\bar{\phi}_i(\mathbf{x}(t)) \in \mathbb{R}$ is such that

$$\bar{\phi}_i(\mathbf{x}(t)) \in \text{co}\{\Omega_{L(i)}\mathbf{x}(t), \Omega_{U(i)}\mathbf{x}(t)\}$$

with $\Omega_{L(i)}, \Omega_{U(i)} \in \mathbb{R}^{1 \times n_x}$. Therefore, $\bar{\phi}_i(\mathbf{x}(t))$ satisfies the inequality

$$\left(\bar{\phi}_i(\mathbf{x}(t)) - \Omega_{L(i)}\mathbf{x}(t)\right) \left(\bar{\phi}_i(\mathbf{x}(t)) - \Omega_{U(i)}\mathbf{x}(t)\right) \leq 0. \quad (2.10)$$

In order to maintain a convex condition, some transformations in the nonlinear term $\bar{\phi}_i(\mathbf{x}(t))$ will be performed. Let $\phi_i(\mathbf{x}(t)) = \bar{\phi}_i(\mathbf{x}(t)) - \Omega_{L(i)}\mathbf{x}(t)$, and substituting $\bar{\phi}_i(\mathbf{x}(t))$ in (2.10), one has that

$$\phi_i(\mathbf{x}(t)) \left(\phi_i(\mathbf{x}(t)) - \Omega_{(i)}\mathbf{x}(t)\right) \leq 0, \quad (2.11)$$

where $\Omega_{(i)} = \Omega_{U(i)} - \Omega_{L(i)}$. Substituting $\bar{\phi}_i(\mathbf{x}(t))$ in (2.9) yields

$$f(\mathbf{x}(t)) = f_a(\mathbf{x}(t)) + f_b(\mathbf{x}(t))\Omega_L\mathbf{x}(t) + f_b(\mathbf{x}(t))\boldsymbol{\phi}(\mathbf{x}(t)),$$

where $\Omega_L = \begin{bmatrix} \Omega_{L(1)}^\top & \Omega_{L(2)}^\top & \cdots & \Omega_{L(n_\phi)}^\top \end{bmatrix}^\top$, and $\boldsymbol{\phi}(\mathbf{x}(t)) = \begin{bmatrix} \phi_1(\mathbf{x}(t)) & \cdots & \phi_{n_\phi}(\mathbf{x}(t)) \end{bmatrix}^\top$. Thus, the nonlinear system (2.9) can be written as follows:

$$\dot{\mathbf{x}}(t) = \bar{f}_a(\mathbf{x}(t)) + g(\mathbf{x}(t))\mathbf{u}(t) + f_b(\mathbf{x}(t))\boldsymbol{\phi}(\mathbf{x}(t)),$$

with $\bar{f}_a(\mathbf{x}(t)) = f_a(\mathbf{x}(t)) + f_b(\mathbf{x}(t))\Omega_L\mathbf{x}(t)$.

As shown previously, the nonlinear functions $\bar{f}_a(\cdot)$, $f_b(\cdot)$ and $g(\cdot)$ can be described by fuzzy techniques (Tanaka and Wang 2001). Consequently, the nonlinear system (2.3) can be expressed by the following N-TS fuzzy model:

$$\begin{aligned} \textbf{Rule } i : & \textbf{IF } z_1(t) \in \mathcal{M}_1^{\alpha_{i1}} \text{ and } \cdots \text{ and } z_p(t) \in \mathcal{M}_p^{\alpha_{ip}}, \\ & \textbf{THEN } \dot{\mathbf{x}}(t) = A_i\mathbf{x}(t) + B_i\mathbf{u}(t) + G_i\boldsymbol{\phi}(\mathbf{x}(t)), \end{aligned} \quad (2.12)$$

where $i \in \mathcal{I}_r$, with r the number of fuzzy rules; $\mathbf{x}(t) \in \mathbb{R}^{n_x}$ is the state vector; $\mathbf{u}(t) \in \mathbb{R}^{n_u}$ is the control input vector; $\boldsymbol{\phi}(\mathbf{x}(t)) \in \mathbb{R}^{n_\phi}$ is the nonlinearities vector; $\mathbf{z}(t) \in \mathbb{R}^p$ is the premise variables vector ($z_j(t)$ is the j -th element of vector $\mathbf{z}(t)$); $A_i \in \mathbb{R}^{n_x \times n_x}$, $B_i \in \mathbb{R}^{n_x \times n_u}$ and $G_i \in \mathbb{R}^{n_x \times n_\phi}$ are constant matrices describing the local dynamics of the system; $\mathcal{M}_j^{\alpha_{ij}}$ is the fuzzy set related to the premise variable $z_j(t)$.

The rule set (2.12) and membership functions (2.5) yield the following inferred N-TS fuzzy model:

$$\dot{\mathbf{x}}(t) = \sum_{i=1}^r \varsigma_i(\mathbf{z}(t)) (A_i\mathbf{x}(t) + B_i\mathbf{u}(t) + G_i\boldsymbol{\phi}(t)). \quad (2.13)$$

One of the advantages of the N-TS fuzzy models is to generate less rules compared to traditional TS fuzzy systems, since it incorporates the nonlinearity $\varphi(x)$. Aiming to obtain a smaller number of rules, an approximate representation of the nonlinearities is usually used to create the TS fuzzy system, which can lead to serious performance problems or in extreme cases, closed-loop instability.

Thus, the N-TS fuzzy model allows a better convex representation, where some system nonlinearities are exactly transformed into a convex sum, and the others are nonlinearities belonging to the sector satisfying Property 2.3.

Example 2.5. To highlight the advantage of using N-TS fuzzy models, we consider two-inverted pendulums connected via a linear spring, which are depicted in Figure 2.3.

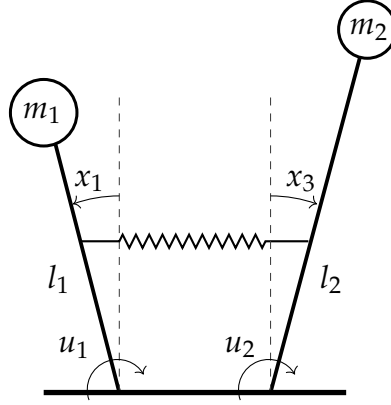


Figure 2.3: Two-inverted pendulums connected via linear springs.

The system dynamics can be described by the following continuous-time state-space representation:

$$\begin{aligned}
 \dot{x}_1 &= x_2, \\
 \dot{x}_2 &= \frac{g}{l_1} \sin x_1 + \frac{1}{m_1 l_1^2} u_1 + \frac{k a^2}{m_1 l_1^2} (\sin x_3 \cos x_3 - \sin x_1 \cos x_1), \\
 \dot{x}_3 &= x_4, \\
 \dot{x}_4 &= \frac{g}{l_2} \sin x_3 + \frac{1}{m_2 l_2^2} u_2 + \frac{k a^2}{m_2 l_2^2} (\sin x_1 \cos x_1 - \sin x_3 \cos x_3),
 \end{aligned} \tag{2.14}$$

where x_1 and x_3 are the rod angles with respect to the vertical axis and x_2 and x_4 are state variables stand for the angular velocities of each rod; m_i is the mass, and l_i is the rod length of the i th pendulum; u_i is the torque applied to the base of the i th pendulum; g is the gravitational acceleration; k denotes the spring elastic constants, and a is their connection heights.

Defining the premise variables, $z_1 = \sin x_1$ and $z_2 = \sin x_3$, and assuming that $|x_{2i-1}| \leq \pi/2$, $\forall i \in \mathcal{I}_2$, each premise variable can be written as local sector nonlinearity, i.e. $\sin x_{2i-1} \in \text{co}\{b_2 x_{2i-1}, b_1 x_{2i-1}\}$, with $b_1 = 1$ and $b_2 = 2/\pi$. Therefore, one

can represent $z_i = \sin x_{2i-1}$ as follows:

$$z_i = \left(\sum_{j=1}^2 \mu_i^j(z_i) b_j \right) x_{2i-1},$$

where the normalized membership functions can be calculated as

$$\mu_i^1(z_i) = \begin{cases} \frac{z_i - \frac{2}{\pi} \sin^{-1} z_i}{(1 - \frac{2}{\pi}) \sin^{-1} z_i}, & z_i \neq 0, \\ 1, & \text{otherwise,} \end{cases}$$

and $\mu_i^2(z_i) = 1 - \mu_i^1(z_i)$, $\forall i \in \mathcal{I}_2$.

Furthermore, the remaining nonlinearities also belong to a local sector if $|x_{2i-1}| \leq \pi/2$, i.e. $\phi_i(\mathbf{x}) = \sin x_{2i-1} \cos x_{2i-1} \in \text{co}\{0, x_{2i-1}\}$, for $i \in \mathcal{I}_2$. Indeed, for each nonlinearity $\phi_i(\mathbf{x})$ one has that

$$\begin{aligned} \phi_1(\mathbf{x}) &\in \text{co} \left\{ \begin{bmatrix} 0 & 0 & 0 & 0 \end{bmatrix} \mathbf{x}, \begin{bmatrix} 1 & 0 & 0 & 0 \end{bmatrix} \mathbf{x} \right\}, \\ \phi_2(\mathbf{x}) &\in \text{co} \left\{ \begin{bmatrix} 0 & 0 & 0 & 0 \end{bmatrix} \mathbf{x}, \begin{bmatrix} 0 & 0 & 1 & 0 \end{bmatrix} \mathbf{x} \right\}. \end{aligned}$$

Thus, the nonlinear system (2.14) is represented by the following N-TS fuzzy model:

$$\begin{aligned} \textbf{Rule } \kappa : & \textbf{IF } z_1(t) \in \mathcal{M}_1^{\alpha_{i1}} \text{ and } z_2(t) \in \mathcal{M}_2^{\alpha_{i2}} \\ & \textbf{THEN } \dot{\mathbf{x}} = A_\kappa \mathbf{x} + B_\kappa \mathbf{u} + G_\kappa \boldsymbol{\phi}(\mathbf{x}). \end{aligned}$$

The inferred TS membership functions $h_\kappa(\mathbf{z})$ is constructed as follows

$$\begin{aligned} \alpha_{11} &= 1, \alpha_{12} = 1, & \varsigma_1(\mathbf{z}) &= \mu_1^1(z_1) \mu_2^1(z_2), \\ \alpha_{21} &= 1, \alpha_{22} = 2, & \varsigma_2(\mathbf{z}) &= \mu_1^1(z_1) \mu_2^2(z_2), \\ \alpha_{31} &= 2, \alpha_{32} = 1, & \varsigma_3(\mathbf{z}) &= \mu_1^2(z_1) \mu_2^1(z_2), \\ \alpha_{41} &= 2, \alpha_{42} = 2, & \varsigma_4(\mathbf{z}) &= \mu_1^2(z_1) \mu_2^2(z_2). \end{aligned}$$

Finally, the inferred fuzzy model is given by

$$\dot{\mathbf{x}} = \sum_{\kappa=1}^4 \varsigma_\kappa(\mathbf{z}) (A_\kappa \mathbf{x} + B_\kappa \mathbf{u} + G_\kappa \boldsymbol{\phi}(\mathbf{x})),$$

with

$$A_\kappa = \begin{bmatrix} 0 & 1 & 0 & 0 \\ \frac{g}{l_1} b_i & 0 & 0 & 0 \\ 0 & 0 & 0 & 1 \\ 0 & 0 & \frac{g}{l_1} b_j & 0 \end{bmatrix}, \quad B_\kappa = \begin{bmatrix} 0 & 0 \\ \frac{1}{m_1 l_1^2} & 0 \\ 0 & 0 \\ 0 & \frac{1}{m_2 l_2^2} \end{bmatrix}, \quad G_\kappa = \begin{bmatrix} 0 & 0 \\ -\frac{ka^2}{m_1 l_1^2} & \frac{ka^2}{m_1 l_1^2} \\ 0 & 0 \\ \frac{ka^2}{m_2 l_2^2} & -\frac{ka^2}{m_2 l_2^2} \end{bmatrix},$$

and $i, j \in \mathcal{I}_2$, $\kappa = j + 2(i - 1)$.

Remark 2.3

Notice that just as in the classical TS fuzzy model, different choices of premise variables can be made. Transforming all nonlinearities in a fuzzy description as in Example 2.4, $z_{2i-1} = \sin x_{2i-1}$, $z_{2i} = \sin x_{2i-1} \cos x_{2i-1}$, for $i \in \mathcal{I}_2$, then 2^4 fuzzy rules are required to build a regular – with affine consequent – TS fuzzy model (2.6). However, as shown in the Example 2.5, if we use the N-TS fuzzy model (2.13), the number of fuzzy rules would be reduced to only 2^2 .

Analogously, if we had N series-connected inverted pendulums, the number of fuzzy rules would be reduced from 2^{2N} to 2^N . As a result, both conservativeness and computational complexity for stability analysis and control design can be drastically reduced when using N-TS fuzzy models for continuous-time (Dong, Wang, and Yang 2009) and discrete-time systems (Dong, Wang, and Yang 2011).

2.3 Interconnected N-TS Fuzzy Systems

Consider a continuous-time large-scale system which consists of N interconnected nonlinear subsystems with nonlinear interconnections and subject to control input saturation. Each i -th subsystem is described as follows:

$$\dot{\mathbf{x}}_i(t) = f_i(\mathbf{x}_i(t)) + g_i(\mathbf{x}_i(t))\text{sat}(\mathbf{u}_i(t)) + \sum_{j \in \mathcal{N}_i} h_{ij}(\mathbf{x}_i(t), \mathbf{x}_j(t)), \quad (2.15)$$

where $i \in \mathcal{I}_N$, $\mathbf{x}_i(t) \in \mathbb{R}^{n_{x_i}}$ is the state vector of i -th subsystem; $\mathbf{u}_i(t) \in \mathbb{R}^{n_{u_i}}$ is the i -th control input vector; f_i , g_i and h_{ij} are smooth nonlinear functions and h_{ij} can be divided into a linear function and a bounded sector nonlinear one.

As it was demonstrated in the Section 2.2, TS fuzzy models can be used to approximate nonlinear functions from fuzzy rules (Takagi and Sugeno 1985). Thus, if we transform only local nonlinearities, $f_i(\mathbf{x}_i(t))$ and $g_i(\mathbf{x}_i(t))$ in (2.15), using fuzzy rules, we should obtain the following N-TS fuzzy model for each subsystem in (2.15):

$$\begin{aligned} \text{Rule } \mathcal{R}_i^l : & \text{ IF } z_{i1}(t) \in \mathcal{M}_{i1}^{\alpha_{i1}^1} \text{ and } z_{i2}(t) \in \mathcal{M}_{i2}^{\alpha_{i2}^2} \text{ and } \cdots \text{ and } z_{ip_i}(t) \in \mathcal{M}_{ip_i}^{\alpha_{ip_i}^{p_i}} \\ & \text{ THEN } \dot{\mathbf{x}}_i(t) = A_i^l \mathbf{x}_i(t) + B_i^l \text{sat}(\mathbf{u}_i(t)) \\ & \quad + \sum_{j \in \mathcal{N}_i} \left(H_{ii}^l \mathbf{x}_i(t) - H_{ij}^l \mathbf{x}_j(t) \right) + G_i^l \left(\sum_{j \in \mathcal{N}_i} \varphi_{ij}(\mathbf{x}_i(t), \mathbf{x}_j(t)) \right) \end{aligned}$$

where $i \in \mathcal{I}_N$; $l \in \mathcal{I}_{r_i}$, with r_i the number of rules; \mathcal{R}_i^l denotes the l -th fuzzy rule of i -th subsystem; $\mathbf{z}_i(t) \in \mathbb{R}^{p_i}$ is the premise variables vector associated to i -th subsystem ($z_{ij}(t)$ is the j -th element of vector $\mathbf{z}_i(t)$); $\mathcal{M}_{ij}^{\alpha_{ij}^j}$ is the fuzzy set related to the premise variable

$\mathbf{z}_{ij}(t); \mathbf{x}_i(t) \in \mathbb{R}^{n_{x_i}}$ is the state vector of i -th subsystem; $\mathbf{u}_i(t) \in \mathbb{R}^{n_{u_i}}$ is the i -th input vector subject to saturation; $\varphi_{ij}(\cdot)$ are functions describing the nonlinear interconnections between the i -th and j -th subsystems; \mathcal{N}_i is the set of indexes related to the subsystems in the network that are directly connected to the i -th subsystem, i.e. $j \in \mathcal{N}_i \Leftrightarrow \alpha_{ij} \neq 0$; A_i^l and B_i^l are known constant matrices of appropriate dimensions; with H_{ij}^l working as a weighing of the contributions of the *linear* couplings between interconnected systems, and G_i^l weighing the corresponding contributions of *nonlinear* couplings for the l -th local model.

After using fuzzy combination of rules, we can directly obtain the i -th inferred N-TS fuzzy model as follows

$$\begin{aligned} \dot{\mathbf{x}}_i(t) = \sum_{l=1}^{r_i} \zeta_i^l(\mathbf{z}_i(t)) & \left[A_i^l \mathbf{x}_i(t) + B_i^l \text{sat}(\mathbf{u}_i(t)) \right. \\ & \left. + \sum_{j \in \mathcal{N}_i} \left(H_{ii}^l \mathbf{x}_i(t) - H_{ij}^l \mathbf{x}_j(t) \right) + G_i^l \left(\sum_{j \in \mathcal{N}_i} \varphi_{ij}(\mathbf{x}_i(t), \mathbf{x}_j(t)) \right) \right], \end{aligned} \quad (2.16)$$

where $i \in \mathcal{I}_N$, A_i^l , B_i^l , H_{ij}^l and G_i^l are known constant matrices with appropriate dimensions; with the nonlinearities φ_{ij} satisfying Property 2.3.

From the above description, the state and input vectors of the whole large-scale system are given, respectively, by $\mathbf{x}(t) = [\mathbf{x}_1^\top(t) \ \mathbf{x}_2^\top(t) \ \cdots \ \mathbf{x}_N^\top(t)]^\top \in \mathbb{R}^{n_x}$, and $\mathbf{u}(t) = [\mathbf{u}_1^\top(t) \ \mathbf{u}_2^\top(t) \ \cdots \ \mathbf{u}_N^\top(t)]^\top \in \mathbb{R}^{n_u}$, with $n_x = \sum_{i=1}^N n_{x_i}$ and $n_u = \sum_{i=1}^N n_{u_i}$, such that the entire network dynamics can be expressed as

$$\dot{\mathbf{x}}(t) = (\mathbf{A}_N + \mathbf{H}_N \circ \mathbf{L}) \mathbf{x}(t) + \mathbf{B}_N \text{sat}(\mathbf{u}(t)) + \mathbf{G}_N [(A_G \circ \Phi(\mathbf{x}(t))) \mathbf{1}_N], \quad (2.17)$$

with $\text{sat}(\mathbf{u}) = [\text{sat}(\mathbf{u}_1(t))^\top \ \text{sat}(\mathbf{u}_2(t))^\top \ \cdots \ \text{sat}(\mathbf{u}_N(t))^\top]^\top$; \mathbf{A}_N is a block diagonal matrix, i.e., $\mathbf{A}_N = \bigoplus_{i=1}^N (\sum_{l=1}^{r_i} \zeta_i^l(\mathbf{z}_i(t)) A_i^l)$, and similarly the same holds for \mathbf{B}_N and \mathbf{G}_N ; $\mathbf{H}_N = [\sum_{l=1}^{r_i} \zeta_i^l(\mathbf{z}_i(t)) H_{ij}^l]$, $\mathbf{L} = [L_{ij}] = \ell_{ij} \mathbf{1}_{n_{x_i} \times n_{x_j}}$ and $\Phi(\mathbf{x}) = [\varphi_{ij}(\mathbf{x}_i, \mathbf{x}_j)] \in \mathbb{R}^{N \times N}$ is a matrix of nonlinear functions; and A_G is Adjacency matrix associated with the interconnection graph \mathcal{G} of the large-scale system. Notice that the term $(A_G \circ \Phi(\mathbf{x}))$ could be further simplified by defining that $\varphi_{ij}(\mathbf{x}_i, \mathbf{x}_j) = 0$, if $\alpha_{ij} = 0$, such that the information on the network connectivity is incorporated in the definition of the nonlinear coupling functions.

Notice that if the i -th and j -th subsystems are not interconnected, then the nonlinearity $\varphi_{ij}(\mathbf{x}_i, \mathbf{x}_j)$ does not exist and it can cause numerical problems in the design conditions and it should not be taken into consideration. Thus, $\boldsymbol{\varphi}_i(\mathbf{x}(t)) = [\varphi_{ij_1} \ \varphi_{ij_2} \ \cdots \ \varphi_{ij_{d_{ii}}}]^\top \in \mathbb{R}^{d_{ii}}$ is defined as a *column* vector formed by stacking the nonlinear functions φ_{ij_κ} , with $j_\kappa \in \mathcal{N}_i$, $\kappa \in \mathcal{I}_{d_{ii}}$. This notation is illustrated in the following example.

Example 2.6. Consider the interconnected system represented by the graph in Figure 2.4. The neighborhood associated with the 4th subsystem is given by $\mathcal{N}_4 = \{1, 3, 5\}$, with

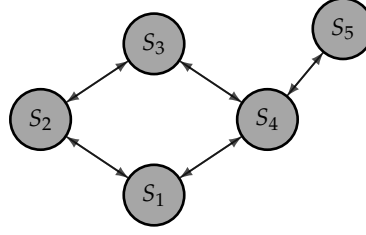


Figure 2.4: Graph of interconnected system.

$\kappa \in \mathcal{I}_3$ and $j_1 = 1$, $j_2 = 3$, and $j_3 = 5$.

Hence, $\boldsymbol{\phi}_4(\mathbf{x}(t)) = \begin{bmatrix} \varphi_{41}(\mathbf{x}_4, \mathbf{x}_1) & \varphi_{43}(\mathbf{x}_4, \mathbf{x}_3) & \varphi_{45}(\mathbf{x}_4, \mathbf{x}_5) \end{bmatrix}^\top$.

Thus, the entire network (2.17) can be rewritten taking this aspect into account, such that

$$\dot{\mathbf{x}}(t) = (\mathbf{A}_N + \mathbf{H}_N \circ \mathbf{L}) \mathbf{x}(t) + \mathbf{B}_N \text{sat}(\mathbf{u}(t)) + \bar{\mathbf{G}}_N \boldsymbol{\phi}(\mathbf{x}(t)), \quad (2.18)$$

where $\bar{\mathbf{G}}_N$ is also block diagonal matrix and incorporates the information on the number of interconnections of each subsystem, i.e., $\bar{\mathbf{G}}_N = \bigoplus_{i=1}^N \left(\sum_{l=1}^{r_i} \varsigma_i^l(\mathbf{z}_i(t)) G_i^l \mathbf{1}_{d_{ii}}^\top \right)$, and $\boldsymbol{\phi}(t) = \begin{bmatrix} \boldsymbol{\phi}_1^\top(t) & \boldsymbol{\phi}_2^\top(t) & \cdots & \boldsymbol{\phi}_N^\top(t) \end{bmatrix}^\top$. Therefore, the i -th N-TS fuzzy model can be simplified as follows:

$$\begin{aligned} \dot{\mathbf{x}}_i(t) = \sum_{l=1}^{r_i} \varsigma_i^l(\mathbf{z}_i(t)) & \left[A_i^l \mathbf{x}_i(t) + B_i^l \text{sat}(\mathbf{u}_i(t)) \right. \\ & \left. + \sum_{j \in \mathcal{N}_i} \left(H_{ii}^l \mathbf{x}_i(t) - H_{ij}^l \mathbf{x}_j(t) \right) + G_i^l \mathbf{1}_{d_{ii}}^\top \boldsymbol{\phi}_i(\mathbf{x}(t)) \right]. \end{aligned} \quad (2.19)$$

The entire network model (2.18) and its subsystems (2.19) will be used in Chapter 3 to obtain synthesis conditions.

Remark 2.4

Notice that since each function $\varphi_{ij}(\mathbf{x}_i, \mathbf{x}_j)$ satisfies Property 2.3, and considering the definition of $\boldsymbol{\phi}_i(\mathbf{x})$, it follows that each $\boldsymbol{\phi}_i(\mathbf{x})$ also satisfies Property 2.3, i.e., there exists given matrix $\boldsymbol{\Omega}_i = \begin{bmatrix} \Omega_{i1} & \Omega_{i2} & \cdots & \Omega_{iN} \end{bmatrix} \in \mathbb{R}^{d_{ii} \times n_x}$, $n_x = \sum_{i=1}^N n_{x_i}$, with $\Omega_{ij} \in \mathbb{R}^{d_{ii} \times n_{x_j}}$, $\forall j \in \mathcal{I}_N$, such that the following inequality holds

$$\boldsymbol{\phi}_i(\mathbf{x})^\top \Lambda_i^{-1} (\boldsymbol{\phi}_i(\mathbf{x}) - \boldsymbol{\Omega}_i \mathbf{x}) \leq 0, \quad (2.20)$$

where $\Lambda_i \in \mathbb{R}^{d_{ii} \times d_{ii}}$ is any positive definite diagonal matrix which is responsible for inserting degrees of freedom in (2.11).

Example 2.7. To exemplify the construction of interconnected N-TS fuzzy models consider a network of interconnected inverted pendulums. The following modifications are done in the system of inverted pendulums coupled by springs (Šiljak 2012, Chapter I):

- (i) Consider the problem with more than two interconnected inverted pendulums, such that their interconnections are represented by the corresponding graph Adjacency matrix;
- (ii) Linear springs are replaced by the so-called hardening springs (Khalil 2002), with restoring forces modeled as cubic functions of their displacements, as follows $h(y) = k(1 + a^2 y^2)y$, and we assume that all springs are equal;
- (iii) Assume also that the pendulums can have different masses and rod lengths, while being subjected to control input saturation.

Thus, the system of multiple interconnected inverted pendulums can be described by

$$\begin{aligned}\dot{x}_{i1}(t) &= x_{i2}(t), \\ \dot{x}_{i2}(t) &= \frac{g}{l_i} \sin(x_{i1}(t)) + \frac{1}{m_i l_i^2} \text{sat}(u_i(t)) \\ &\quad - \frac{k a^2}{m_i l_i^2} \sum_{j \in \mathcal{N}_i} (x_{i1}(t) - x_{j1}(t)) - \frac{k a^2 \gamma^2}{m_i l_i^2} \sum_{j \in \mathcal{N}_i} (x_{i1}(t) - x_{j1}(t))^3,\end{aligned}\tag{2.21}$$

where $i \in \mathcal{I}_N$, N is the number of pendulums; the state vector of the i -th subsystem is $\mathbf{x}_i(t) = [x_{i1}(t) \ x_{i2}(t)]^\top$, $x_{i1}(t)$ is the rod angle with respect to the upright position, $x_{i2}(t)$ is the angular velocity, and $u_i(t)$ is the torque applied to the base of the i -th pendulum; g denotes the gravitational acceleration, m_i is the mass, and l_i is the rod length of the i -th pendulum. Since the springs are equal, thus k and γ denote the linear and nonlinear elastic coefficients, respectively, and a is the height of the their connection at the pendulums rods.

Notice that the system of multiple interconnected inverted pendulums (2.21) can be rewritten in the form given in (2.19) using the approach presented in Section 2.2. However, the N-TS fuzzy models is only valid if $|x_{i1}(t)| \leq \bar{\theta}$, which defines the validity region of the model (2.16). As discussed below, this constraint directly enables the use of sector-boundedness conditions for the nonlinear functions.

A 2-rule N-TS fuzzy model (2.19) can be obtained to each i -pendulum applying the sector nonlinearity approach previously illustrated, choosing $z_i(t) = \sin(x_{i1}(t)) \in \text{co}\left\{\frac{\sin \bar{\theta}}{\bar{\theta}}, 1\right\}$ as the premise variable of the i -th subsystem, and $\varphi_{ij_\kappa}(\mathbf{x}_i, \mathbf{x}_{j_\kappa}) = (x_{i1} - x_{j_\kappa 1})^3 \in \text{co}\left\{0, \Omega_{i(\kappa)} x\right\}$, with $\kappa \in \mathcal{I}_{d_{ii}}$, and $\Omega_i = [\Omega_{i1} \ \Omega_{i2} \ \cdots \ \Omega_{iN}]$, $\Omega_{ii(\kappa)} = [4\bar{\theta}^2 \ 0]$, $\forall i \in \mathcal{I}_N$, for $\Omega_{ij_\kappa(\kappa)} = -\Omega_{ii(\kappa)}$, if $j_\kappa \in \mathcal{N}_i$ and $\Omega_{ij(\kappa)} = [0 \ 0]$,

otherwise. The i -th local state-space matrices are given by

$$A_i^1 = \begin{bmatrix} 0 & 1 \\ \frac{g}{l_i} & 0 \end{bmatrix}, A_i^2 = \begin{bmatrix} 0 & 1 \\ \frac{g \sin \bar{\theta}}{l_i} & 0 \end{bmatrix}, B_i^1 = B_i^2 = \begin{bmatrix} 0 \\ \frac{1}{m_i l_i^2} \end{bmatrix},$$

$$H_{ij}^1 = H_{ij}^2 = \begin{bmatrix} 0 & 0 \\ -\frac{ka^2}{m_i l_i^2} & 0 \end{bmatrix}, G_i^1 = G_i^2 = \begin{bmatrix} 0 \\ -\frac{ka^2 \gamma^2}{m_i l_i^2} \end{bmatrix}.$$

2.3.1 Fuzzy Summations and Interconnected Systems

The great advantage of interconnected N-TS fuzzy systems is the only local nonlinearity of N interconnected nonlinear subsystems is transformed by fuzzy rules and nonlinear interconnections satisfy the sector condition.

In this context, the analysis and synthesis conditions will usually present N sets of double fuzzy summations, i.e. each subsystem has corresponding double fuzzy summations, in other words, each subsystem has its proper set of membership functions. Based on this, Lemmas 2.1 and 2.2 are not adequate to address this scenario, because they consider only one set of fuzzy summations and a generalization to N sets is required.

Therefore, we will use the notion of multisets (Singh et al. 2007) that emerges due to multiple sets of membership functions. A similar idea has been mainly utilized in the context of discrete-time systems (Coutinho et al. 2019; Coutinho et al. 2020) concerning multisets of delay, which are inserted in the membership function to reduce the conservativeness.

Next, we provide fundamental concepts about multisets. The notation used is based on the one proposed in (Coutinho et al. 2020).

Definition 2.4: Multisets (Singh et al. 2007)

Let $\mathcal{S} = \{\varsigma_1, \varsigma_2, \dots, \varsigma_n\}$ be a set. A multiset \mathcal{S}_ς over \mathcal{S} is a cardinal-valued function $\mathcal{S}_\varsigma : \mathcal{S} \mapsto \mathbb{N}$ such that for $\varsigma \in \text{Dom}(\mathcal{S}_\varsigma)$ implies the cardinal $|\varsigma|_{\mathcal{S}_\varsigma}$. The value $|\varsigma|_{\mathcal{S}_\varsigma}$ denotes the multiplicity of ς , i.e. the number of times ς occurs in \mathcal{S}_ς . A multiset \mathcal{S}_ς is denoted here by the set of pairs $\mathcal{S}_\varsigma = \{\langle |\varsigma_1|_{\mathcal{S}_\varsigma}, \varsigma_1 \rangle, \dots, \langle |\varsigma_n|_{\mathcal{S}_\varsigma}, \varsigma_n \rangle\}$.

Example 2.8. If the multiplicity of a given element $\varsigma \in \mathcal{S}_\varsigma$ is 1, it is simply denoted $\langle 1, \varsigma \rangle = \varsigma$. Particularly, synthesis conditions in this thesis present only multisets of double fuzzy summations, i.e. the multiplicity of membership functions of i -th subsystem is $|\varsigma_i|_{\mathcal{S}_\varsigma} = 2$ and the multiset of membership functions associated to overall system is $\mathcal{S}_\varsigma = \{\langle 2, \varsigma_1 \rangle, \dots, \langle 2, \varsigma_n \rangle\}$.

Definition 2.5: Index set and multi-index

The i -th index set of a multiple fuzzy summation with multiset of membership functions \mathcal{S}_ζ is the set of all indexes in the sum associated with subset $\mathcal{S}_{\zeta_i} \subset \mathcal{S}_\zeta$. It is denoted here by $\mathbb{I}_{\zeta_i} = \{\iota_i = (\iota_{i,1}, \dots, \iota_{i,|\mathcal{S}_{\zeta_i}|}) \mid \iota_{i,j} \in \mathcal{I}_{r_i}, j \in \mathcal{I}_{|\mathcal{S}_{\zeta_i}|}\}$. An element $\iota_i \in \mathbb{I}_{\zeta_i}$ is called multi-index of i -th subset of multiset \mathcal{S}_ζ .

Example 2.9. Consider (2.19) with $N = 2$, a generic multiple fuzzy summation with double fuzzy summations of each subsystem can be written by:

$$\sum_{\iota_1 \in \mathbb{I}_{\zeta_1}} \sum_{\iota_2 \in \mathbb{I}_{\zeta_2}} \varsigma_1^{\iota_1} \varsigma_2^{\iota_2} Y_{(\iota_1, \iota_2)} = \sum_{\iota_{1,1}=1}^{r_1} \sum_{\iota_{1,2}=1}^{r_1} \sum_{\iota_{2,1}=1}^{r_2} \sum_{\iota_{2,2}=1}^{r_2} \varsigma_1^{\iota_{1,1}} \varsigma_1^{\iota_{1,2}} \varsigma_2^{\iota_{2,1}} \varsigma_2^{\iota_{2,2}} Y_{(\iota_{1,1}, \iota_{1,2}, \iota_{2,1}, \iota_{2,2})}.$$

Lemma 2.3: Multiple fuzzy summation with multiset of membership functions, adapted from Lemma 2 in (Coutinho et al. 2020)

A sufficient condition for the satisfaction of the following inequality dependent on a multiple fuzzy summation with multiset of membership functions

$$\sum_{\iota_1 \in \mathbb{I}_{\zeta_1}} \cdots \sum_{\iota_N \in \mathbb{I}_{\zeta_N}} \left(\prod_{i=1}^N \varsigma_i^{\iota_i} \right) Y_{(\iota_1, \dots, \iota_N)} \succ 0,$$

is that, for every combination of $(\iota_1, \dots, \iota_N)$, where ι_i is a multi-index given by Definition 2.5, the sum of its permutations is positive definite.

Remark 2.5

Given a multidimensional fuzzy summations with multiset of membership functions $\mathcal{S}_{\zeta_i} = \{(|\zeta_i|_{\mathcal{S}_\zeta}, \zeta_i)\}$, $\forall i \in \mathcal{N}$, the number of LMIs to ensure its positiveness obtained with Lemma 2.3 is given by (Coutinho et al. 2020, Remark 7)

$$\prod_{i=1}^N \frac{(r_i + |\zeta_i|_{\mathcal{S}_\zeta} - 1)!}{(|\zeta_i|_{\mathcal{S}_\zeta})!(r_i - 1)!}.$$

Specially in this thesis, a multiplicity of each membership function is equal to 2, i.e. $|\zeta_i|_{\mathcal{S}_\zeta} = 2$. Therefore, the number of LMIs is

$$\prod_{i=1}^N \frac{r_i^2 + r_i}{2}.$$

The Lemma 2.3 is obtained from the recursive application of Lemma 2.2 in each i -th subset of multiset \mathcal{S}_ζ associated with multiple fuzzy summation. This will be illustrated in next example.

Example 2.10. Consider that, we want to check the positiveness of the multiple fuzzy summation in Example 2.9, for $r_1 = r_2 = 2$. Since $N = 2$, the multiset of membership functions is $\mathcal{S}_\zeta = \{\langle 2, \varsigma_1 \rangle, \langle 2, \varsigma_2 \rangle\}$.

$$\sum_{\iota_1 \in \mathbb{I}_{\varsigma_1}} \sum_{\iota_2 \in \mathbb{I}_{\varsigma_2}} \varsigma_1^{\iota_1} \varsigma_2^{\iota_2} Y_{(\iota_1, \iota_2)} \succ 0.$$

By Lemma 2.3, its positiveness is ensured if the following set of conditions hold:

$$\begin{aligned} Y_{(1,1,1,1)} &\succ 0, & Y_{(2,2,2,2)} &\succ 0, & Y_{(1,1,1,2)} + Y_{(1,1,2,1)} &\succ 0, & Y_{(1,1,2,2)} &\succ 0, \\ Y_{(1,2,1,1)} + Y_{(2,1,1,1)} &\succ 0, & Y_{(1,2,1,2)} + Y_{(2,1,1,2)} + Y_{(1,2,2,1)} + Y_{(2,1,2,1)} &\succ 0, \\ Y_{(1,2,2,2)} + Y_{(2,1,2,2)} &\succ 0, & Y_{(2,2,1,1)} &\succ 0, & Y_{(2,2,1,2)} + Y_{(2,2,2,1)} &\succ 0. \end{aligned}$$

Above conditions can also be obtained from the recursive application of Lemma 2.2. Initially, we can apply Lemma 2.2 to multi-index ι_2 , resulting in the conditions:

$$Y_{(\iota_1, 1, 1)} \succ 0, \quad Y_{(\iota_1, 1, 2)} + Y_{(\iota_1, 2, 1)} \succ 0, \quad Y_{(\iota_1, 2, 2)} \succ 0.$$

Next, if we apply Lemma 2.2 to multi-index ι_1 , by considering each one of the previous conditions one has that:

$$\begin{aligned} Y_{(1,1,1,1)} &\succ 0, & Y_{(1,2,1,1)} + Y_{(2,1,1,1)} &\succ 0, & Y_{(2,2,1,1)} &\succ 0, \\ Y_{(1,1,1,2)} + Y_{(1,1,2,1)} &\succ 0, & Y_{(2,2,1,2)} + Y_{(2,2,2,1)} &\succ 0, \\ Y_{(1,2,1,2)} + Y_{(1,2,2,1)} + Y_{(2,1,1,2)} + Y_{(2,1,2,1)} &\succ 0, \\ Y_{(1,1,2,2)} &\succ 0 & Y_{(1,2,2,2)} + Y_{(2,1,2,2)} &\succ 0 & Y_{(2,2,2,2)} &\succ 0 \quad . \end{aligned}$$

According to Remark 2.5, the number of LMIs obtained is equal to 9.

3 Distributed Control of Networked Nonlinear Systems

In this chapter, we investigate the problem of designing nonlinear distributed control laws for a class of continuous-time networked nonlinear heterogeneous systems with sector-bounded nonlinear interconnections. The new sufficient conditions, taking into account state constraints and actuators saturation, are derived in terms of LMIs. In addition, the volume of the DoA estimate for the closed-loop system is maximized.

The presentation and the results in this chapter were based on (Araújo, Torres, and Palhares 2020).

3.1 Introduction

Networked systems consist of several interconnected subsystems by linear or nonlinear couplings. Particularly, this thesis is concerned in the case where subsystems interact physically with each other and interconnections are nonlinear, e.g. nonlinear springs connect the inverted pendulums in the Example 2.7.

In this chapter, we explore the flexibility in the control design provided by using N-TS fuzzy models, together with the advantages of a distributed control approach to designing nonlinear distributed control law for a class of continuous-time networked nonlinear heterogeneous systems with sector-bounded nonlinear interconnections. Besides, here we refer to the large-scale system as a networked system because no decomposition technique is applied to large-scale systems, this case will be addressed in the next chapter.

3.1.1 Regional Stability

Real-world systems are also subject to both state and control input constraints, which may arise either from economic restrictions or safety reasons (Nguyen et al. 2016). State constraints can be considered due to the existence of physical limitations for the system states or when the system's model is valid only in a given bounded region, e.g. when relying on linear models valid around a specific operating point. This also happens when TS fuzzy models are employed to represent nonlinear functions that can be taken as sector nonlinearities only in bounded regions of the state-space, according to what was discussed in Section 2.2.

In this chapter, we consider that the estimate of the domain of attraction for the closed-loop system (to be defined next) is inside a polytopic region in state-space, which establishes the validity region of the system's model. By following this approach, it is possible to ensure that the system trajectories will always evolve within the validity region of the underlying system model, for every initial condition in the estimated domain of attraction. It should be emphasized that this fundamental requirement is often neglected in many works, especially when one deals with fuzzy TS models.

The polytopic set associated with the validity of the model (2.6) representing (2.3) is defined as follows:

$$\mathcal{D}_{\mathbf{x}} = \left\{ \mathbf{x}(t) \in \mathbb{R}^{n_x} : \boldsymbol{\beta}_\nu^\top \mathbf{x}(t) \leq 1, \nu \in \mathcal{I}_{n_e} \right\}, \quad (3.1)$$

with $\boldsymbol{\beta}_\nu \in \mathbb{R}^{n_x}$ being given vectors that define the limits (hyperplanes) of the polytopic set, and n_e the number of hyperplanes.

Domain of Attraction Estimate

In the context of nonlinear systems, equilibrium points are usually only locally asymptotically stable. Therefore, it is important to find the DoA corresponding to the equilibrium point under consideration.

Definition 3.1: *Domain of Attraction (DoA)*

The DoA is a positively invariant region around an equilibrium point of a given nonlinear system such that every trajectory initiating inside it asymptotically converges to the equilibrium point.

To find the exact DoA is usually very challenging. Alternatively, it can be easier to guarantee regional stability considering an estimate of the DoA (Khalil 2002). As a matter of fact, one can estimate the DoA via Lyapunov theory, using Lyapunov functions level sets (Khalil 2002).

Thus, if we consider the following quadratic Lyapunov function in the stability analysis of the nonlinear system in (2.3):

$$V(\mathbf{x}(t)) = \mathbf{x}(t)^\top P \mathbf{x}(t), \quad (3.2)$$

with $P = P^\top \succ 0$, the 1-level set associated with the quadratic Lyapunov function (3.2) is an ellipsoidal region defined as:

$$\mathcal{L}_V = \left\{ \mathbf{x}(t) \in \mathbb{R}^{n_x} : \mathbf{x}(t)^\top P \mathbf{x}(t) \leq 1 \right\}.$$

If $\dot{V}(\mathbf{x}(t)) < 0$ along the trajectories of the nonlinear system (2.3), $\forall \mathbf{x}(t) \in \mathcal{L}_V, \mathbf{x}(t) \neq 0$, then \mathcal{L}_V is a positively invariant ellipsoidal set, and hence it is also a subset of the DoA of the system (Khalil 2002).

In addition, we must ensure that \mathcal{L}_V is a subset of $\mathcal{D}_\mathbf{x}$, the validity region defined in (3.1). This condition is guaranteed if the following inequality holds (Rohr, Pereira, and Coutinho 2009):

$$1 - \mathbf{x}(t)^\top \boldsymbol{\beta}_\nu - \boldsymbol{\beta}_\nu^\top \mathbf{x}(t) + \mathbf{x}(t)^\top P \mathbf{x}(t) \geq 0, \forall \nu \in \mathcal{I}_{n_e}. \quad (3.3)$$

One can achieve this result by rewriting (3.1) as $2 - \mathbf{x}(t)^\top \boldsymbol{\beta}_\nu - \boldsymbol{\beta}_\nu^\top \mathbf{x}(t) \geq 0$, and since $\mathbf{x}(t)^\top P \mathbf{x}(t) \leq 1, \forall \mathbf{x}(t) \in \mathcal{L}_V$, then (3.3) implies that $\mathcal{L}_V \subseteq \mathcal{D}_\mathbf{x}$.

The inequality (3.3) can be rewritten as the quadratic form:

$$\begin{bmatrix} 1 \\ -\mathbf{x}(t) \end{bmatrix}^\top \begin{bmatrix} 1 & \star \\ \boldsymbol{\beta}_\nu & P \end{bmatrix} \begin{bmatrix} 1 \\ -\mathbf{x}(t) \end{bmatrix} \succeq 0, \forall \nu \in \mathcal{I}_{n_e}.$$

Hence, if the next LMI holds

$$\begin{bmatrix} 1 & \star \\ \boldsymbol{\beta}_\nu & P \end{bmatrix} \succeq 0, \forall \nu \in \mathcal{I}_{n_e}, \quad (3.4)$$

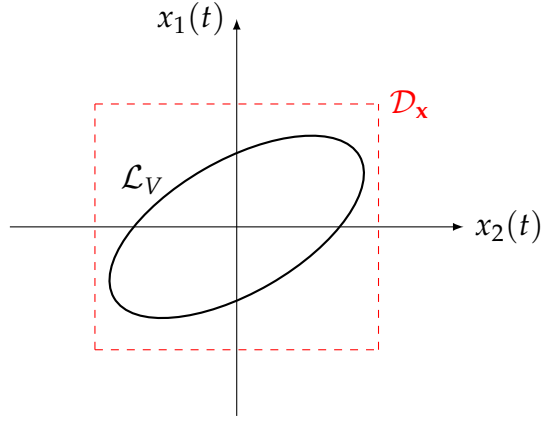
it implies that $\mathcal{L}_V \subseteq \mathcal{D}_\mathbf{x}$. Figure 3.1 illustrates, for case two-dimensional, the inclusion of DoA, \mathcal{L}_V , in the validity region of the model $\mathcal{D}_\mathbf{x}$, which is ensured by LMI constraint (3.4).

Representation of Control Input Saturation

On the other hand, input control constraints or actuator saturation emerge from limitations in actuators and may seriously degrade the closed-loop performance, leading the system to critical conditions and, in extreme cases, it may cause instability if not fully considered in the controller design process (Hu and Lin 2001; Tarbouriech et al. 2011).

Consider the nonlinear system (2.3) subject to control input constraint:

$$\dot{\mathbf{x}}(t) = f(\mathbf{x}(t)) + g(\mathbf{x}(t))\text{sat}(\mathbf{u}(t)).$$


 Figure 3.1: Validity region \mathcal{D}_x and DoA.

The control input, $\mathbf{u}(t)$, is subject to a saturation map $\text{sat}(\cdot) : \mathbb{R}^{n_u} \mapsto \mathbb{R}^{n_u}$, defined as

$$\text{sat}(u_i(t)) = \max(\min(u_i(t), \bar{u}_i), -\bar{u}_i), \forall i \in \mathcal{I}_{n_u},$$

where $\bar{u}_i > 0$ is the absolute bound of the i -th component of the control input.

Different forms can be used to describe saturation, in (Tarbouriech et al. 2011, Chapter 2) 3 different polytopic approaches are presented. In particular, Hu and Lin 2001 also propose a polytopic representation, however, this approach generates 2^{n_u} LMIs to be considered in the control design. In the context of the control of networked systems, this is prohibitive.

Thus, the approach based on a sector nonlinearity model presented in (Tarbouriech et al. 2011, Chapter 3) is used throughout this chapter, where a dead-zone nonlinearity is defined as

$$\boldsymbol{\psi}(\mathbf{u}(t)) = \mathbf{u}(t) - \text{sat}(\mathbf{u}(t)),$$

with $\boldsymbol{\psi}(\mathbf{u}(t)) \in \mathbb{R}^{n_u}$.

Consider a linear state feedback control law $\mathbf{u}(t) = K\mathbf{x}(t)$. The following lemma is useful to deal with dead-zone nonlinearities (Tarbouriech et al. 2011).

Lemma 3.1: *Dead-zone nonlinearity* (Tarbouriech et al. 2011)

Consider the set

$$\mathcal{D}_u = \left\{ \mathbf{x}(t) \in \mathbb{R}^{n_x} : \left| (K - W)_{(i)} \mathbf{x}(t) \right| \leq \bar{u}_i, \forall i \in \mathcal{I}_{n_u} \right\},$$

where $W \in \mathbb{R}^{n_u \times n_x}$ is any matrix.

If $\mathbf{x}(t) \in \mathcal{D}_u$, then

$$\boldsymbol{\psi}(\mathbf{u}(t))^\top U (\boldsymbol{\psi}(\mathbf{u}(t)) - W\mathbf{x}(t)) \leq 0,$$

holds for any positive definite diagonal matrix $U \in \mathbb{R}^{n_u \times n_u}$.

Proof. If $\mathbf{x}(t) \in \mathcal{D}_{\mathbf{u}}$, then we can conclude that, $\forall i \in \mathcal{I}_{n_u}$, one has that:

$$-\bar{u}_i \leq (K - W)_{(i)} \mathbf{x}(t) \leq \bar{u}_i. \quad (3.5)$$

Thus it is necessary to show that, $\forall i \in \mathcal{I}_{n_u}$,

$$\psi(u_i(t))^\top U_{(i,i)} (\boldsymbol{\psi}(\mathbf{u}(t)) - W\mathbf{x}(t))_{(i)} \leq 0, \quad (3.6)$$

where $U_{(i,i)}$ denotes the i -th element of the diagonal of the matrix U . Thus, three possible cases according to the value of $u_i(t)$ have to be considered:

(i) $-\bar{u}_i \leq u_i(t) \leq \bar{u}_i$. It follows that $\psi(u_i(t)) = 0$ and thus (3.6) holds.

(ii) $u_i(t) > \bar{u}_i$. Since $\psi(u_i(t)) = u_i(t) - \bar{u}_i$, then

$$\psi(u_i(t)) = K_{(i)} \mathbf{x}(t) - \bar{u}_i > 0.$$

Notice that from (3.5) then $(K - W)_{(i)} \mathbf{x}(t) \leq \bar{u}_i$ and

$$(\boldsymbol{\psi}(\mathbf{u}(t)) - W\mathbf{x}(t))_{(i)} = (K - W)_{(i)} \mathbf{x}(t) - \bar{u}_i \leq 0.$$

Since $\psi(u_i(t)) > 0$, then inequality (3.6) holds.

(iii) $u_i(t) < -\bar{u}_i$. Since $\psi(u_i(t)) = u_i(t) - \bar{u}_i$, then

$$\psi(u_i(t)) = K_{(i)} \mathbf{x}(t) - \bar{u}_i < 0.$$

Again, it follows from (3.5) that $(K - W)_{(i)} \mathbf{x}(t) \geq -\bar{u}_i$. Hence

$$(\boldsymbol{\psi}(\mathbf{u}(t)) - W\mathbf{x}(t))_{(i)} = (K - W)_{(i)} \mathbf{x}(t) - \bar{u}_i \geq 0.$$

However, $\psi(u_i(t)) < 0$ in this case, then inequality (3.6) holds.

□

Analogously to the previous subsection, we must ensure that \mathcal{L}_V associated with the Lyapunov function (3.2) is a subset of $\mathcal{D}_{\mathbf{u}}$, the region in which saturation is described as dead-zone nonlinearity. Thus, if following inequality holds

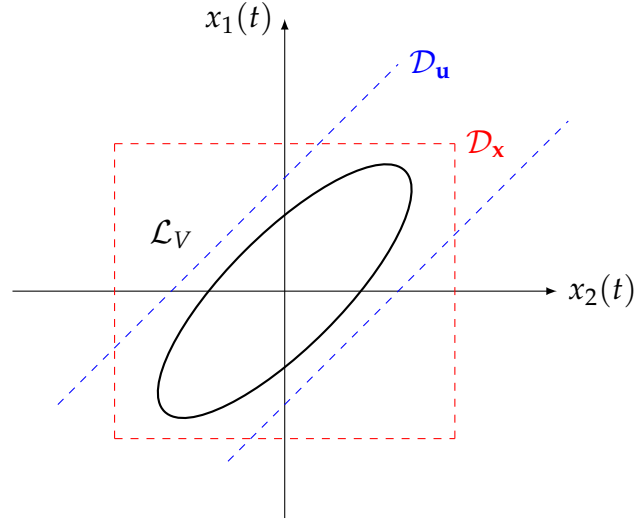
$$V(\mathbf{x}(t)) \geq V(\mathbf{x}(t)) - \frac{\| (K - W)_{(i)} \mathbf{x}(t) \|^2}{\bar{u}_i^2} > 0, \quad (3.7)$$

then, Lemma 3.1 is valid $\forall \mathbf{x}(t) \in \mathcal{L}_V$ and consequently $\mathcal{L}_V \subset \mathcal{D}_{\mathbf{u}}$. Inequality (3.7) also guarantees that the Lyapunov function is positive definite inside of the subset $\mathcal{D}_{\mathbf{u}}$.

In addition, Lemma 3.1 is also used to ensure that the time derivative is negative definite, such that:

$$\dot{V}(\mathbf{x}(t)) \leq \dot{V}(\mathbf{x}(t)) - 2\boldsymbol{\psi}(\mathbf{u}(t))^\top U (\boldsymbol{\psi}(\mathbf{u}(t)) - W\mathbf{x}(t)) < 0.$$

Figure 3.2 illustrates, for case two-dimensional, the inclusion of DoA, \mathcal{L}_V , in the set $\mathcal{D}_{\mathbf{u}}$, which is ensured the stability in presence of saturation.

Figure 3.2: DoA and sets \mathcal{D}_x and \mathcal{D}_u .

3.2 Problem Statement

Consider a continuous-time networked system which consists of N interconnected nonlinear heterogeneous subsystems with nonlinear interconnections and subject to control input saturation. The interconnection among subsystems is represented by an undirected graph $\mathcal{G}(\mathcal{V}, \mathcal{E})$. Each i -th subsystem is described as follows:

$$\dot{\mathbf{x}}_i(t) = f_i(\mathbf{x}_i(t)) + g_i(\mathbf{x}_i(t))\text{sat}(\mathbf{u}_i(t)) + \sum_{j \in \mathcal{N}_i} h_{ij}(\mathbf{x}_i(t), \mathbf{x}_j(t)), \quad (3.8)$$

where $i \in \mathcal{I}_N$, $\mathbf{x}_i(t) \in \mathbb{R}^{n_{x_i}}$ is the state vector of i -th subsystem; $\mathbf{u}_i(t) \in \mathbb{R}^{n_{u_i}}$ is the i -th control input vector; f_i , g_i and h_{ij} are smooth nonlinear functions.

Each subsystem in (3.8) can be represented by a N-TS fuzzy model, according to the discussion in Section 2.3. Thus, the i -th inferred N-TS fuzzy model is given as follows

$$\begin{aligned} \dot{\mathbf{x}}_i(t) = \sum_{l=1}^{r_i} \varsigma_i^l(\mathbf{z}_i(t)) & \left[A_i^l \mathbf{x}_i(t) + B_i^l \text{sat}(\mathbf{u}_i(t)) \right. \\ & \left. + \sum_{j \in \mathcal{N}_i} \left(H_{ii}^l \mathbf{x}_i(t) - H_{ij}^l \mathbf{x}_j(t) \right) + G_i^l \left(\sum_{j \in \mathcal{N}_i} \varphi_{ij}(\mathbf{x}_i(t), \mathbf{x}_j(t)) \right) \right], \end{aligned} \quad (3.9)$$

where $i \in \mathcal{I}_N$, A_i^l , B_i^l , H_{ij}^l and G_i^l are known constant matrices with appropriate dimensions; with the nonlinearities φ_{ij} being sector-bounded and satisfying Property 2.3.

For control design, we will consider the following nonlinear distributed control law for the i -th subsystem:

$$\mathbf{u}_i(t) = \sum_{l=1}^{r_i} \varsigma_i^l(\mathbf{z}_i(t)) K_i^l \mathbf{x}_i(t) + \sum_{j \in \mathcal{N}_i} \Gamma_{ij} \varphi_{ij}(\mathbf{x}_i(t), \mathbf{x}_j(t)) + \sum_{j \in \mathcal{N}_i} F_{ij} \mathbf{x}_j(t),$$

where $K_i^l \in \mathbb{R}^{n_{u_i} \times n_{x_i}}$, $\Gamma_{ij} \in \mathbb{R}^{n_{u_i} \times 1}$, and $F_{ij} \in \mathbb{R}^{n_{u_i} \times n_{x_j}}$, and \mathcal{N}_i is the set of indexes related to the subsystems in the network that are directly connected to the i -th subsystem; i.e.,

$j \in \mathcal{N}_i \Leftrightarrow \alpha_{ij} \neq 0$. To simplify the notation, henceforward matrices Γ_{ij} will be grouped by defining $\Gamma_i = \begin{bmatrix} \Gamma_{ij_1} & \Gamma_{ij_2} & \cdots & \Gamma_{ij_{d_{ii}}} \end{bmatrix} \in \mathbb{R}^{n_{u_i} \times d_{ii}}$, with $j_\kappa \in \mathcal{N}_i$, $\kappa \in \mathcal{I}_{d_{ii}}$, similarly to $\phi_i(\mathbf{x}(t))$ in Section 2.3, such that

$$\mathbf{u}_i(t) = \sum_{l=1}^{r_i} \varsigma_i^l(\mathbf{z}_i(t)) K_i^l \mathbf{x}_i(t) + \Gamma_i \phi_i(\mathbf{x}(t)) + \sum_{j \in \mathcal{N}_i} F_{ij} \mathbf{x}_j(t). \quad (3.10)$$

Example 3.1. For instance, considering Example 2.6, the neighborhood associated with the 4th subsystem is $\mathcal{N}_4 = \{1, 3, 5\}$. Therefore, matrix Γ_4 associated with the 4th subsystem is $\Gamma_4 = \begin{bmatrix} \Gamma_{41} & \Gamma_{43} & \Gamma_{45} \end{bmatrix}$.

The following assumption is considered in order to have a consistent control law in (3.10).

Assumption 3.1

The state vector $\mathbf{x}_j(t)$ is available for the i -th subsystem, and the nonlinear functions $\phi_{ij}(\mathbf{x}_i, \mathbf{x}_j)$ are known for the i -th subsystem, if $j \in \mathcal{N}_i$.

Similarly to (Dong, Wang, and Yang 2009), the nonlinearities $\phi_i(x(t))$ were incorporated in the nonlinear distributed control law (3.10). This *a priori* additional information aims to improve the system response by reducing conservativeness in the controller synthesis procedure. The same approach has been used in several works on N-TS fuzzy systems either for continuous-time (Dong, Wang, and Yang 2009; Moodi et al. 2019) or for discrete-time systems (Coutinho et al. 2020; Dong, Wang, and Yang 2011; Klug, Castelan, and Coutinho 2015; Klug et al. 2015).

Remark 3.1

A decentralized control law can be obtained by taking $\Gamma_i = 0$ and $F_{ij} = 0$, $\forall i \in \mathcal{I}_N$ and $\forall j \in \mathcal{N}_i$. A distributed control law that is *linear* with respect to state variables from neighboring subsystems corresponds to $\Gamma_i = 0$, $\forall i \in \mathcal{I}_N$. On the other hand, a *nonlinear* distributed control law inspired in the one in (Dong, Wang, and Yang 2009)^a, would be obtained by taking $F_{ij} = 0$, $\forall i \in \mathcal{I}_N$ and $\forall j \in \mathcal{N}_i$. The last one is a distributed control law since the nonlinear interconnections also depend on the states of subsystems in the neighborhood of the i -th subsystem.

^aDong, Wang, and Yang 2009 deals only with a single system and the control law is considered centralized.

Using the representation of saturation as dead-zone nonlinearity and substituting (3.10) into (3.9) leads to the following closed-loop subsystem:

$$\begin{aligned}\dot{\mathbf{x}}_i(t) = & \sum_{k=1}^{r_i} \sum_{l=1}^{r_i} \varsigma_i^k(\mathbf{z}_i(t)) \varsigma_j^l(\mathbf{z}_i(t)) \left(A_i^k + B_i^k K_i^l + d_{ii} H_{ii}^k \right) \mathbf{x}_i(t) \\ & + \sum_{j \in \mathcal{N}_i} \sum_{k=1}^{r_i} \varsigma_i^k(\mathbf{z}_i(t)) \left(B_i^k F_{ij} - H_{ij}^k \right) \mathbf{x}_j(t) \\ & + \sum_{k=1}^{r_i} \varsigma_i^k(\mathbf{z}_i(t)) \left(B_i^k \Gamma_i + G_i^k \mathbf{1}_{d_{ii}}^\top \right) \boldsymbol{\phi}_i(\mathbf{x}(t)) - \sum_{k=1}^{r_i} \varsigma_i^k(\mathbf{z}_i(t)) B_i^k \boldsymbol{\psi}_i(\mathbf{u}_i(t))\end{aligned}\quad (3.11)$$

where $\boldsymbol{\psi}_i(\mathbf{u}_i(t)) = \mathbf{u}_i(t) - \text{sat}(\mathbf{u}_i(t))$ is the dead-zone nonlinearity.

Remark 3.2

To consider systems without saturation, one must eliminate terms with regard to the dead-zone nonlinearity in (3.11).

According to what was discussed in section 3.1.1, state and control input constraints should be considered, since the set of interconnected closed-loop subsystems are only valid in a local region $\mathcal{D}_{\mathbf{x}}$, besides, saturation is described as dead-zone nonlinearity and defines a region $\mathcal{D}_{\mathbf{u}}$. Further, the maximization of the volume of the DoA estimate is pursued. Thus, we establish the following problem.

Problem 3.1

Design a nonlinear distributed controller (3.10) for each i -th subsystem (3.9), such that the volume of the DoA estimate, $\mathcal{L}_V \subset \mathcal{D}_{\mathbf{x}} \cap \mathcal{D}_{\mathbf{u}}$, of the networked nonlinear closed-loop system, composed by the interconnected subsystems (3.11), is maximized.

3.3 Stabilization of Interconnected N-TS Fuzzy Systems

It is known that Lyapunov inequalities for linear systems admit block-diagonal solutions (Sootla, Zheng, and Papachristodoulou 2017, 2019). Thus, the following quadratic block-diagonal Lyapunov function candidate is considered in the stability analysis of the N interconnected closed-loop subsystems in (3.11):

$$V(\mathbf{x}(t)) = \sum_{i=1}^N \mathbf{x}_i(t)^\top P_i \mathbf{x}_i(t) = \mathbf{x}(t)^\top \mathbf{P}_N \mathbf{x}(t), \quad (3.12)$$

where $\mathbf{x}(t) = \begin{bmatrix} \mathbf{x}_1(t)^\top & \mathbf{x}_2(t)^\top & \cdots & \mathbf{x}_N(t)^\top \end{bmatrix}^\top$, $\mathbf{P}_N = \bigoplus_{i=1}^N P_i$, with $P_i = P_i^\top \succ 0$.

Initially, to demonstrate the effects of multiple fuzzy summation when dealing with a networked system, we will consider that subsystems are free from both state and control input constraints, see Remark 3.2.

The next theorem provides sufficient conditions to ensure that the origin of the networked nonlinear system is asymptotically stable. As the theorem addresses all subsystems of the whole network, the notation of multi-index introduced in Section 2.3 will be used.

Theorem 3.1: Stabilization of networked system I

Let $\mathbf{\Omega}_i, \forall i \in \mathcal{I}_N$ given. If there exist matrices $Q_i \succ 0$, diagonal matrices $\Lambda_i \succ 0$, and any matrices $R_i^{l_{i,2}}, S_{ij}$ and $T_i, \forall i \in \mathcal{I}_N, \forall l_{i,2} \in \mathcal{I}_{r_i}$ and $\forall j \in \mathcal{N}_i$, satisfying (3.13):

$$\sum_{l_{1,1}=1}^{r_1} \sum_{l_{1,2}=1}^{r_1} \cdots \sum_{l_{N,1}=1}^{r_N} \sum_{l_{N,2}=1}^{r_N} \varsigma_1^{l_{1,1}} \varsigma_1^{l_{1,2}} \cdots \varsigma_N^{l_{N,1}} \varsigma_N^{l_{N,2}} \begin{bmatrix} \mathbf{\Theta}_N + \mathbf{\Delta} & \star \\ \mathbf{\Pi}_N + \mathbf{\Omega} \mathbf{Q}_N & -2\mathbf{\Lambda}_N \end{bmatrix} \prec 0, \quad (3.13)$$

where,

$$\begin{aligned} \mathbf{\Theta}_N &= \bigoplus_{i=1}^N \left(\left(A_i^{l_{i,1}} Q_i + d_{ii} H_{ii}^{l_{i,1}} Q_i + B_i^{l_{i,1}} R_i^{l_{i,2}} \right)^\top + \left(A_i^{l_{i,1}} Q_i + d_{ii} H_{ii}^{l_{i,1}} Q_i + B_i^{l_{i,1}} R_i^{l_{i,2}} \right) \right), \\ \mathbf{Q}_N &= \bigoplus_{i=1}^N Q_i, \mathbf{\Lambda}_N = \bigoplus_{i=1}^N \Lambda_i, \mathbf{\Pi}_N = \bigoplus_{i=1}^N \left(B_i^{l_{i,1}} T_i + G_i^{l_{i,1}} \mathbf{1}_{d_{ii}}^\top \Lambda_i \right)^\top, \mathbf{\Omega} = \left[\mathbf{\Omega}_1^\top \quad \cdots \quad \mathbf{\Omega}_N^\top \right]^\top \\ \mathbf{\Delta} &= \begin{cases} \Delta_{ij} = \mathbf{0}_{n_{x_i} \times n_{x_j}}, & \text{if } \alpha_{ij} = 0 \\ \Delta_{ij} = B_i^{l_{i,1}} S_{ij} + S_{ji}^\top B_j^{l_{j,1}}^\top - H_{ij}^{l_{i,1}} Q_j - Q_i H_{ji}^{l_{j,1}}^\top, & \text{if } \alpha_{ij} = 1 \end{cases}. \end{aligned}$$

Then continuous-time networked nonlinear system represented by a given undirected graph $\mathcal{G}(\mathcal{V}, \mathcal{E})$, composed by N interconnected closed-loop subsystems given in (3.11), is stable and the control gains in (3.10) are: $K_i^{l_{i,1}} = R_i^{l_{i,1}} Q_i^{-1}$, $\Gamma_i = T_i \Lambda_i^{-1}$ and $F_{ij} = S_{ij} Q_j^{-1}$.

Proof. If inequality (3.13) holds, taking $R_i^{l_{i,1}} = K_i^{l_{i,1}} Q_i$, $T_i = \Gamma_i \Lambda_i$, and $S_{ij} = F_{ij} Q_j$, $\forall i \in \mathcal{I}_N, \forall l_{i,1} \in \mathcal{I}_{r_i}$ and $\forall j \in \mathcal{N}_i$; and applying the congruence transformation $\text{diag}(\mathbf{P}_N, \mathbf{\Lambda}_N^{-1}, U^{-1})$, leads to the matrix inequality:

$$\sum_{l_{1,1}=1}^{r_1} \sum_{l_{1,2}=1}^{r_1} \cdots \sum_{l_{N,1}=1}^{r_N} \sum_{l_{N,2}=1}^{r_N} \varsigma_1^{l_{1,1}} \varsigma_1^{l_{1,2}} \cdots \varsigma_N^{l_{N,1}} \varsigma_N^{l_{N,2}} \begin{bmatrix} \tilde{\mathbf{\Theta}}_N + \tilde{\mathbf{\Delta}} \\ \tilde{\mathbf{\Pi}}_N + \mathbf{\Lambda}_N^{-1} \mathbf{\Omega} & -2\mathbf{\Lambda}_N^{-1} \end{bmatrix} \prec 0, \quad (3.14)$$

with

$$\begin{aligned}\tilde{\Theta}_N &= \bigoplus_{i=1}^N \left(\left(A_i^{l_{i,1}} + B_i^{l_{i,1}} K_i^{l_{i,2}} + d_{ii} H_{ii}^{l_{i,1}} \right)^\top P_i + P_i \left(A_i^{l_{i,1}} + B_i^{l_{i,1}} K_i^{l_{i,2}} + d_{ii} H_{ii}^{l_{i,1}} \right) \right), \\ \tilde{\Delta} &= \begin{cases} \tilde{\Delta}_{ij} = \mathbf{0}_{n_{x_i} \times n_{x_j}}, & \text{if } \alpha_{ij} = 0 \\ \tilde{\Delta}_{ij} = P_i B_i^{l_{i,1}} F_{ij} + F_{ji}^\top B_j^{l_{j,2}^\top} P_j - P_i H_{ij}^{l_{i,1}} - H_{ji}^{l_{j,2}^\top} P_j, & \text{if } \alpha_{ij} = 1 \end{cases}, \\ \tilde{\Pi}_N &= \bigoplus_{i=1}^N \left(B_i^{l_{i,1}} \Gamma_i + G_i^{l_{i,1}} \mathbf{1}_{d_{ii}}^\top \right)^\top P_i.\end{aligned}$$

Pre- and pos-multiplying (3.14) by $\begin{bmatrix} \mathbf{x}^\top & \boldsymbol{\phi}(\mathbf{x})^\top \end{bmatrix}$ and its transpose, and considering (3.11) and (3.12), one has that

$$\dot{V}(\mathbf{x}) - 2 \sum_{i \in \mathcal{I}_N} \boldsymbol{\phi}_i(\mathbf{x})^\top \Lambda_i^{-1} (\boldsymbol{\phi}_i(\mathbf{x}) - \boldsymbol{\Omega}_i \mathbf{x}) < 0. \quad (3.15)$$

Notice that since each nonlinearity $\boldsymbol{\phi}_i(\mathbf{x})$ verifies a sector condition as in (2.20), the inequality (3.15) defines an upper bound for the time derivative of the Lyapunov function (3.12), implying $\dot{V}(\mathbf{x}) < 0$, $\forall \mathbf{x} \neq 0$. This completes the proof. \square

One of the main difficulties when dealing with interconnected systems using TS fuzzy models is to obtain conditions from the combinations of the rules of each subsystem (Tanaka and Wang 2001), since with the increasing amount of subsystems the number of LMIs grows exponentially. This happens in Theorem 3.1, since Lemma 2.3 must be used to obtain a finite number of LMIs.

To avoid this problem and to ensure that the asymptotic stability of the subsystem trajectories, we propose conditions based on LMI constraints obtained in a similar way as the one presented in (Lam and Lauber 2012; Lin, Wang, and Yang 2007), where membership functions have been used together with state variables to define a quadratic form.

For this, Lemma 2.1 is applied into each i -th closed-loop subsystem (3.11), thus, an equivalent form of (3.11) is given by

$$\begin{aligned}\dot{\mathbf{x}}_i(t) &= \sum_{k=1}^{r_i} (\varsigma_i^k(\mathbf{z}_i(t)))^2 \mathbb{A}_i^{kk} \mathbf{x}_i(t) + 2 \sum_{k=1}^{r_i-1} \sum_{l=k+1}^{r_i} \varsigma_i^k(\mathbf{z}_i(t)) \varsigma_i^l(\mathbf{z}_i(t)) \left(\frac{\mathbb{A}_i^{kl} + \mathbb{A}_i^{lk}}{2} \right) \mathbf{x}_i(t) \\ &\quad + \sum_{j \in \mathcal{N}_i} \sum_{k=1}^{r_i} \varsigma_i^k(\mathbf{z}_i(t)) \left(B_i^k F_{ij} - H_{ij}^k \right) \mathbf{x}_j(t) \\ &\quad + \sum_{k=1}^{r_i} \varsigma_i^k(\mathbf{z}_i(t)) \left(B_i^k \Gamma_i + G_i^k \mathbf{1}_{d_{ii}}^\top \right) \boldsymbol{\phi}_i(\mathbf{x}(t)) - \sum_{k=1}^{r_i} \varsigma_i^k(\mathbf{z}_i(t)) B_i^k \boldsymbol{\psi}_i(\mathbf{u}_i(t))\end{aligned} \quad (3.16)$$

where $\mathbf{A}_i^{kl} = A_i^k + B_i^k K_i^l + d_{ii} H_{ii}^k$ and $\boldsymbol{\psi}_i(\mathbf{u}_i(t)) = \mathbf{u}_i(t) - \text{sat}(\mathbf{u}_i(t))$ is the dead-zone nonlinearity. In addition, the following vector is defined:

$$\bar{\mathbf{x}} = \left[\boldsymbol{\varsigma}_1^\top \otimes \mathbf{x}_1^\top \quad \boldsymbol{\varsigma}_2^\top \otimes \mathbf{x}_2^\top \quad \cdots \quad \boldsymbol{\varsigma}_N^\top \otimes \mathbf{x}_N^\top \right]^\top, \quad (3.17)$$

where $\boldsymbol{\varsigma}_i = \left[\varsigma_i^1(\mathbf{z}_i(t)) \quad \varsigma_i^2(\mathbf{z}_i(t)) \quad \cdots \quad \varsigma_i^{r_i}(\mathbf{z}_i(t)) \right]^\top$ is the vector of membership functions of the i -th subsystem.

To deal with saturation, a modified version of Lemma 3.1 is presented in Lemma 3.2 to consider the control law (3.10).

Lemma 3.2: *Dead-zone nonlinearity* for distributed control law (3.10)

Consider the set

$$\mathcal{D}_{\mathbf{u}} = \left\{ \mathbf{x} \in \mathbb{R}^{n_x} : \left| (\mathbf{K}_N + \mathbf{F} - W)_{(l)} \bar{\mathbf{x}} + (\boldsymbol{\Gamma}_N - J)_{(l)} \boldsymbol{\phi}(\mathbf{x}) \right| \leq \bar{u}_l, \forall l \in \mathcal{I}_{n_u} \right\}, \quad (3.18)$$

where $W \in \mathbb{R}^{n_u \times n_{\bar{x}}}$ and $J \in \mathbb{R}^{n_u \times n_{\phi}}$ are any matrices with dimensions defined by $n_{\bar{x}} = \sum_{i=1}^N r_i n_{x_i}$, $n_u = \sum_{i=1}^N n_{u_i}$, and $n_{\phi} = \sum_{i=1}^N d_{ii}$; $\mathbf{K}_N = \bigoplus_{i=1}^N \begin{bmatrix} K_i^1 & \cdots & K_i^{r_i} \end{bmatrix}$, $\boldsymbol{\Gamma}_N = \bigoplus_{i=1}^N \boldsymbol{\Gamma}_i$, the block matrix $\mathbf{F} = [\bar{F}_{ij}]$, with $\bar{F}_{ij} = \mathbf{1}_{r_j}^\top \otimes F_{ij}$, if $\alpha_{ij} = 1$ and $F_{ii} = \mathbf{0}_{n_{u_i} \times r_j n_{x_j}}$, if $\alpha_{ij} = 0$.

If $\mathbf{x} \in \mathcal{D}_{\mathbf{u}}$, then

$$\boldsymbol{\psi}(\mathbf{u})^\top U^{-1} (\boldsymbol{\psi}(\mathbf{u}) - W \bar{\mathbf{x}} - J \boldsymbol{\phi}(\mathbf{x})) \leq 0, \quad (3.19)$$

holds for any positive definite diagonal matrix $U \in \mathbb{R}^{n_u \times n_u}$, with $\boldsymbol{\phi}(\mathbf{x}) = \left[\boldsymbol{\phi}_1(\mathbf{x})^\top \quad \cdots \quad \boldsymbol{\phi}_N(\mathbf{x})^\top \right]^\top$, and $\boldsymbol{\psi}(\mathbf{u}) = \left[\boldsymbol{\psi}_1(\mathbf{u}_1)^\top \quad \cdots \quad \boldsymbol{\psi}_N(\mathbf{u}_N)^\top \right]^\top$.

Proof. The proof follows the same steps of Lemma 3.1 and has been omitted here. \square

The following theorem provides sufficient conditions to ensure that the origin of the networked nonlinear system is locally asymptotically stable.

Theorem 3.2: Stabilization of networked system II (Araújo, Torres, and Palhares 2020)

Let $\beta_v, \bar{u}_l, \forall v \in \mathcal{I}_{n_e}, \forall l \in \mathcal{I}_{n_u}$, and $\Omega_i, \forall i \in \mathcal{I}_N$ given. If there exist matrices $Q_i \succ 0$, diagonal matrices $\Lambda_i \succ 0, U \succ 0$, and any matrices W, J, R_i^l, S_{ij} and $T_i, \forall i \in \mathcal{I}_N, \forall l \in \mathcal{I}_{r_i}$ and $\forall j \in \mathcal{N}_i$, satisfying the following LMIs:

$$\begin{bmatrix} 1 & \star \\ Q_N \beta_v & Q_N \end{bmatrix} \succeq 0, \quad \forall v \in \mathcal{I}_{n_e}, \quad (3.20)$$

$$\begin{bmatrix} \tilde{Q}_N & \star & \star \\ -\tilde{\Omega} \tilde{Q}_N & 2\Lambda_N & \star \\ (R_N + S - W)_{(l)} & (T_N - J)_{(l)} & \bar{u}_l^2 \end{bmatrix} \succ 0, \quad \forall l \in \mathcal{I}_{n_u}, \quad (3.21)$$

$$\begin{bmatrix} \Theta_N + \Delta & \star & \star \\ \Pi_N + \tilde{\Omega} \tilde{Q}_N & -2\Lambda_N & \star \\ -UB_N + W & J & -2U \end{bmatrix} \prec 0, \quad (3.22)$$

where,

$$Q_N = \bigoplus_{i=1}^N Q_i, \quad \bar{Q}_N = \bigoplus_{i=1}^N (I_{r_i} \otimes Q_i), \quad \tilde{Q}_N = \bigoplus_{i=1}^N (\mathbf{1}_{r_i \times r_i} \otimes Q_i), \quad \Lambda_N = \bigoplus_{i=1}^N \Lambda_i,$$

$$R_N = \bigoplus_{i=1}^N \begin{bmatrix} R_i^1 & \cdots & R_i^{r_i} \end{bmatrix}, \quad T_N = \bigoplus_{i=1}^N T_i, \quad B_N = \bigoplus_{i=1}^N \begin{bmatrix} B_i^{1^\top} & \cdots & B_i^{r_i^\top} \end{bmatrix},$$

$$\Theta_N = \bigoplus_{i=1}^N \begin{bmatrix} \Theta_i^{11} & \cdots & \Theta_i^{1r_i} \\ \vdots & \ddots & \vdots \\ \Theta_i^{r_i 1} & \cdots & \Theta_i^{r_i r_i} \end{bmatrix}, \quad \Theta_i^{kl} = \left(\frac{\bar{A}_i^{kl} + \bar{A}_i^{lk}}{2} \right)^\top + \left(\frac{\bar{A}_i^{kl} + \bar{A}_i^{lk}}{2} \right),$$

$$\bar{A}_i^{kl} = A_i^k Q_i + d_{ii} H_{ii}^k Q_i + B_i^k R_i^l,$$

$$\Delta = \begin{cases} \Delta_{ij} = \mathbf{0}_{r_i n_{x_i} \times r_j n_{x_j}}, & \text{if } \alpha = 0 \\ \Delta_{ij} = [\Delta_{ij}^{kl}], & \text{if } \alpha = 1, \text{ with } \Delta_{ij}^{kl} = B_i^k S_{ij} + S_{ji}^\top B_j^{l^\top} - H_{ij}^k Q_j - Q_i H_{ji}^{l^\top} \end{cases},$$

$$\Pi_N = \bigoplus_{i=1}^N \begin{bmatrix} \Pi_i^1 & \cdots & \Pi_i^{r_i} \end{bmatrix}, \quad \Pi_i^k = \left(B_i^k T_i + G_i^k \mathbf{1}_{d_{ii}}^\top \Lambda_i \right)^\top,$$

$$\bar{\Omega} = \begin{bmatrix} \bar{\Omega}_1^\top & \bar{\Omega}_2^\top & \cdots & \bar{\Omega}_N^\top \end{bmatrix}^\top, \quad \text{with } \bar{\Omega}_i = \begin{bmatrix} \mathbf{1}_{r_1}^\top \otimes \Omega_{i1} & \mathbf{1}_{r_2}^\top \otimes \Omega_{i2} & \cdots & \mathbf{1}_{r_N}^\top \otimes \Omega_{iN} \end{bmatrix},$$

$$S = [\bar{S}_{ij}], \quad \text{with } \bar{S}_{ij} = \mathbf{1}_{r_j}^\top \otimes S_{ij}, \text{ if } \alpha_{ij} = 1, \text{ or } \bar{S}_{ij} = \mathbf{0}_{n_{u_i} \times r_j n_{x_j}}, \text{ if } \alpha_{ij} = 0.$$

Then continuous-time networked nonlinear system represented by a given undirected graph $\mathcal{G}(\mathcal{V}, \mathcal{E})$, composed by N interconnected closed-loop subsystems given in (3.16), is stable and the control gains in (3.10) are: $K_i^l = R_i^l Q_i^{-1}$, $\Gamma_i = T_i \Lambda_i^{-1}$ and $F_{ij} = S_{ij} Q_j^{-1}$.

Proof. Assume that (3.20) is satisfied. Applying the congruence transformation $\text{diag}(1, \mathbf{P}_N)$, with $P_i = Q_i^{-1}$, $\forall i \in \mathcal{I}_N$, in (3.20) one has that

$$\begin{bmatrix} 1 & \star \\ \boldsymbol{\beta}_v & \mathbf{P}_N \end{bmatrix} \succeq 0, \quad \forall v \in \mathcal{I}_{n_e},$$

and pre- and pos-multiplying the last inequality by $\begin{bmatrix} 1 & -\mathbf{x}^\top \end{bmatrix}$ and its transpose, respectively, it results:

$$1 - \mathbf{x}^\top \boldsymbol{\beta}_v - \boldsymbol{\beta}_v^\top \mathbf{x} + \mathbf{x}^\top \mathbf{P}_N \mathbf{x} \geq 0.$$

Since $\mathbf{x}^\top \mathbf{P}_N \mathbf{x} \leq 1$, $\forall \mathbf{x} \in \mathcal{L}_V$, then $2 - \mathbf{x}^\top \boldsymbol{\beta}_v - \boldsymbol{\beta}_v^\top \mathbf{x} \geq 0$ holds $\forall \mathbf{x} \in \mathcal{L}_V$, implying that $\boldsymbol{\beta}_v^\top \mathbf{x} \leq 1$. Hence, $\mathcal{L}_V \subseteq \mathcal{D}_\mathbf{x}$, with $\mathcal{D}_\mathbf{x}$ defined in (3.1).

Next, applying a congruence transformation to (3.21) with $\text{diag}(\bar{\mathbf{P}}_N, \boldsymbol{\Lambda}_N^{-1}, 1)$, with $\bar{\mathbf{P}}_N = \bigoplus_{i=1}^N (I_{r_i} \otimes P_i)$, $\boldsymbol{\Lambda}_N^{-1} = \bigoplus_{i=1}^N \Lambda_i^{-1}$ and $\bar{\mathbf{P}}_N = \bar{\mathbf{Q}}_N^{-1}$, followed by the application of the Schur complement Lemma, we obtain

$$\begin{bmatrix} \bar{\mathbf{P}}_N & \star \\ -\boldsymbol{\Lambda}_N^{-1} \bar{\boldsymbol{\Omega}} & 2\boldsymbol{\Lambda}_N^{-1} \end{bmatrix} - \frac{1}{\bar{u}_l^2} \mathbf{Y}_{(l)}^\top \mathbf{Y}_{(l)} \succ 0, \quad \forall l \in \mathcal{I}_{n_u}, \quad (3.23)$$

where $\bar{\mathbf{P}}_N = \bigoplus_{i=1}^N (1_{r_i \times r_i} \otimes P_i)$, and $\mathbf{Y} = \begin{bmatrix} \mathbf{K}_N + \mathbf{F} - \tilde{\mathbf{W}} & \boldsymbol{\Gamma}_N - \tilde{\mathbf{J}} \end{bmatrix}$, with $\tilde{\mathbf{W}} = \mathbf{W} \bar{\mathbf{P}}_N$ and $\tilde{\mathbf{J}} = \mathbf{J} \boldsymbol{\Lambda}_N^{-1}$. Pre- and pos-multiplying (3.23) by $\begin{bmatrix} \bar{\mathbf{x}}^\top & \boldsymbol{\phi}(\mathbf{x})^\top \end{bmatrix}$ and its transpose, considering (3.16) and using (3.12) as Lyapunov function, it leads to

$$\begin{aligned} V(\mathbf{x}) + 2 \sum_{i \in \mathcal{I}_N} \boldsymbol{\phi}_i(\mathbf{x})^\top \Lambda_i^{-1} (\boldsymbol{\phi}_i(\mathbf{x}) - \bar{\boldsymbol{\Omega}}_i \bar{\mathbf{x}}) \\ - \frac{\| (\mathbf{K}_N + \mathbf{F} - \tilde{\mathbf{W}})_{(l)} \bar{\mathbf{x}} + (\boldsymbol{\Gamma}_N - \tilde{\mathbf{J}})_{(l)} \boldsymbol{\phi}(\mathbf{x}) \|^2}{\bar{u}_l^2} > 0. \end{aligned}$$

Thus, since each nonlinearity $\boldsymbol{\phi}_i(\mathbf{x})$ verifies a sector condition (according to Remark 2.4), Lemma 3.2 it valid $\forall \mathbf{x}(t) \in \mathcal{L}_V$ and it follows that $\mathcal{L}_V \subset \mathcal{D}_u$, with \mathcal{D}_u defined in (3.18).

Finally, if inequality (3.22) holds, taking $R_i^l = K_i^l Q_i$, $T_i = \Gamma_i \Lambda_i$, and $S_{ij} = F_{ij} Q_j$, $\forall i \in \mathcal{I}_N$, $\forall l \in \mathcal{I}_{r_i}$ and $\forall j \in \mathcal{N}_i$; and applying the congruence transformation $\text{diag}(\bar{\mathbf{P}}_N, \boldsymbol{\Lambda}_N^{-1}, U^{-1})$, it leads to the matrix inequality:

$$\begin{bmatrix} \tilde{\boldsymbol{\Theta}}_N + \tilde{\boldsymbol{\Delta}} & \star & \star \\ \tilde{\boldsymbol{\Pi}}_N + \boldsymbol{\Lambda}_N^{-1} \bar{\boldsymbol{\Omega}} & -2\boldsymbol{\Lambda}_N^{-1} & \star \\ -\mathbf{B}_N \bar{\mathbf{P}}_N + U^{-1} \mathbf{W} \bar{\mathbf{P}}_N & U^{-1} \mathbf{J} \boldsymbol{\Lambda}_N^{-1} & -2U^{-1} \end{bmatrix} \prec 0, \quad (3.24)$$

with

$$\begin{aligned}\tilde{\Theta}_N &= \bigoplus_{i=1}^N \begin{bmatrix} \tilde{\Theta}_i^{11} & \dots & \tilde{\Theta}_i^{1r_i} \\ \vdots & \ddots & \vdots \\ \tilde{\Theta}_i^{r_i 1} & \dots & \tilde{\Theta}_i^{r_i r_i} \end{bmatrix}, \quad \tilde{\Theta}_i^{kl} = \left(\frac{\mathbb{A}_i^{kl} + \mathbb{A}_i^{lk}}{2} \right)^\top P_i + P_i \left(\frac{\mathbb{A}_i^{kl} + \mathbb{A}_i^{lk}}{2} \right), \\ \tilde{\Delta} &= \begin{cases} \tilde{\Delta}_{ij} = \mathbf{0}_{r_i n_{x_i} \times r_j n_{x_j}}, & \text{if } \alpha = 0 \\ \tilde{\Delta}_{ij} = [\tilde{\Delta}_{ij}^{kl}], & \text{if } \alpha = 1, \text{ with } \tilde{\Delta}_{ij}^{kl} = P_i B_i^k F_{ij} + F_{ji}^\top B_j^l P_j - P_i H_{ij}^k - H_{ji}^{l\top} P_j \end{cases}, \\ \tilde{\Pi}_N &= \bigoplus_{i=1}^N \begin{bmatrix} \tilde{\Pi}_i^1 & \dots & \tilde{\Pi}_i^{r_i} \end{bmatrix}, \quad \tilde{\Pi}_i^k = \left(B_i^k \Gamma_i + G_i^k \mathbf{1}_{d_{ii}}^\top \right)^\top P_i.\end{aligned}$$

Pre- and pos-multiplying (3.24) by $\begin{bmatrix} \bar{\mathbf{x}}^\top & \boldsymbol{\phi}(\mathbf{x})^\top & \boldsymbol{\psi}(\mathbf{u})^\top \end{bmatrix}$ and its transpose, and considering (3.12), one has that

$$\dot{V}(\mathbf{x}) - 2 \sum_{i \in \mathcal{I}_N} \boldsymbol{\phi}_i(\mathbf{x})^\top \Lambda_i^{-1} (\boldsymbol{\phi}_i(\mathbf{x}) - \bar{\mathbf{\Omega}}_i \bar{\mathbf{x}}) - 2 \boldsymbol{\psi}(\mathbf{u})^\top U^{-1} (\boldsymbol{\psi}(\mathbf{u}) - \tilde{W} \bar{\mathbf{x}} - \tilde{J} \boldsymbol{\phi}(\mathbf{x})) < 0. \quad (3.25)$$

Notice that since each nonlinearity $\boldsymbol{\phi}_i(\mathbf{x})$ verifies a sector condition as in (2.20) and $\boldsymbol{\psi}(\mathbf{u})$ is a dead-zone nonlinearity and satisfies (3.19), inequality (3.25) defines an upper bound for the time derivative of the Lyapunov function (3.12), implying $\dot{V}(\mathbf{x}) < 0, \forall \mathbf{x} \neq 0$. This completes the proof. \square

Remark 3.3

Notice that the combination of membership functions of different subsystems is avoided in LMI constraint (3.22), because Lemma 2.1 is applied in each i -th subsystem and then using the membership functions together with states to generate the quadratic form.

Theorem 3.2 provides sufficient conditions to ensure asymptotic stability and an estimate of the DoA, \mathcal{L}_V , of the networked nonlinear system. However, we are interested in finding the largest estimate considering $\mathcal{D}_{\mathbf{x}}$ and $\mathcal{D}_{\mathbf{u}}$, i.e., $\mathcal{L}_V \subset \mathcal{D}_{\mathbf{x}} \cap \mathcal{D}_{\mathbf{u}}$. The following Corollary solves Problem 3.1 incorporating the maximization of the volume of \mathcal{L}_V , while still considering the sufficient conditions in Theorem 3.2.

Corollary 3.1: Maximization of the DoA estimate

If the optimization problem,

$$\begin{aligned} & \max_{Q_i, \Lambda_i, U, W, J, R_i^l, S_{ij}, T_i} \det(Q_N)^{1/n_x} \\ & \text{subject to (3.20), (3.21) and (3.22)} \end{aligned}$$

is feasible, then Problem 3.1 has a solution that gives the largest positively invariant ellipsoidal set \mathcal{L}_V under the considered constraints.

Proof. Note that maximizing $\det(Q_N)^{1/n_x}$ implies on minimizing $\det(P_N)^{1/n_x}$ and hence the volume of the set \mathcal{L}_V associated with the Lyapunov function (3.12) is maximized. The rest of the proof is a direct consequence of Theorem 3.2. \square

Remark 3.4

Notice that in the case when saturation is not taken into account, it is necessary to exclude in the Theorem 3.2 the LMI constraint (3.21) as well as 3th row and 3th column in LMI constraint (3.22). Furthermore, one has to pay attention when using Corollary 3.1 since if there is no saturation on the control inputs, the state constraints must form a compact polytopic set such that the cost function in the optimization problem remains bounded.

3.4 Illustrative Examples

In this section, two study cases are presented to illustrate the effectiveness of the nonlinear distributed control strategy. The first example is an electrical power system composed of two-machine subsystems discussed in Lin, Wang, and Yang 2007. The second one is a network of multiple inverted pendulums coupled by nonlinear springs presented in the Example 2.7, which is a modified version of the example presented in (Šiljak 2012).

All simulation results presented throughout this chapter were obtained using the Yalmip parser (Löfberg 2004) and Mosek solver (Mosek 2017) performing on software Matlab R2018b.

3.4.1 Two-machine Subsystems

Consider an electrical power system composed of two-machine subsystems and given as in (Lin, Wang, and Yang 2007):

$$\begin{aligned}\dot{x}_{i1}(t) &= x_{i2}(t), \\ \dot{x}_{i2}(t) &= -\frac{D_i}{M_i}x_{i2}(t) + \frac{1}{M_i}u_i(t) \\ &\quad + \sum_{j=1}^2 \frac{V_i V_j Y_{ij}}{M_i} \times [\cos(\delta_{ij}^0 - \theta_{ij}) - \cos(x_{i1}(t) - x_{j1}(t) + \delta_{ij}^0 - \theta_{ij})],\end{aligned}\tag{3.26}$$

where $i \in \mathcal{I}_2$, $x_{i1}(t)$ denotes the absolute rotor angle and $x_{i2}(t)$ is the angular velocity of the i -th machine. Parameters M_i , D_i , V_i , and Y_{ij} denote the inertia coefficient, damping coefficient, internal voltage, and the modulus of the transfer admittance between the i -th and j -th machine, respectively. All parameter values are the same used in (Lin, Wang, and Yang 2007).

For $i \in \mathcal{I}_2$, one has $x(t) = [x_{11} \ x_{12} \ x_{21} \ x_{22}]^\top$, note that by considering $x_{i1}(t) \in [-\pi/2, \pi/2]$ nonlinear interconnections $\varphi_{ij}(x_i, x_j) = \cos(\delta_{ij}^0 - \theta_{ij}) - \cos(x_{i1} - x_{j1} + \delta_{ij}^0 - \theta_{ij})$ belong to the sector $\varphi_{ij}(x_i, x_j) \in \text{co}\{\Omega_L x(t), \Omega_U x(t)\}$, with $\Omega_L = [-0.813 \ 0 \ 0.813 \ 0]$, $\Omega_U = [0.628 \ 0 \ -0.628 \ 0]$, which can be transformed in a sector nonlinearity $\bar{\varphi}_{ij}(x_i, x_j) = \cos(\delta_{ij}^0 - \theta_{ij}) - \cos(x_{i1} - x_{j1} + \delta_{ij}^0 - \theta_{ij}) - \Omega_L x \in \text{co}\{0, \Omega_i x(t)\}$, where $\Omega_i = \Omega_U - \Omega_L$ as in (Dong, Wang, and Yang 2009). Thus, the system of two-machine in (3.26) can be described as follows:

$$\begin{aligned}\dot{x}_{i1}(t) &= x_{i2}(t), \\ \dot{x}_{i2}(t) &= -\frac{D_i}{M_i}x_{i2}(t) + \frac{1}{M_i}u_i(t) + \sum_{j=1}^2 \frac{V_i V_j Y_{ij}}{M_i}(\bar{\varphi}_{ij}(x_i, x_j) + E_L x(t)),\end{aligned}\tag{3.27}$$

Although the model in (3.27) does not have local nonlinearities. Thus, the whole networked system is represented by only one rule independently of the subsystems number, which is an advantage over the approach in (Lin, Wang, and Yang 2007), where 9 rules are required to describe the system with two machines. Notice that this number will increase exponentially in the case of adding more machines. In addition, in (Lin, Wang, and Yang 2007) an approximate approach is used to obtain the fuzzy rules describing the system (Takagi and Sugeno 1985), and it is not possible to estimate a DoA since there is no guarantee of convergence for any initial condition.

In order to compare the approaches, the LMI given in (3.20) has been added in the condition of Remark 1 in (Lin, Wang, and Yang 2007), which ensures the validity of the model; as well as the cost function in Corollary 3.1, which aims to compare the volume of the DoA that this approach would generate if it would be possible to compute. In this case, the proposed methodology has been performed disregarding saturation, i.e. the LMI condition (3.21) and 3th row and 3th column in LMI condition (3.22) has been excluded.

In addition, constraint $x_{i2}(t) \in [-2\pi, 2\pi]$ is also considered in order to avoid that the cost function of the optimization problem is unbounded. Table 3.1 presents values of $\det(\mathbf{Q}_N)^{1/n_x}$, which is proportional to volume of DoA obtained with the aforementioned approaches. Note that the methodology in Section 3.3 returns a DoA greater with regarding to the proposed extension from (Lin, Wang, and Yang 2007).

Table 3.1: Values of $\det(\mathbf{Q}_N)^{1/n_x}$ obtained with extension of (Lin, Wang, and Yang 2007) and Corollary 3.1.

| Method | $\det(\mathbf{Q}_N)^{1/n_x}$ |
|---|------------------------------|
| Extension of (Lin, Wang, and Yang 2007) | 8.2996 |
| Corollary 3.1 | 9.8696 |

Figures 3.3 and 3.4 illustrate the trajectories of angular positions of two-machines obtained using the extension of (Lin, Wang, and Yang 2007) previously described, considering the initial conditions $x_0(t) = [0.7732 \ 0 \ -0.5203 \ 0]^\top$, which belongs to stability regions obtained by both methods.

Note that the quality of the responses is worse (greater settling times and control input magnitudes, although this not is always guaranteed) than those obtained from the method proposed in Section 3.3, illustrated in Figures 3.5 and 3.6.

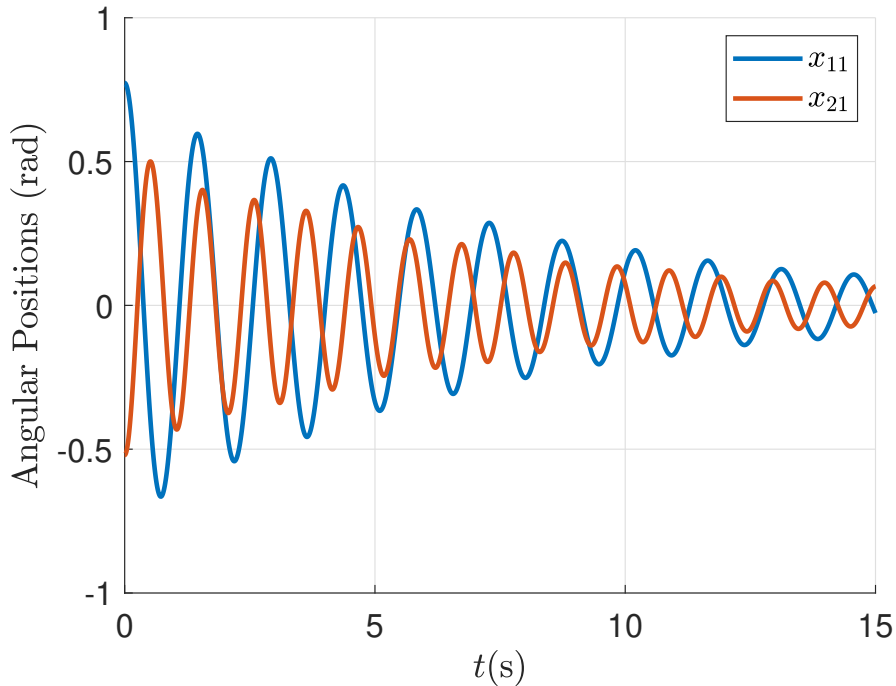


Figure 3.3: Trajectories of angular positions of two-machines in Section 3.4.1 – Extension of (Lin, Wang, and Yang 2007).

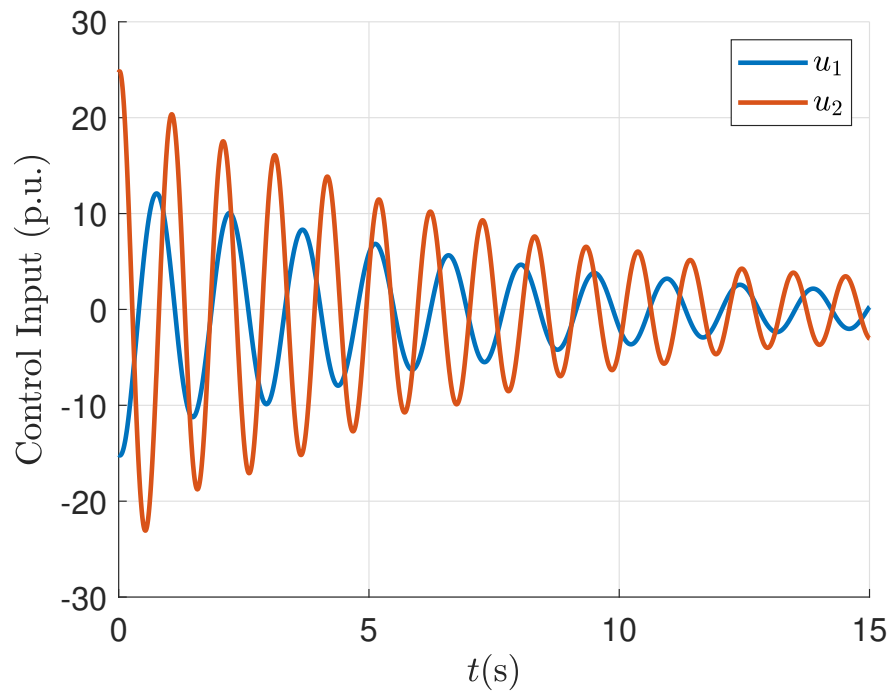


Figure 3.4: Control signals of two-machines in Section 3.4.1 – Extension of (Lin, Wang, and Yang 2007).

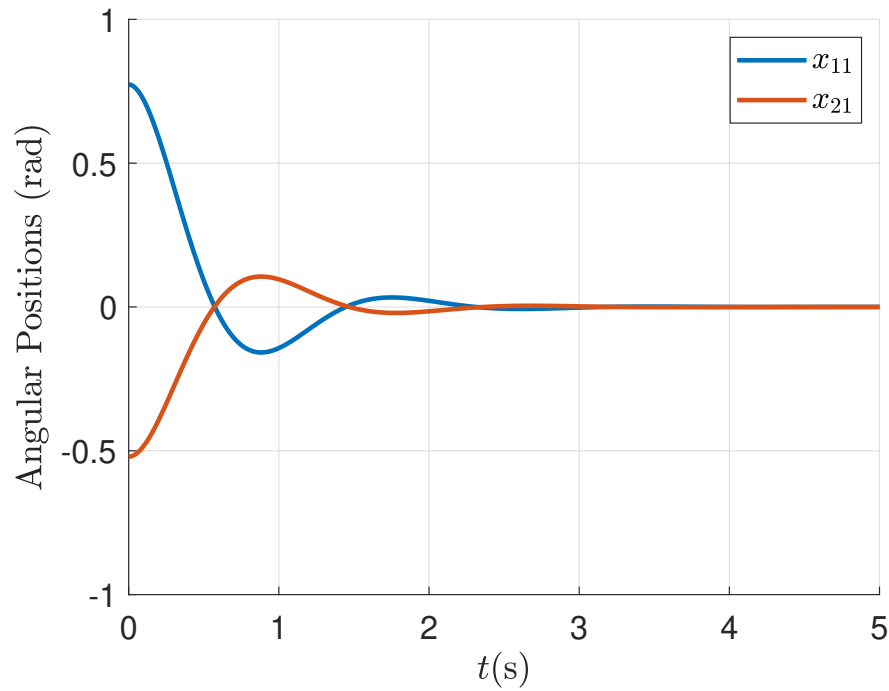


Figure 3.5: Trajectories of angular positions of two-machines in Section 3.4.1 – Corollary 3.1.

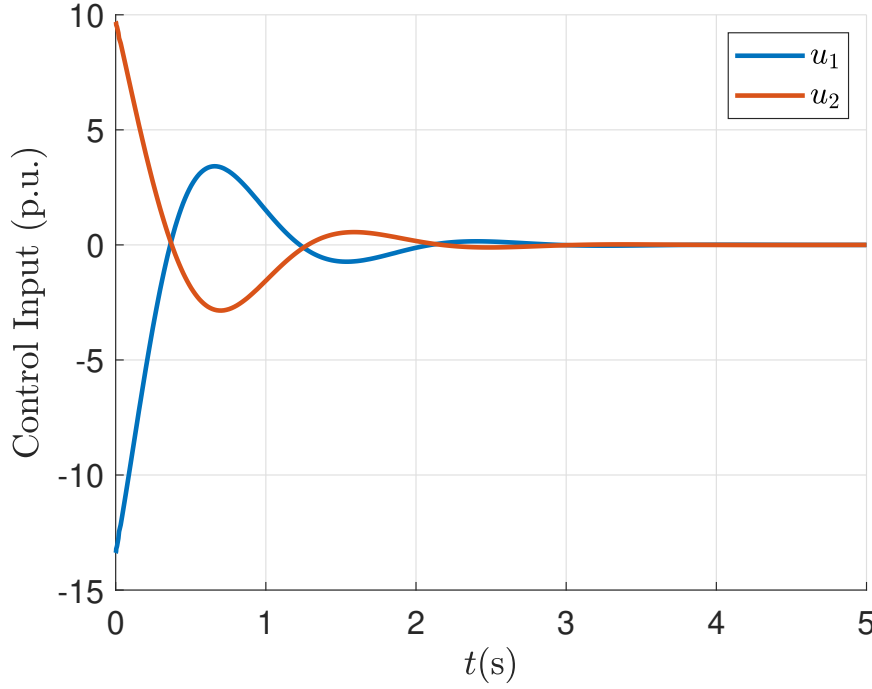


Figure 3.6: Control signals of two-machines in Section 3.4.1 – Corollary 3.1.

3.4.2 Multiple Inverted Pendulums

The networked system composed by multiple inverted pendulums coupled by nonlinear springs described in the Example 2.7 will be used to demonstrate the effectiveness of the proposed design approach. The system parameters are $N = 9$, $g = 9.8\text{m/s}^2$, $k = 80\text{N/m}$, $\gamma = 0.8\text{m}^{-1}$, $a = 0.5\text{m}$, the saturation of the control input is defined as $\bar{u}_i = 25\text{Nm}$, $\forall i \in \mathcal{I}_N$ and the other parameters (masses (m_i) and lengths (l_i)) are shown in Table 3.2.

Table 3.2: Parameters of the multiple inverted pendulums.

| Subsystem | m_i (kg) | l_i (m) | x_{i10} (rad) |
|-----------|------------|-----------|-----------------|
| S_1 | 0.35 | 1.2 | -0.1652 |
| S_2 | 0.35 | 1.2 | -0.1007 |
| S_3 | 0.30 | 1.3 | -0.1094 |
| S_4 | 0.25 | 0.9 | -0.1511 |
| S_5 | 0.25 | 1.1 | 0.1267 |
| S_6 | 0.45 | 1.1 | 0.1072 |
| S_7 | 0.40 | 1.1 | -0.1344 |
| S_8 | 0.25 | 0.9 | 0.1008 |
| S_9 | 0.45 | 1.2 | 0.1587 |

The graph representing the interconnections between the nine pendulums is depicted in Figure 3.7. From that one obtains the Adjacency and Degree matrices of the networked system, respectively, $A_{\mathcal{G}}$ and $D_{\mathcal{G}}$. Obviously, the value of the volume of the DoA estimate depends on the level of the control input saturation and limits the trajectories of the states.

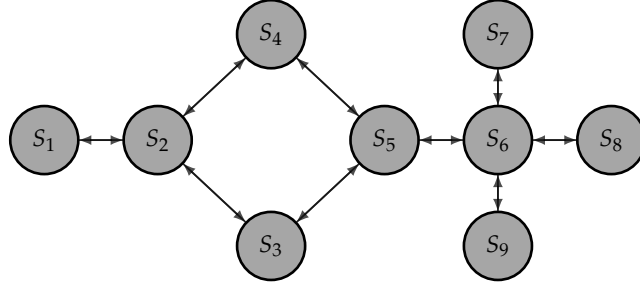


Figure 3.7: Networked system graph of the interconnected inverted pendulums.

However, in this case, the limits of the state variable $x_{i1}(t)$ also modify the nonlinearity sector. Thus, the value of $\bar{\theta}$ which generates the greatest DoA estimate is $\bar{\theta} = 0.3927$.

The reduction in the conservativeness is illustrated by the values of $\det(\mathbf{Q}_N)^{1/n_x}$ obtained from the optimization in Corollary 3.1. The values for the control law (3.10) and their modifications discussed in Remark 3.1 are shown in Table 3.3. Notice that the volume of the set \mathcal{L}_V can be increased with the addition of terms in the control law as proposed in this thesis.

Table 3.3: Values of $\det(\mathbf{Q}_N)^{1/n_x}$ obtained with Corollary 3.1, and alternatives of control in the Remark 3.1.

| Controller | $\det(\mathbf{Q}_N)^{1/n_x}$ |
|---|------------------------------|
| Decentralized ($\Gamma_i = 0$ and $F_{ij} = 0$) | 1.5763 |
| Linear Distributed ($\Gamma_i = 0$) | 1.7223 |
| Nonlinear Distributed ($F_{ij} = 0$, inspired in (Dong, Wang, and Yang 2009)) | 2.2391 |
| Nonlinear Distributed (Eq. (3.10)) | 2.3355 |

The closed-loop behavior of the system is depicted in Figure 3.8, considering, as initial conditions, all pendulums at rest and their angular positions x_{i10} as given in Table 3.2. It is worth pointing out that the nonlinear distributed controller is the only one guaranteeing the stabilization considering the set of initial conditions. The corresponding control signals are depicted in Figure 3.9. Note that although the saturation is taken into account, the proposed nonlinear distributed controller prevents its occurrence and guarantees the asymptotic stability of the closed-loop system.

3.5 Conclusions

This chapter investigated the nonlinear distributed control problem for a class of continuous-time networked heterogeneous systems with bounded sector nonlinear interconnections subject to both control input saturation and state constraints, which are described by interconnected nonlinear Takagi-Sugeno fuzzy systems. A quadratic block-diagonal Ly-

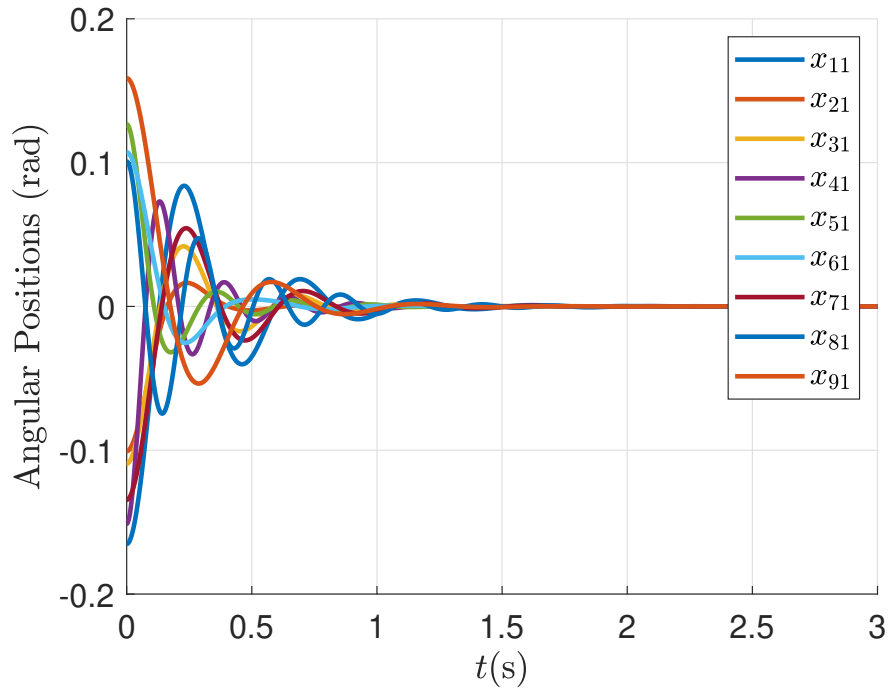


Figure 3.8: Time evolution of the angular positions for the nine interconnected inverted pendulums in Section 3.4.2.

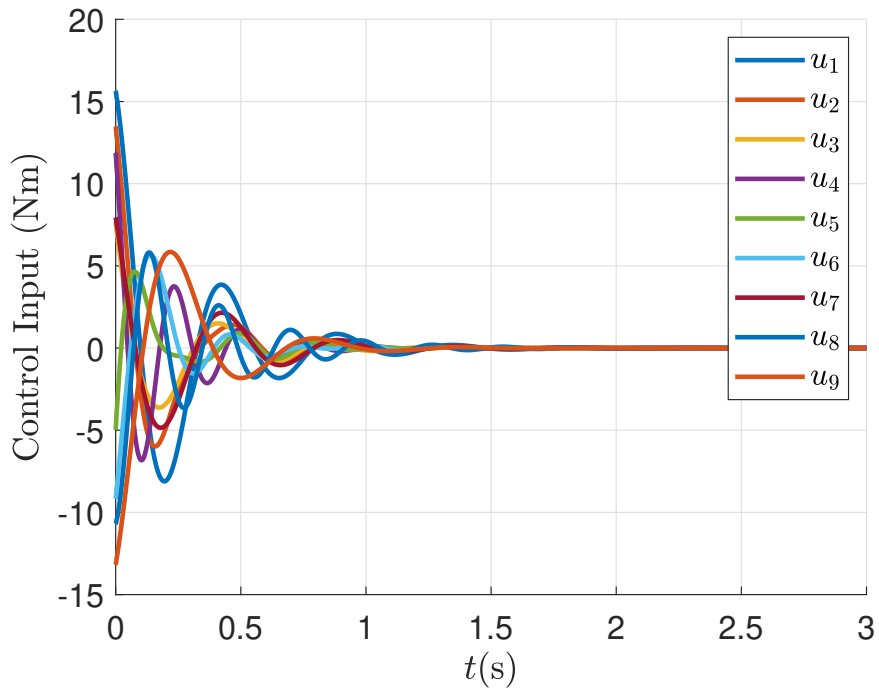


Figure 3.9: Control signals of the nine interconnected inverted pendulums in Section 3.4.2.

punov function was used to obtain sufficient conditions to solve the problem by means of LMIs, and two theorems were proposed from this.

Although Theorem 3.1 ensures the stability of the networked system, it is prohibitive,

even considering a small number of subsystems, since a large number of LMIs is obtained due to application of Lemma 2.3. Theorem 3.2 was proposed to overcome this problem, which using the membership functions of subsystems to define the augmented vector (3.17), dealing with the combination of membership functions of subsystems in a single LMI constraint.

It has been shown that if the associated optimization problem is feasible, the closed-loop networked control system is asymptotically stable, and the corresponding estimated ellipsoidal DoA is maximized. Finally, two examples of networked systems were employed to show the effectiveness of the proposed control approach, with respect to other works and over decentralized and linear distributed control laws derived following the same method.

4 Distributed Control of Large-Scale Systems

In this chapter, we investigate the problem of distributed controller synthesis for a class of large-scale systems. For this, the chordal decomposition is used to extend the result based on the multisets of membership functions presented in the previous chapter. Besides, it presents the analysis of the computational complexity of the approach when the number of interconnected subsystems increases.

4.1 Introduction

A system is large-scale when its dimension is such that traditional modeling, analysis, control, and computation techniques cannot provide solutions with reasonable computational efforts (Jamshidi 1997). The methods enumerated in Section 1, either using fuzzy TS models or not, to deal with nonlinear interconnections among subsystems are not scalable when the number of subsystems is large.

In this context, the chordal decomposition (Blair and Peyton 1993; Vandenberghe and Andersen 2015) has been used to reduce the complexity of the resulting problems, mainly when the graph associated with the large-scale system is sparse. This technique was used to design distributed control of interconnected systems in (Zheng, Mason, and Papachristodoulou 2018), although all components were considered linear, including subsystems, interconnections and controllers.

As discussed in Chapter 3, Theorem 3.1 is impractical even when the number of the subsystems is relatively small, and although Theorem 3.2 can provide solutions for a higher number of subsystems, it does not take advantage of sparsity of the graph that represents the networked system.

In this chapter, the chordal decomposition is used to deal with large scale systems in order to extend the previously developed approach to the case where the number of subsystems is large. Finally, we will provide an analysis of the computational complexity of the proposed methods aiming to illustrate the advantages of using the chordal decomposition.

4.1.1 Sparse Block Matrices and Chordal Decomposition

According to the discussion in Chapter 3, the occurrence of block matrices is natural when we deal with large-scale systems. Therefore, we provide an extension of the Chordal Decomposition Theorem presented in Theorem 2.4 for the case where \mathbf{X} is a block matrix, i.e. $\mathbf{X} = [X_{ij}]$.

Given a vector $\boldsymbol{\lambda} = \{\lambda_1, \lambda_2, \dots, \lambda_N\}$; with $\lambda_i \in \mathbb{R}$, $i \in \mathcal{I}_N$; a block matrix $\mathbf{X} \in \mathbb{S}^{n_x}$ has $\boldsymbol{\lambda}$ -partitioning with $n_x = \sum_{i=1}^N \lambda_i$, such that

$$\mathbf{X} = \begin{bmatrix} X_{11} & X_{12} & \cdots & X_{1N} \\ X_{21}^\top & X_{22} & \cdots & X_{2N} \\ \vdots & \vdots & \ddots & \vdots \\ X_{1N}^\top & X_{2N}^\top & \cdots & X_{NN} \end{bmatrix},$$

where each block $X_{ij} \in \mathbb{S}^{\lambda_i \times \lambda_j}$, $\forall i, j \in \mathcal{I}_N$. For an undirected graph $\mathcal{G}(\mathcal{V}, \mathcal{E})$, the space of $\boldsymbol{\lambda}$ -partitioned symmetric matrices with sparsity pattern \mathcal{E} is defined as

$$\mathbb{S}_{\boldsymbol{\lambda}}^{n_x}(\mathcal{E}, 0) = \{\mathbf{X} \in \mathbb{S}^{n_x} \mid X_{ij} = X_{ji}^\top = 0, \text{ if } i \neq j \text{ and } (i, j) \notin \mathcal{E}\},$$

and the space of sparse block positive semidefinite matrices is

$$\mathbb{S}_{\boldsymbol{\lambda},+}^{n_x}(\mathcal{E}, 0) = \{\mathbf{X} \in \mathbb{S}_{\boldsymbol{\lambda}}^{n_x}(\mathcal{E}, 0) \mid \mathbf{X} \succeq 0\}.$$

Similar to Section 2.1, if $\mathbf{X} \in \mathbb{S}_{\boldsymbol{\lambda}}^{n_x}(\mathcal{E}, 0)$ and $\mathcal{E} \subset \hat{\mathcal{E}}^1$, then \mathbf{X} also has sparsity pattern $\hat{\mathcal{E}}$, i.e. $\mathbf{X} \in \mathbb{S}_{\boldsymbol{\lambda}}^{n_x}(\hat{\mathcal{E}}, 0)$.

To extend the chordal decomposition theorem, we define a block version of the principle submatrices. Given a clique \mathcal{C}_k of a chordal graph $\mathcal{G}(\mathcal{V}, \mathcal{E})$ and a partition $\boldsymbol{\lambda}$, the block-wise principle submatrices of a sparsity pattern \mathcal{E} are matrices $E_{\mathcal{C}_k, \boldsymbol{\lambda}} \in \mathbb{R}^{|\mathcal{C}_k|_{\boldsymbol{\lambda}} \times n_x}$, $\forall k \in \mathcal{I}_t$ with $|\mathcal{C}_k|_{\boldsymbol{\lambda}} = \sum_{i \in \mathcal{C}_k} \lambda_i$, and $n_x = \sum_{i=1}^N \lambda_i$ with entries

$$(E_{\mathcal{C}_k, \boldsymbol{\lambda}})_{ij} = \begin{cases} I_{\lambda_i}, & \text{if } \mathcal{C}_k(i) = j, \\ \mathbf{0}_{\lambda_i \times \lambda_j}, & \text{otherwise,} \end{cases} \quad (4.1)$$

where $\mathcal{C}_k(i)$ is the i -th vertex in \mathcal{C}_k , whose vertices are sorted in the natural ordering. Thus, the following theorem extends Theorem 2.4 to the case of sparse block matrices.

¹ $\hat{\mathcal{E}}$ denotes the edges set of a chordal extension of graph \mathcal{G} , see Section 2.1.

Theorem 4.1: Block-chordal decomposition theorem (Zheng 2019)

Let $\mathcal{G}(\mathcal{V}, \mathcal{E})$ be a chordal graph with maximal cliques $\{\mathcal{C}_1, \mathcal{C}_2, \dots, \mathcal{C}_t\}$. Given a partition $\lambda = \{\lambda_1, \lambda_2, \dots, \lambda_N\}$ and $n_x = \sum_{i=1}^N \lambda_i$, then, $\mathbf{X} \in \mathbb{S}_{\lambda,+}^{n_x}(\mathcal{E}, 0)$ if and only if there exist matrices $\mathbf{X}_k \in \mathbb{S}_+^{|\mathcal{C}_k|\lambda}$ for $k \in \mathcal{I}_t$ such that

$$\mathbf{X} = \sum_{k=1}^t E_{\mathcal{C}_k, \lambda}^\top \mathbf{X}_k E_{\mathcal{C}_k, \lambda}.$$

Note that when $\lambda_i = 1, \forall i \in \mathcal{I}_N$, $E_{\mathcal{C}_k, \lambda} = E_{\mathcal{C}_k}$ and Theorem 4.1 is reduced to Theorem 2.4. In this thesis, each element of partition corresponds to the order of each subsystem, i.e. $\lambda_i = n_{x_i}$.

Example 4.1. In this example Theorem 4.1 will be applied to illustrate how to obtain fewer constraints from a sparse inequality. Consider the chordal graph $\mathcal{G}(\mathcal{V}, \mathcal{E})$ in Figure 4.1 and the block matrix (4.2) with the same sparsity pattern of the graph.

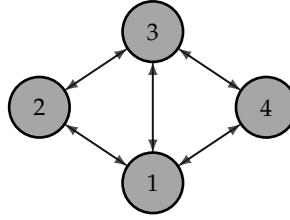


Figure 4.1: Graph of large-scale system.

$$\mathbf{X} = \begin{bmatrix} X_{11} & X_{12} & X_{13} & X_{14} \\ X_{12}^\top & X_{22} & X_{23} & 0 \\ X_{13}^\top & X_{23}^\top & X_{33} & X_{34} \\ X_{14}^\top & 0 & X_{34}^\top & X_{44} \end{bmatrix} \in \mathbb{S}_{\lambda,+}^{n_x}(\mathcal{E}, 0). \quad (4.2)$$

Maximal cliques associated to the graph are $\mathcal{C}_1 = \{1, 2, 3\}$ and $\mathcal{C}_2 = \{1, 3, 4\}$, and its block principle submatrices are build as in (4.1). Thus, from Theorem 4.1, one has that the following set of constraints is equivalent to (4.2).

$$\mathbf{X}_1 = \begin{bmatrix} Y_1 & X_{12} & Y_2 \\ X_{12}^\top & X_{22} & X_{23} \\ Y_2^\top & X_{23}^\top & Y_3 \end{bmatrix} \in \mathbb{S}_+^{|\mathcal{C}_1|\lambda}, \quad \mathbf{X}_2 = \begin{bmatrix} W_1 & W_2 & X_{14} \\ W_2^\top & W_3 & X_{34} \\ X_{14}^\top & X_{34}^\top & X_{44} \end{bmatrix} \in \mathbb{S}_+^{|\mathcal{C}_2|\lambda}, \quad (4.3)$$

$Y_i + W_i = X_{ii}, i = \{1, 3\}, \text{ and } Y_2 + W_2 = X_{13}.$

Notice that equality constraints in the example above arise due to overlapping elements in the graph, i.e. if a vertex or an edge appear in more than one maximal clique. In

this thesis, we will consider that the overlapping elements are divided equally between inequality constraints, eliminating the equality constraints. For this, we define $Z = [\zeta_{ij}] \in \mathbb{S}^N(\mathcal{E}, 0)$, with each element equal to the number of times vertices, if $i = j$, and edges (i, j) , if $i \neq j$, appears in a clique tree \mathcal{T} of the graph.

Then, matrix $\bar{Z} = [\bar{\zeta}_{ij}]$ of averaging factors for decomposing the overlapping elements is defined as:

$$\bar{\zeta}_{ij} = \begin{cases} \frac{1}{\zeta_{ij}}, & \text{if } i \in \mathcal{T} \forall i = j, \text{ or } (i, j) \in \mathcal{T} \forall i \neq j \\ 0, & \text{otherwise} \end{cases}. \quad (4.4)$$

Example 4.2. Considering the previous example, the clique tree \mathcal{T} of the graph in Figure 4.1 is shown in Figure 4.2.

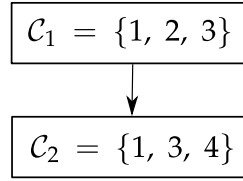


Figure 4.2: Clique tree of the chordal graph in Figure 4.1.

Notice that vertices 1 and 3 appear twice in the clique tree, as well as the $(1, 3)$ and $(3, 1)$ edges. Also, the $(2, 4)$ and $(4, 2)$ edges not belong to the graph, i.e. $\zeta_{24} = \zeta_{42} = 0$. Therefore,

$$Z = \begin{bmatrix} 2 & 1 & 2 & 1 \\ 1 & 1 & 1 & 0 \\ 2 & 1 & 2 & 1 \\ 1 & 0 & 1 & 1 \end{bmatrix}.$$

Hence, the matrix \bar{Z} of averaging factors for decomposing the overlapping elements can be obtained as in (4.4). Thus, constraints (4.3) are transformed as follows:

$$\begin{aligned} \mathbf{X}_1 &= \begin{bmatrix} \bar{\zeta}_{11}X_{11} & X_{12} & \bar{\zeta}_{13}X_{13} \\ X_{12}^\top & X_{22} & X_{23} \\ \bar{\zeta}_{13}X_{13}^\top & X_{23}^\top & \bar{\zeta}_{33}X_{33} \end{bmatrix} \in \mathbb{S}_+^{|\mathcal{C}_1|_\lambda}, \\ \mathbf{X}_2 &= \begin{bmatrix} \bar{\zeta}_{11}X_{11} & \bar{\zeta}_{13}X_{13} & X_{14} \\ \bar{\zeta}_{13}X_{13}^\top & \bar{\zeta}_{33}X_{33} & X_{34} \\ X_{14}^\top & X_{34}^\top & X_{44} \end{bmatrix} \in \mathbb{S}_+^{|\mathcal{C}_2|_\lambda}. \end{aligned} \quad (4.5)$$

Based on this, constraints (4.2), (4.3) and (4.5) are equivalent.

4.2 Problem Statement

Consider a continuous-time large-scale system which consists of N interconnected nonlinear heterogeneous subsystems with nonlinear interconnections. The interconnection

among subsystems is represented by an undirected graph $\mathcal{G}(\mathcal{V}, \mathcal{E})$. Each i -th subsystem is described as follows:

$$\dot{\mathbf{x}}_i(t) = f_i(\mathbf{x}_i(t)) + g_i(\mathbf{x}_i(t))\mathbf{u}_i(t) + \sum_{j \in \mathcal{N}_i} h_{ij}(\mathbf{x}_i(t), \mathbf{x}_j(t)), \quad (4.6)$$

where $i \in \mathcal{I}_N$, $\mathbf{x}_i(t) \in \mathbb{R}^{n_{x_i}}$ is the state vector of i -th subsystem; $\mathbf{u}_i(t) \in \mathbb{R}^{n_{u_i}}$ is the i -th control input vector; f_i , g_i and h_{ij} are smooth nonlinear functions.

According to the discussion in Section 2.3, each subsystem in (4.6) can be represented by a N-TS fuzzy model. Thus, the i -th inferred N-TS fuzzy model is given by

$$\begin{aligned} \dot{\mathbf{x}}_i(t) = \sum_{l=1}^{r_i} \varsigma_i^l(\mathbf{z}_i(t)) & \left[A_i^l \mathbf{x}_i(t) + B_i^l \mathbf{u}_i(t) \right. \\ & \left. + \sum_{j \in \mathcal{N}_i} \left(H_{ii}^l \mathbf{x}_i(t) - H_{ij}^l \mathbf{x}_j(t) \right) + G_i^l \left(\sum_{j \in \mathcal{N}_i} \varphi_{ij}(\mathbf{x}_i(t), \mathbf{x}_j(t)) \right) \right], \end{aligned} \quad (4.7)$$

where $i \in \mathcal{I}_N$, A_i^l , B_i^l , H_{ij}^l and G_i^l are known constant matrices with appropriate dimensions; with the nonlinearities φ_{ij} being sector-bounded ones and satisfying the Property 2.3.

As in the previous chapter, we will consider the same nonlinear distributed control law for the i -th subsystem (4.7):

$$\mathbf{u}_i(t) = \sum_{l=1}^{r_i} \varsigma_i^l(\mathbf{z}_i(t)) K_i^l \mathbf{x}_i(t) + \sum_{j \in \mathcal{N}_i} \Gamma_{ij} \varphi_{ij}(\mathbf{x}_i(t), \mathbf{x}_j(t)) + \sum_{j \in \mathcal{N}_i} F_{ij} \mathbf{x}_j(t), \quad (4.8)$$

where Assumption 3.1 is still considered valid, together with the observations made in Remark 3.1 regarding modifications in the control law. Furthermore, we will consider subsystems without saturation in its control inputs, according to Remark 3.2. Thus, substituting (4.8) into (4.7) it leads to the following closed-loop subsystem:

$$\begin{aligned} \dot{\mathbf{x}}_i(t) = \sum_{k=1}^{r_i} \sum_{l=1}^{r_i} \varsigma_i^k(\mathbf{z}_i(t)) \varsigma_j^l(\mathbf{z}_i(t)) & \left(A_i^k + B_i^k K_i^l + d_{ii} H_{ii}^k \right) \mathbf{x}_i(t) \\ & + \sum_{j \in \mathcal{N}_i} \sum_{k=1}^{r_i} \varsigma_i^k(\mathbf{z}_i(t)) \left(B_i^k F_{ij} - H_{ij}^k \right) \mathbf{x}_j(t) + \sum_{j \in \mathcal{N}_i} \sum_{k=1}^{r_i} \varsigma_i^k(\mathbf{z}_i(t)) \left(B_i^k \Gamma_{ij} + G_i^k \right) \varphi_{ij}(\mathbf{x}(t)) \end{aligned} \quad (4.9)$$

As discussed earlier, the approach proposed in Chapter 3 is not applicable when the number of interconnected subsystems is large. In this chapter, we take advantage of the sparsity of the underlying interconnection graph to solve the following problem with reasonable computational efforts.

Problem 4.1

Design a nonlinear distributed controller (4.8) for each i -th subsystem (4.7), such that the large-scale nonlinear closed-loop system, composed by the interconnected subsystems (4.9), is stable.

4.3 Stabilization of Large-Scale Systems

The sufficient conditions for distributed stabilization of large-scale systems presented in this section are obtained through of the following quadratic block-diagonal Lyapunov function candidate (Sootla, Zheng, and Papachristodoulou 2017, 2019):

$$V(\mathbf{x}(t)) = \sum_{i=1}^N \mathbf{x}_i(t)^\top P_i \mathbf{x}_i(t) = \mathbf{x}(t)^\top \mathbf{P}_N \mathbf{x}(t),$$

where $\mathbf{x}(t) = \begin{bmatrix} \mathbf{x}_1(t)^\top & \mathbf{x}_2(t)^\top & \cdots & \mathbf{x}_N(t)^\top \end{bmatrix}^\top$, $\mathbf{P}_N = \bigoplus_{i=1}^N P_i$, with $P_i = P_i^\top \succ 0$.

Particularly, this choice is justified because the sparsity pattern of the graph associated with the N interconnected subsystems is maintained in the LMI constraints generated from it. Theorem 4.2 provides sufficient conditions to guarantee that the origin of the large-scale nonlinear system is asymptotically stable.

Theorem 4.2: Stabilization of large-scale system

Let the matrices $\mathbf{\Omega}_i$ associated with the sector nonlinearities in each subsystem (4.7), $\forall i \in \mathcal{I}_N$, according to (2.20), be given. Let $\mathcal{G}(\mathcal{V}, \mathcal{E})$ be an undirected graph, with a chordal extension that has maximal cliques $\{\mathcal{C}_1, \mathcal{C}_2, \dots, \mathcal{C}_t\}$. Assume that there exist matrices $Q_i \succ 0$, diagonal matrices $\Lambda_{ij} \succ 0$, and any matrices $R_i^{l_{i,2}}$, S_{ij} and T_{ij} , $\forall i \in \mathcal{I}_N$, $\forall l_{i,2} \in \mathcal{I}_{r_i}$ and $\forall j \in \mathcal{N}_i$, satisfying (4.10):

$$\prod_{i \in \mathcal{C}_k} \left(\sum_{l_{i,1}=1}^{r_i} \sum_{l_{i,2}=1}^{r_i} \varsigma_i^{l_{i,1}} \varsigma_i^{l_{i,2}} \right) \begin{bmatrix} \mathbf{\Theta}^k + \mathbf{\Delta}^k & \star \\ \mathbf{\Pi}^k + \mathbf{\Omega}^k \mathbf{Q}^k & -2\mathbf{\Lambda}^k \end{bmatrix} \prec 0, \quad \forall k \in \mathcal{I}_t \quad (4.10)$$

where,

$$\mathbf{\Theta}^k = \bigoplus_{i \in \mathcal{C}_k} \frac{1}{\varsigma_{ii}} \left(\left(A_i^{l_{i,1}} Q_i + d_{ii} H_{ii}^{l_{i,1}} Q_i + B_i^{l_{i,1}} R_i^{l_{i,2}} \right)^\top + \left(A_i^{l_{i,1}} Q_i + d_{ii} H_{ii}^{l_{i,1}} Q_i + B_i^{l_{i,1}} R_i^{l_{i,2}} \right) \right),$$

$$\mathbf{Q}^k = \bigoplus_{i \in \mathcal{C}_k} Q_i, \quad \mathbf{\Lambda}^k = \bigoplus_{(i,j) \in \mathcal{E}_{\mathcal{C}_k}} \frac{1}{\varsigma_{ij}} \Lambda_{ij}, \quad \mathbf{\Pi}^k = \bigoplus_{(i,j) \in \mathcal{E}_{\mathcal{C}_k}} \frac{1}{\varsigma_{ij}} \left(B_i^{l_{i,1}} T_{ij} + G_i^{l_{i,1}} \Lambda_{ij} \right)^\top,$$

$$\mathbf{\Delta}^k = E_{\mathcal{C}_k, \lambda} \mathbf{\Delta} E_{\mathcal{C}_k, \lambda}^\top, \quad \mathbf{\Omega}^k = E_{\mathcal{C}_k, d} \left(E_{\mathcal{C}_k, \lambda} \mathbf{\Omega} E_{\mathcal{C}_k, \lambda}^\top \right), \text{ for } \mathbf{\Delta} \text{ and } \mathbf{\Omega} \text{ in Theorem 3.1,}$$

$$\text{with } E_{\mathcal{C}_k, d} \in \mathbb{R}^{|\mathcal{E}_{\mathcal{C}_k}| \times |\mathcal{C}_k|_\lambda}, \quad (E_{\mathcal{C}_k, d})_{ij} = \begin{cases} 1, & \text{if } \mathcal{E}_{\mathcal{C}_k}(i) = \mathcal{E}(j), \\ 0, & \text{otherwise,} \end{cases}$$

where $\mathcal{E}_{\mathcal{C}_k}(i)$ and $\mathcal{E}(j)$ are the i -th and j -th edge in $\mathcal{G}_{\mathcal{C}_k}$ and \mathcal{G} , respectively, sorted in the natural ordering.

Then the continuous-time large-scale nonlinear system represented by the graph \mathcal{G} , composed by N interconnected closed-loop subsystems given in (4.9), is stable and the control gains in (4.8) are given by: $K_i^{l_{i,1}} = R_i^{l_{i,1}} Q_i^{-1}$, $\Gamma_{ij} = T_{ij} \Lambda_{ij}^{-1}$ and $F_{ij} = S_{ij} Q_j^{-1}$.

Proof. From Theorem 4.1, constraints (4.10) are equivalent to the constraint (3.13) in Theorem 3.1. The rest of the proof is a direct consequence of the proof of Theorem 3.1. \square

Since the constraints (4.10) in Theorem 4.2 are nonlinear ones, one has to use Lemma 2.3 to obtain a finite number of LMI.

The main advantage of Theorem 4.2 over Theorem 3.1 is the possibility of dealing with a large number of interconnected subsystems by taking into account the sparsity of the graph that represents the large-scale interconnected system. The higher the sparsity of the graph, the smaller the size of the LMIs to be considered. A graph with high sparsity means that it has a large number of maximal cliques with a small number of vertices in each clique.

Notice that the chordal extension of the graph is used only to obtain the maximal cliques, which indicate which subsystems participate in each constraint defined by a corresponding maximal clique, while the original graph is taken into account to mounting the block matrices of each constraint.

Remark 4.1

Notice that if the number of maximal cliques in the graph represents interconnections of the large-scale system is unitary, i.e. the graph is complete, then Theorem 4.2 is reduced to Theorem 3.1.

4.4 Analysis of the Computational Complexity

In this section, it is discussed the analysis of the computational complexity of Theorems 3.1 and 3.2 presented in Chapter 3 in comparison to the computational complexity of Theorem 4.2 proposed in Section 4.3.

As Theorems 3.1 and 4.2 do not take into account both state and control input constraints, for the Theorem 3.2 we will consider only the LMI constraint (3.22) and the observations in Remark 3.4 to evaluate its computational complexity.

The computational complexity of an LMI solver based on interior point methods can be estimated as being proportional to $\log(N_d^3 N_l)$, where N_d is the number of decision variables and N_l is the number of LMI rows (Nguyen et al. 2016). In general, the number of decision variables depends only on the control law, dimension of the system and Lyapunov function used to obtain LMI conditions. Thus, since all theorems use the same control law and Lyapunov function, the number of decision variables can be computed as follows:

$$N_d = \sum_{i=1}^N \left(n_{x_i} \left(\frac{n_{x_i} + 1}{2} \right) + d_{ii} + n_{u_i} n_{x_i} r_i + \sum_{j \in \mathcal{N}_i} n_{u_i} n_{x_j} + n_{u_i} d_{ii} \right).$$

And the number of LMI rows is computed as shown in Table 4.1. Particularly, the number of LMI rows in Theorems 3.2 and 4.2 are obtained by following the observations in Remark 2.5.

Table 4.1: Comparison of the number of LMI rows in Theorems 3.1, 3.2 and 4.2.

| Method | N_l |
|-------------|--|
| Theorem 3.1 | $\left(\sum_{i=1}^N (n_{x_i} + d_{ii}) \right) \left(\prod_{i=1}^N \frac{r_i^2 + r_i}{2} \right)$ |
| Theorem 3.2 | $\sum_{i=1}^N (r_i n_{x_i} + d_{ii})$ |
| Theorem 4.2 | $\sum_{k=1}^t \left(\left(\sum_{i \in \mathcal{C}_k} n_{x_i} + \frac{ \mathcal{C}_k !}{(\mathcal{C}_k -2)!} \right) \left(\prod_{i \in \mathcal{C}_k} \frac{r_i^2 + r_i}{2} \right) \right)$ |

Notice that when the graph that represents interconnections in a large-scale system is complete, the number of maximal cliques is $t = 1$ and $|\mathcal{C}_k| = N$, with $k = 1$, where N denotes the number of subsystems. Hence $\sum_{i=1}^N d_{ii} = \frac{N!}{(N-2)!}$, and the number of LMI rows in Theorems 3.1 and 4.2 are equal (see Remark 4.1).

Theorem 3.2 reduces the combination between membership functions by using the augmented vector (3.17), and consequently avoiding the use of Lemma 2.3. However, the procedure increases the sparsity of the LMI constraint since the order of the matrix grows beyond the number r_i of fuzzy rules for each subsystem. On the other hand, Theorem 4.2 takes advantage of the graph sparsity to reduce the size of the LMI constraints. Thus the number of LMI rows will be smaller than the corresponding number of rows in the theorems as long as the sizes of the maximal cliques are small, such that the product will be reduced, although the sum that depends on the number k of maximal cliques grows.

Next, the network of multiple inverted pendulums coupled by nonlinear springs presented in Example 2.7 will be used again to illustrate these issues and to compare the computational complexity of proposed theorems when the number of subsystems is relatively large.

4.4.1 Multiple Inverted Pendulums

For the network of multiple inverted pendulums presented in Section 2.3, the number of fuzzy rules is $r_i = 2$, and the size of state and control input vectors for each i -th subsystem are $n_{x_i} = 2$ and $n_{u_i} = 1$, $\forall i \in \mathcal{I}_N$.

To compare the application of theorems developed in Chapter 3 with the application of Theorem 4.2, we have analyzed their computational complexity and their running times, considering different graph sizes. Different chordal graphs were generated with the number of vertices (subsystems) between 20 and 1020, with the size of the largest maximal clique defined by

$$\tau = \max_{k \in \mathcal{I}_t} |\mathcal{C}_k|,$$

modified accordingly to illustrate the increasing in the computational complexity for $\tau = 2$, $\tau = 6$ and $\tau = 10$.

All simulation results presented throughout this section were conducted on an otherwise idle computer equipped with Intel Core i3 3.06GHz, with 4 GB of RAM, and Mac OS 10.13.6, using the Yalmip parser (Löfberg 2004) and Mosek solver (Mosek 2017) performing on software Matlab R2017b. All presented execution times are Matlab times, i.e. time intervals spent between the call to *tic* and *toc* commands used to measure execution time.

Computational Complexity

According to Table 4.1, the computational complexity of the Theorem 3.1 is high, even for a small number of subsystems, due to the combination of all membership functions of the subsystems. For instance, for $N = 120$, the computational complexity is proportional to 69.8, and for $N = 1020$, it is proportional to approximately 500, which makes the theorem impractical.

On the other hand, the computational complexity associated with Theorem 4.2 depends on the number of maximal cliques of the graph and their sizes, i.e. the complexity is small if the sizes of the largest maximal cliques are small. Figures 4.3, 4.4 and 4.5 illustrate the increasing computational complexity for Theorems 3.2 and 4.2, considering that the size of the largest maximal clique of the corresponding graph is $\tau = 2$, $\tau = 6$ and $\tau = 10$, respectively.

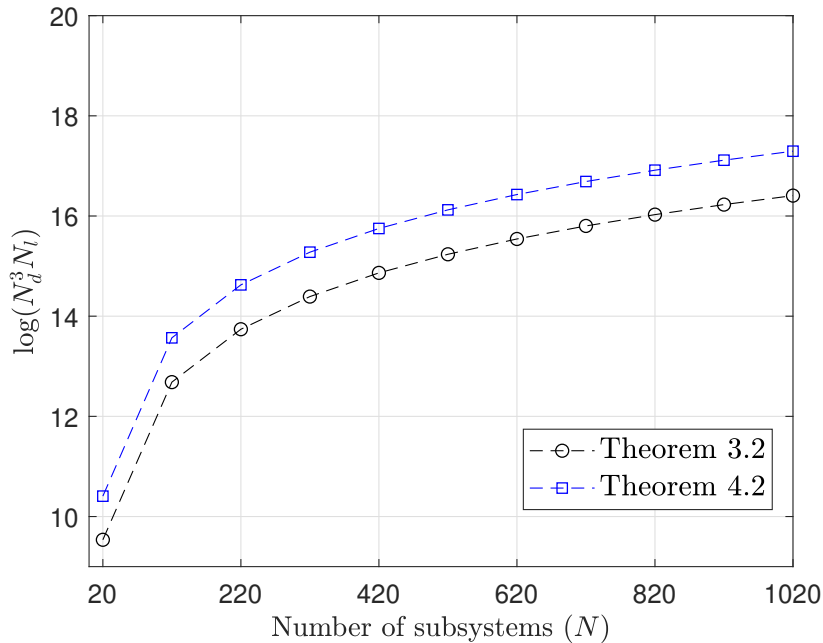


Figure 4.3: Comparison of the computational complexity associated with Theorems 3.2 and 4.2, considering the largest maximal clique size $\tau = 2$.

We have verified that the computational complexity in Theorem 4.2 increases with the size of the largest maximal clique, although the number of maximal cliques is reduced. Besides, if the size of the largest maximal clique increases, the computational complexity in Theorem 4.2 approximates that in Theorem 3.1. When $\tau = N$, they are equal according to Remark 4.1, but it is worth noticing that this scenario is rarely found in practice.

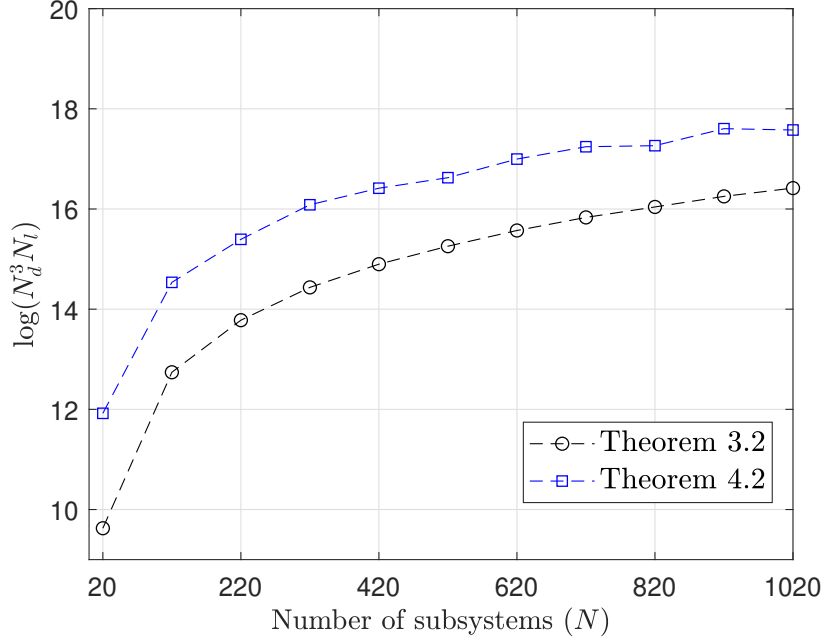


Figure 4.4: Comparison of the computational complexity of Theorems 3.2 and 4.2, considering the largest maximal clique size $\tau = 6$.

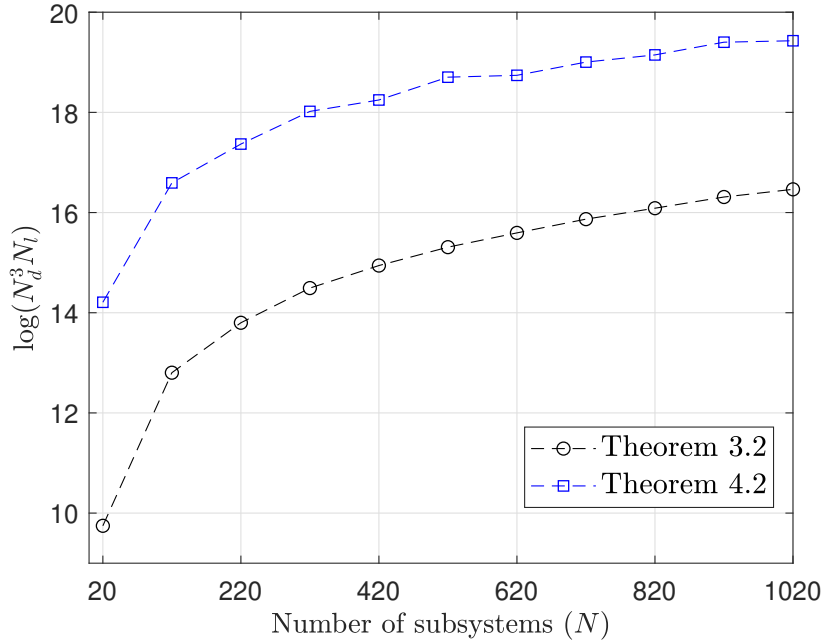


Figure 4.5: Comparison of the computational complexity of Theorems 3.2 and 4.2, considering the largest maximal clique size $\tau = 10$.

Running Time

Although the computational complexity in Theorem 3.2 is smaller than that found for the best case in Theorem 4.2 ($\tau = 2$), it is not scalable to a large number of subsystems, as illustrated in Figures 4.6 and 4.7.

Figure 4.6 shows the total running time, i.e. the summation of time intervals spent on assembling the LMIs, parsing them using Yalmip, and running the optimization solver, considering $\tau = 2$. Notice that the time required to solve the problem with $N = 220$ subsystems using Theorem 3.2 is higher than the time required to solve the problem with $N = 720$ subsystems using Theorem 4.2.

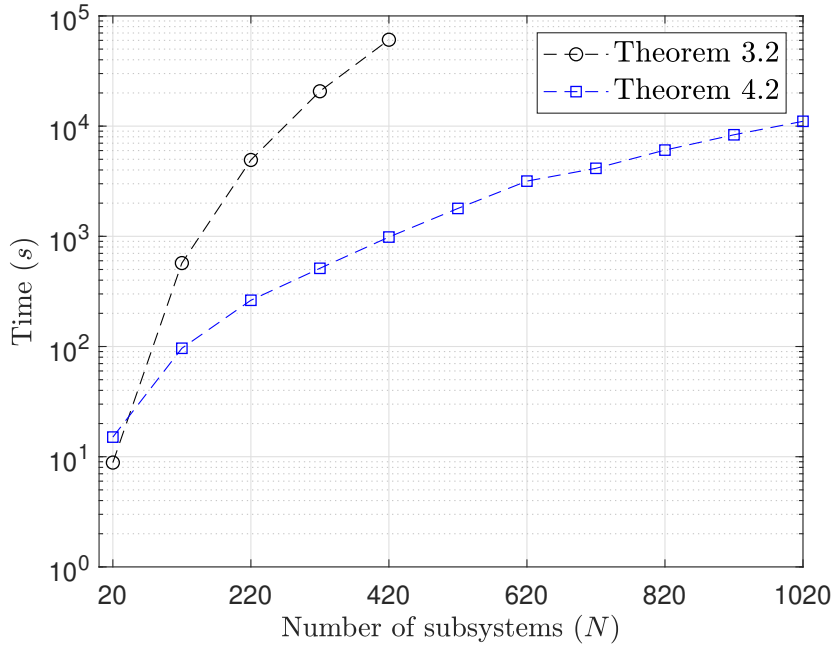
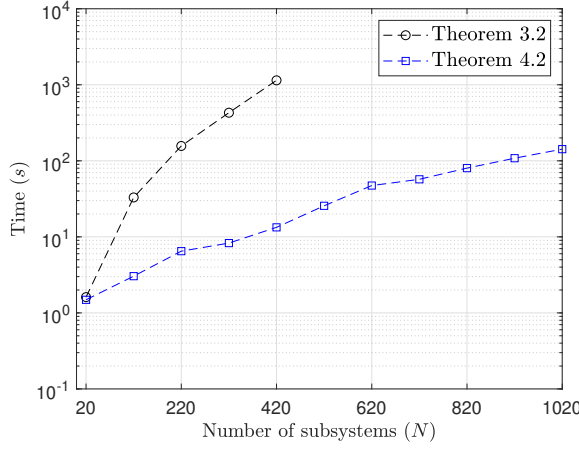


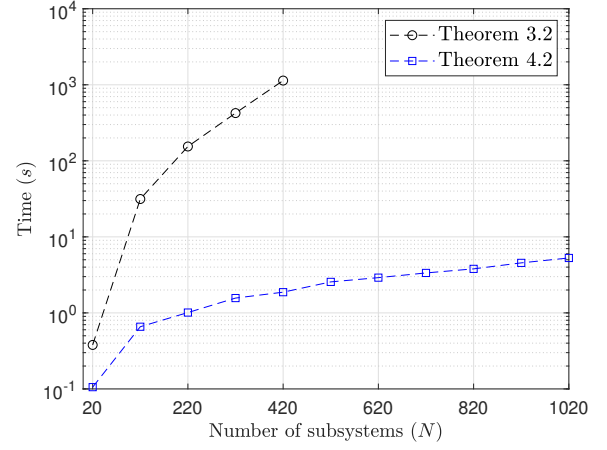
Figure 4.6: Comparison of the total running time associated with Theorems 3.2 and 4.2, considering the largest maximal clique size $\tau = 2$.

This happens due to the difficulty of the solver to deal with sparse constraints, as evidenced in Figure 4.7. Comparing Figures 4.7(a) and (b), notice that the Yalmip parser time is minimal with respect to Theorem 3.2, such it has only one LMI constraint. In contrast, Theorem 4.2 creates several smaller LMI constraints, eliminating its sparsity such that the solver is much faster. For instance, for $N = 420$, the solver running time is 500 times smaller than the solver running time associated with Theorem 3.2. Moreover, the solver time does not increase as rapidly as for Theorem 3.2, even when considering a large number of subsystems.

The same behavior described above is repeated for case $\tau = 6$, according with depicted in Figures 4.8 and 4.9. Again, Theorem 4.2 presents better performing when the number of subsystems increases. Notably, in this case, the solver running time sometimes decreases when the number of subsystems increases. This variation occurs because, although the



(a) Yalmip parser plus solver running time.



(b) Solver running time.

Figure 4.7: Comparison of the Yalmip parser plus solver running time and only solver running time associated with Theorems 3.2 and 4.2, considering the largest maximal clique size $\tau = 2$.

size of the largest maximal clique is 6, the size of other maximal cliques is small, causing variation in the size of the constraints.

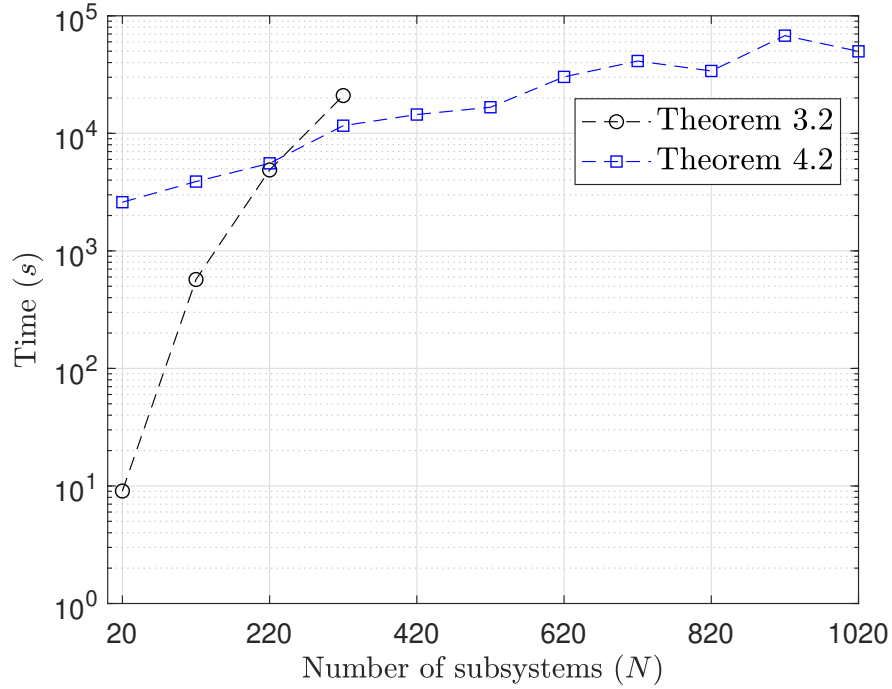


Figure 4.8: Comparison of the total running time associated with Theorems 3.2 and 4.2, considering the largest maximal clique size $\tau = 6$.

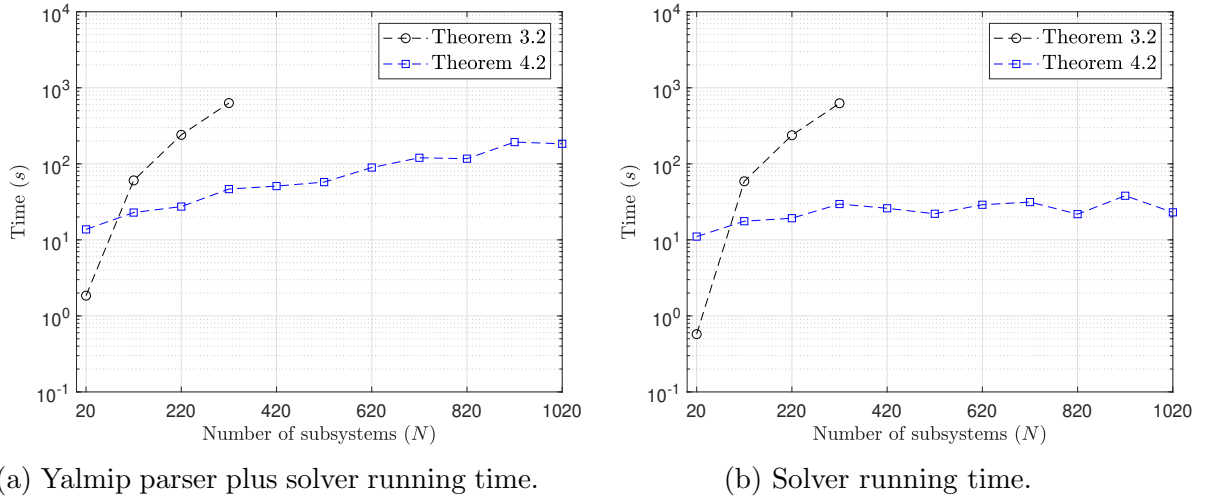


Figure 4.9: Comparison of the Yalmip parser plus solver running time and only solver running time associated with Theorems 3.2 and 4.2, considering the largest maximal clique size $\tau = 6$.

4.5 Conclusions

This chapter discussed how a chordal decomposition can be employed to deal with higher computational complexity in Theorem 3.1 when a large number of subsystems must be considered, i.e. a large-scale interconnected system is under consideration.

In this context, Theorem 4.2 was proposed to explore the graph sparsity in order to reduce the computational complexity in Theorem 3.1. For this, the chordal decomposition can be used such that the number of combinations of membership functions between subsystems is significantly reduced.

Although both Theorem 3.2, proposed in Chapter 3, and Theorem 4.2 reduce the computational complexity associated with Theorem 3.1, only the last one is scalable, i.e. can solve the problem when the number of subsystems becomes large, as it can be seen in the comparison of running times presented in the last section. This happens because the sparsity of constraints is removed before handing them over to the optimization solver. This prevents the high computational burden that would be present, since ordinary solvers are not capable of exploring sparse constraints.

5 Conclusions and Future Directions

In this chapter we present the main conclusions as well as the final remarks with respect to the problems investigated in this doctoral thesis. We also discuss possible future research directions.

5.1 An Overview of the Research

This thesis investigated the distributed control problem for a class of continuous-time large-scale systems.

We have considered that the large-scale systems are described as a network of heterogeneous subsystems that has an underlying graph topology (Section 2.1), such that each subsystem can be described as a nonlinear Takagi-Sugeno (N-TS) fuzzy model, i.e. a Takagi-Sugeno fuzzy model with nonlinear consequent (Section 2.2). In addition, we have also assumed that the subsystems are linked together relying on sector-bounded nonlinear interconnections (Section 2.3).

Distributed control synthesis procedures, represented as LMI semidefinite programs, were proposed by taking into account the presence or absence of input saturation in each subsystem of the network (Chapter 3).

Furthermore, we have also proposed a new control synthesis procedure aiming to use the graph sparsity to reduce the total running time to solve the associated optimization problem when the number of subsystems increases together with the problem computational complexity (Chapter 4).

5.2 Main Conclusions

Chapter 3 presents an alternative method to obtain sufficient conditions for distributed stabilization of the networked system. It is based on quadratic block-diagonal Lyapunov

functions and include saturation of the control inputs in the interconnected subsystems. It has been shown that if the associated optimization problem is feasible, the closed-loop networked control system is asymptotically stable, and the corresponding estimated ellipsoidal Domain of Attraction (DoA) is maximized. Two examples of networked systems are employed to show the effectiveness of the proposed control approach, which is able to be used in the synthesis of not only distributed but also decentralized controllers. Notably, it is illustrated in Section 3.4.1, the advantage of the N-TS fuzzy models over the TS fuzzy models, since less conservative results are achieved with a lower number of rules.

Chapter 4 presents another way to reduce the total running time to solve the associated optimization problem when dealing with large-scale systems, despite the increased computational complexity. Sufficient conditions of positiveness of the multiple fuzzy summations with a multiset of membership functions without the need to use the approach based on the augmented vector (3.17) are obtained relying on the graph chordal decomposition. The combinations of fuzzy rules among interconnected subsystems are reduced as the more sparse is the graph representing the subsystems interconnections in the large-scale system. In Section 4.4, it is illustrated that the approach developed is more scalable in comparison to the one in Chapter 3 when the number of interconnected subsystems is large. The elimination of the sparsity in the constraints before handing them over to the optimization solver leads to this improvement, since commercial solvers for semidefinite programs, such as Mosek, are usually not ready to deal with sparse constraints.

5.3 Possible Future Directions

As a direct extension of methods developed to decrease the computational complexity of the problem, we intend to combine both approaches, i.e. to use the chordal decomposition together with the augmented vector ideas, to improve the performance of the solver, mainly when the size of the largest maximal clique is high.

One possibility for future research is the extension of the method to deal with the addition of subsystems in the large-scale system, such that the graph is also extended by the inclusion of a new vertex and edges. This can allow creating a *plug and play* approach on the network of interconnected subsystems, similarly to the method used in (Riverso, Farina, and Ferrari-Trecate 2013; Riverso and Ferrari-Trecate 2012) to synthesize a distributed controller for interconnected linear systems.

Other topics for future research include the extension of the proposed method to deal with:

1. large-scale systems where observers have to be used to estimate either the instantaneous values of the nonlinear interconnections or the states of adjacent subsystems;
2. control of discrete-time large-scale systems; or

3. sampled-data based control incorporating effects of communication network induced delays (Kim, Park, and Joo [2017](#)).

Moreover, other types of Lyapunov function candidates, together with more general control structures, could be used to reduce the conservativeness of the proposed solutions.

It is interesting to notice also that, in the context of fault tolerant control, the property of chordal graphs can be used to ensure the stability of a particular subsystem from its physical interconnections even if all of its actuators fail.

Furthermore, another topic of interest would be the synchronization of multi-agent systems. In this kind of problem, the subsystems have to perform a specific task together. Thus, nonlinear consensus protocols could be used to improve stabilization conditions, similarly to what was investigated in (Andreasson et al. [2014](#)).

Bibliography

- Agler, J., W. Helton, S. McCullough, and L. Rodman (1988). “Positive semidefinite matrices with a given sparsity pattern”. In: *Linear Algebra and its Applications* 107, pp. 101–149. DOI: [10.1016/0024-3795\(88\)90240-6](https://doi.org/10.1016/0024-3795(88)90240-6).
- Andreasson, M., D. V. Dimarogonas, H. Sandberg, and K. H. Johansson (2014). “Distributed control of networked dynamical systems: Static feedback, integral action and consensus”. In: *IEEE Transactions on Automatic Control* 59.7, pp. 1750–1764. DOI: [10.1109/TAC.2014.2309281](https://doi.org/10.1109/TAC.2014.2309281).
- Antoulas, A. C. (2005). *Approximation of Large-Scale Dynamical Systems*. Society for Industrial and Applied Mathematics.
- Araújo, R. F., L. A. B. Torres, and R. M. Palhares (2020). “Distributed control of networked nonlinear systems via interconnected Takagi–Sugeno fuzzy systems with nonlinear consequent”. In: *IEEE Transactions on Systems, Man, and Cybernetics: Systems*. To appear, pp. 1–10. DOI: [10.1109/tsmc.2019.2945500](https://doi.org/10.1109/tsmc.2019.2945500).
- Bakule, L. (2008). “Decentralized control: An overview”. In: *Annual Reviews in Control* 32, pp. 87–98. DOI: [10.1016/j.arcontrol.2008.03.004](https://doi.org/10.1016/j.arcontrol.2008.03.004).
- Bakule, L. (2014). “Decentralized control: Status and outlook”. In: *Annual Reviews in Control* 38, pp. 71–80. DOI: [10.1016/j.arcontrol.2014.03.007](https://doi.org/10.1016/j.arcontrol.2014.03.007).
- Blair, J. R. S. and B. Peyton (1993). “An introduction to chordal graphs and clique trees”. In: *Graph Theory and Sparse Matrix Computation*. New York, NY, USA: Springer, pp. 1–29.
- Boyd, S., L. El Ghaoui, E. Feron, and V. Balakrishnan (1994). *Linear Matrix Inequalities in System and Control theory*. Vol. 15. Philadelphia, PA, USA: Society for Industrial and Applied Mathematics.
- Bullo, F., J. Cortés, and S. Martínez (2009). *Distributed Control of Robotic Networks*. Applied Mathematics Series. Princeton University Press.
- Chang, W., W.-J. Wang, N.-J. Li, H.-G. Chou, and J.-W. Chang (2014). “ \mathcal{H}_∞ control synthesis for the large-scale system based on a linear decomposition of nonlinear interconnections”. In: *International Journal of Fuzzy Systems* 16.1, pp. 97–110.

- Coutinho, P. H. S., J. Lauber, M. Bernal, and R. M. Palhares (2019). “Efficient LMI conditions for enhanced stabilization of discrete-time Takagi-Sugeno models via delayed nonquadratic Lyapunov functions”. In: *IEEE Transactions on Fuzzy Systems* 27.9, pp. 1833–1843. DOI: [10.1109/TFUZZ.2019.2892341](https://doi.org/10.1109/TFUZZ.2019.2892341).
- Coutinho, P. H. S., R. F. Araújo, A.-T. Nguyen, and R. M. Palhares (2020). “A multiple-parameterization approach for local stabilization of constrained Takagi–Sugeno fuzzy systems with nonlinear consequents”. In: *Information Sciences* 506, pp. 295–307. DOI: [10.1016/j.ins.2019.08.008](https://doi.org/10.1016/j.ins.2019.08.008).
- Dhbaibi, S., A. S. Tlili, S. Elloumi, and N. B. Braiek (2009). “ \mathcal{H}_∞ Decentralized observation and control of nonlinear interconnected systems”. In: *ISA Transactions* 48.4, pp. 458–467. DOI: [10.1016/j.isatra.2009.05.006](https://doi.org/10.1016/j.isatra.2009.05.006).
- Dong, J., Y. Wang, and G. Yang (2009). “Control synthesis of continuous-time T-S fuzzy systems with local nonlinear models”. In: *IEEE Transactions on Systems, Man, and Cybernetics, Part B (Cybernetics)* 39.5, pp. 1245–1258. DOI: [10.1109/TSMCB.2009.2014961](https://doi.org/10.1109/TSMCB.2009.2014961).
- Dong, J., Y. Wang, and G. Yang (2011). “ \mathcal{H}_∞ and mixed $\mathcal{H}_2/\mathcal{H}_\infty$ control of discrete-time T-S fuzzy systems with local nonlinear models”. In: *Fuzzy Sets and Systems* 164.1, pp. 1–24. DOI: [10.1016/j.fss.2010.09.014](https://doi.org/10.1016/j.fss.2010.09.014).
- Fukuda, M., M. Kojima, K. Murota, and K. Nakata (2001). “Exploiting Sparsity in Semidefinite Programming via Matrix Completion I: General Framework”. In: *SIAM Journal on Optimization* 11.3, pp. 647–674. DOI: [10.1137/S1052623400366218](https://doi.org/10.1137/S1052623400366218).
- Godsil, C. and G. Royle (2001). *Algebraic Graph Theory*. Springer New York.
- Hu, T. and Z. Lin (2001). *Control Systems with Actuator Saturation: Analysis and Design*. Boston, MA, USA: Birkhäuser Boston.
- Jamshidi, M. (1997). *Large-Scale Systems: Modeling, Control, and Fuzzy Logic*. Upper Saddle River, NJ, USA: Prentice Hall.
- Kakimura, N. (2010). “A direct proof for the matrix decomposition of chordal-structured positive semidefinite matrices”. In: *Linear Algebra and its Applications* 433.4, pp. 819–823. DOI: [10.1016/j.laa.2010.04.012](https://doi.org/10.1016/j.laa.2010.04.012).
- Kazempour, F. and J. Ghaisari (2013). “Stability analysis of model-based networked distributed control systems”. In: *Journal of Process Control* 23, pp. 444–452. DOI: [10.1016/j.jprocont.2012.12.010](https://doi.org/10.1016/j.jprocont.2012.12.010).
- Khalil, H. K. (2002). *Nonlinear Systems*. 3rd. Upper Saddle River, NJ, USA: Prentice Hall.
- Kim, H. S., J. B. Park, and Y. H. Joo (2017). “Decentralized sampled-data tracking control of large-scale fuzzy systems: An exact discretization approach”. In: *IEEE Access* 5, pp. 12668–12681. DOI: [10.1109/ACCESS.2017.2723982](https://doi.org/10.1109/ACCESS.2017.2723982).
- Klug, M., E. B. Castelan, and D. Coutinho (2015). “A T–S fuzzy approach to the local stabilization of nonlinear discrete-time systems subject to energy-bounded disturbances”.

- In: *Journal of Control, Automation and Electrical Systems* 26.3, pp. 191–200. DOI: [10.1007/s40313-015-0172-8](https://doi.org/10.1007/s40313-015-0172-8).
- Klug, M., E. B. Castelan, V. J. S. Leite, and L. F. P. Silva (2015). “Fuzzy dynamic output feedback control through nonlinear Takagi-Sugeno models”. In: *Fuzzy Sets and Systems* 263, pp. 92–111. DOI: [10.1016/j.fss.2014.05.019](https://doi.org/10.1016/j.fss.2014.05.019).
- Koo, G. B., J. B. Park, and Y. H. Joo (2014). “Decentralized fuzzy observer-based output-feedback control for nonlinear large-scale systems: An LMI approach”. In: *IEEE Transactions on Fuzzy Systems* 22.2, pp. 406–419. DOI: [10.1109/TFUZZ.2013.2259497](https://doi.org/10.1109/TFUZZ.2013.2259497).
- Lam, H. and J. Lauber (2012). “Stability analysis of nonlinear-function fuzzy-model-based control systems”. In: *Journal of the Franklin Institute* 349.10, pp. 3102–3120. DOI: [10.1016/j.jfranklin.2012.09.013](https://doi.org/10.1016/j.jfranklin.2012.09.013).
- Li, Y., Y. Wu, and S. He (2018). “Synchronization of network systems subject to nonlinear dynamics and actuators saturation”. In: *Circuits, Systems, and Signal Processing* 38.4, pp. 1596–1618. DOI: [10.1007/s00034-018-0940-3](https://doi.org/10.1007/s00034-018-0940-3).
- Lin, W., W. Wang, and S. Yang (2007). “A novel stabilization criterion for large-scale T–S fuzzy systems”. In: *IEEE Transactions on Systems, Man, and Cybernetics, Part B (Cybernetics)* 37.4, pp. 1074–1079. DOI: [10.1109/TSMCB.2007.896016](https://doi.org/10.1109/TSMCB.2007.896016).
- Liu, Y. and X.-Y. Li (2002). “Decentralized robust adaptive control of nonlinear systems with unmodeled dynamics”. In: *IEEE Transactions on Automatic Control* 47.5, pp. 848–856. DOI: [10.1109/TAC.2002.1000285](https://doi.org/10.1109/TAC.2002.1000285).
- Löfberg, J. (2004). “YALMIP: A toolbox for modeling and optimization in MATLAB”. In: *2004 IEEE International Symposium on Computer Aided Control Systems Design*. Taipei, Taiwan, pp. 284–289. DOI: [10.1109/CACSD.2004.1393890](https://doi.org/10.1109/CACSD.2004.1393890).
- Lunze, J. (1992). *Feedback Control of Large Scale Systems*. New York, NY, USA: Prentice Hall.
- Mahmoud, M. S. (2011). *Decentralized Systems with Design Constraints*. London, U.K.: Springer.
- Meyn, S. (2007). *Control Techniques for Complex Networks*. Cambridge University Press.
- Moodi, H., M. Farrokhi, T. M. Guerra, and J. Lauber (2019). “On stabilization conditions for T–S systems with nonlinear consequent parts”. In: *International Journal of Fuzzy Systems* 21.1, pp. 84–94. DOI: [10.1007/s40815-018-0548-6](https://doi.org/10.1007/s40815-018-0548-6).
- Mosek, A. (2017). *The MOSEK optimization toolbox for MATLAB manual*.
- Nakata, K., K. Fujisawa, M. Fukuda, M. Kojima, and K. Murota (2003). “Exploiting sparsity in semidefinite programming via matrix completion II: implementation and numerical results”. In: *Mathematical Programming* 95.2, pp. 303–327. DOI: [10.1007/s10107-002-0351-9](https://doi.org/10.1007/s10107-002-0351-9).
- Nguyen, A.-T., T. Laurain, R. M. Palhares, J. Lauber, C. Sentouh, and J.-C. Popieul (2016). “LMI-based control synthesis of constrained Takagi-Sugeno fuzzy systems sub-

- ject to \mathcal{L}_2 or \mathcal{L}_∞ disturbances”. In: *Neurocomputing* 207, pp. 793–804. DOI: [10.1016/j.neucom.2016.05.063](https://doi.org/10.1016/j.neucom.2016.05.063).
- Nguyen, A., T. Taniguchi, L. Eciolaza, V. Campos, R. Palhares, and M. Sugeno (2019). “Fuzzy control systems: Past, present and future”. In: *IEEE Computational Intelligence Magazine* 14.1, pp. 56–68. DOI: [10.1109/MCI.2018.2881644](https://doi.org/10.1109/MCI.2018.2881644).
- Peng, D., N. H. El-Farra, Z. Geng, and Q. Zhu (2015). “Distributed data-based fault identification and accommodation in networked process systems”. In: *Chemical Engineering Science* 136, pp. 88–105. DOI: [10.1016/j.ces.2015.04.040](https://doi.org/10.1016/j.ces.2015.04.040).
- Rhee, B.-J. and S. Won (2006). “A new fuzzy Lyapunov function approach for a Takagi-Sugeno fuzzy control system design”. In: *Fuzzy Sets and Systems* 157.9, pp. 1211–1228. DOI: [10.1016/j.fss.2005.12.020](https://doi.org/10.1016/j.fss.2005.12.020).
- Riverso, S., M. Farina, and G. Ferrari-Trecate (2013). “Plug-and-play decentralized model predictive control for linear systems”. In: *IEEE Transactions on Automatic Control* 58.10, pp. 2608–2614. DOI: [10.1109/TAC.2013.2254641](https://doi.org/10.1109/TAC.2013.2254641).
- Riverso, S. and G. Ferrari-Trecate (2012). “Tube-based distributed control of linear constrained systems”. In: *Automatica* 48.11, pp. 2860–2865. DOI: [10.1016/j.automatica.2012.08.024](https://doi.org/10.1016/j.automatica.2012.08.024).
- Rohr, E. R., L. F. A. Pereira, and D. F. Coutinho (2009). “Robustness analysis of nonlinear systems subject to state feedback linearization”. In: *SBA: Controle & Automação* 20.4, pp. 482–489.
- Sala, A. (2009). “On the conservativeness of fuzzy and fuzzy-polynomial control of nonlinear systems”. In: *Annual Reviews in Control* 33.1, pp. 48–58. DOI: [10.1016/j.arcontrol.2009.02.001](https://doi.org/10.1016/j.arcontrol.2009.02.001).
- Sala, A. and C. Ariño (2009). “Polynomial fuzzy models for nonlinear control: A Taylor series approach”. In: *IEEE Transactions on Fuzzy Systems* 17.6, pp. 1284–1295. DOI: [10.1109/TFUZZ.2009.2029235](https://doi.org/10.1109/TFUZZ.2009.2029235).
- Sala, A. and C. Ariño (2007). “Asymptotically necessary and sufficient conditions for stability and performance in fuzzy control: Applications of Polya's theorem”. In: *Fuzzy Sets and Systems* 158.24, pp. 2671–2686. DOI: [10.1016/j.fss.2007.06.016](https://doi.org/10.1016/j.fss.2007.06.016).
- Šiljak, D. (2007). *Large-Scale Dynamic Systems: Stability and Structure*. Dover Civil and Mechanical Engineering Series. Mineola, NY, USA: Dover Publications.
- Šiljak, D. and A. Zečević (2005). “Control of large-scale systems: Beyond decentralized feedback”. In: *Annual Reviews in Control* 29, pp. 169–179. DOI: [10.1016/j.arcontrol.2005.08.003](https://doi.org/10.1016/j.arcontrol.2005.08.003).
- Šiljak, D. D. (2012). *Decentralized Control of Complex Systems*. Mineola, NY, USA: Dover.
- Singh, D., A. Ibrahim, T. Yohanna, and J. Singh (2007). “An overview of the applications of multisets”. In: *Novi Sad Journal of Mathematics* 37.3, pp. 73–92.
- Skogestad, S. and I. Postlethwaite (2005). *Multivariable Feedback Control: Analysis and Design*. Hoboken, NJ, USA: John Wiley.

- Sootla, A., Y. Zheng, and A. Papachristodoulou (2017). “Block-diagonal solutions to Lyapunov inequalities and generalisations of diagonal dominance”. In: *2017 IEEE 56th Annual Conference on Decision and Control (CDC)*, pp. 6561–6566. DOI: [10.1109/CDC.2017.8264648](https://doi.org/10.1109/CDC.2017.8264648).
- Sootla, A., Y. Zheng, and A. Papachristodoulou (2019). “On the existence of block-Diagonal solutions to Lyapunov and \mathcal{H}_∞ Riccati inequalities”. In: *IEEE Transactions on Automatic Control*, pp. 1–1. DOI: [10.1109/TAC.2019.2948194](https://doi.org/10.1109/TAC.2019.2948194).
- Stanković, S. S., D. M. Stipanović, and D. D. Šiljak (2007). “Decentralized dynamic output feedback for robust stabilization of a class of nonlinear interconnected systems”. In: *Automatica* 43.5, pp. 861–867. DOI: [10.1016/j.automatica.2006.11.010](https://doi.org/10.1016/j.automatica.2006.11.010).
- Takagi, T. and M. Sugeno (1985). “Fuzzy identification of systems and its applications to modeling and control”. In: *IEEE Transactions on Systems, Man, and Cybernetics* SMC-15, pp. 116–132. DOI: [10.1109/TSMC.1985.6313399](https://doi.org/10.1109/TSMC.1985.6313399).
- Tanaka, K., H. Yoshida, H. Ohtake, and H. Wang (2009). “A sum-of-squares approach to modeling and control of nonlinear dynamical systems with polynomial fuzzy systems”. In: *IEEE Transactions on Fuzzy Systems* 17.4, pp. 911–922. DOI: [10.1109/TFUZZ.2008.924341](https://doi.org/10.1109/TFUZZ.2008.924341).
- Tanaka, K. and H. O. Wang (2001). *Fuzzy Control Systems Design and Analysis: A Linear Matrix Inequality Approach*. New York, NY, USA: John Wiley & Sons, Inc.
- Tarbouriech, S., G. Garcia, J. Gomes da Silva Jr, and I. Queinnec (2011). *Stability and Stabilization of Linear Systems with Saturating Actuators*. London, UK: Springer.
- Vandenberghe, L., M. S. Andersen, et al. (2015). *Chordal graphs and semidefinite optimization*. Vol. 1. 4. Now Publishers, Inc., pp. 241–433.
- Ye, X. (2011). “Decentralized adaptive stabilization of large-scale nonlinear time-delay systems with unknown high-frequency-gain signs”. In: *IEEE Transactions on Automatic Control* 56.6, pp. 1473–1478. DOI: [10.1109/TAC.2011.2132270](https://doi.org/10.1109/TAC.2011.2132270).
- Yu, W., G. Wen, G. Chen, and J. Cao (2016). *Distributed Cooperative Control of Multi-agent Systems*. John Wiley & Sons Singapore Pte. Ltd.
- Zečević, A. I. and D. D. Šiljak (2004). “Design of robust static output feedback for large-scale systems”. In: *IEEE Transactions on Automatic Control* 49.11, pp. 2040–2044. DOI: [10.1109/TAC.2004.837542](https://doi.org/10.1109/TAC.2004.837542).
- Zečević, A., E. Cheng, and D. Šiljak (2010). “Control design for large-scale Lur’e systems with arbitrary information structure constraints”. In: *Applied Mathematics and Computation* 217.3, pp. 1277–1286. DOI: [10.1016/j.amc.2010.01.119](https://doi.org/10.1016/j.amc.2010.01.119).
- Zečević, A. and D. D. Šiljak (2010). *Control of Complex Systems: Structural Constraints and Uncertainty*. New York, NY, USA: Springer.
- Zhang, H., H. Zhong, and C. Dang (2012). “Delay-dependent decentralized \mathcal{H}_∞ filtering for discrete-time nonlinear interconnected systems with time-varying delay based on

- the T-S fuzzy model”. In: *IEEE Transactions on Fuzzy Systems* 20, pp. 431–443. DOI: [10.1109/TFUZZ.2011.2175231](https://doi.org/10.1109/TFUZZ.2011.2175231).
- Zhang, X. and Y. Lin (2014). “Nonlinear decentralized control of large-scale systems with strong interconnections”. In: *Automatica* 50, pp. 2419–2423. DOI: [10.1016/j.automatica.2014.07.024](https://doi.org/10.1016/j.automatica.2014.07.024).
- Zheng, Y. (2019). “Chordal Sparsity in Control and Optimization of Large-Scale Systems”. PhD thesis. University of Oxford.
- Zheng, Y., R. P. Mason, and A. Papachristodoulou (2018). “Scalable design of structured controllers using chordal decomposition”. In: *IEEE Transactions on Automatic Control* 63.3, pp. 752–767. DOI: [10.1109/TAC.2017.2726578](https://doi.org/10.1109/TAC.2017.2726578).
- Zhong, Z., Y. Zhu, and H. Lam (2018). “Asynchronous piecewise output-feedback control for large-scale fuzzy systems via distributed event-triggering schemes”. In: *IEEE Transactions on Fuzzy Systems* 26, pp. 1688–1703. DOI: [10.1109/TFUZZ.2017.2744599](https://doi.org/10.1109/TFUZZ.2017.2744599).
- Zhou, Y., D. Li, J. Lu, Y. Xi, and L. Cen (2018). “Networked and distributed predictive control of non-linear systems subject to asynchronous communication”. In: *IET Control Theory Applications* 12, pp. 504–514. DOI: [10.1049/iet-cta.2017.0674](https://doi.org/10.1049/iet-cta.2017.0674).